Novel Aspects of Interference Alignment in Wireless Communications

Von der Fakultät für Ingenieurwissenschaften,
Abteilung Elektrotechnik und Informationstechnik
der Universität Duisburg-Essen

zur Erlangung des akademischen Grades

Doktor der Ingenieurwissenschaften (Dr.-Ing.)

genehmigte Dissertation

von

Mohammed El-Absi

aus

Gaza, Palestine

Gutachter:

Prof. Dr.-Ing. Thomas Kaiser

Ao.Univ.Prof. Dipl.-Ing. Dr.techn. Gerald Matz

Tag der mündlichen Prüfung: 21.05.2015

Fachgebiet Digitale Signalverarbeitung (DSV)
Universität Duisburg-Essen
Bismarckstrasse 81
47057 Duisburg
Germany
Tel.: +49 (203) 3 79-32 87
Fax : +49 (203) 3 78-34 98

Referent: Prof. Dr.-Ing. Thomas Kaiser
Co-Referent: Ao.Univ.Prof. Dipl.-Ing. Dr.techn. Gerald Matz
Vorsitzende: Univ. Prof. Dr.-Ing. habil. István Erlich
Tag der Promotion: 21.05.2015

Mit Unterstützung des Deutschen
Akademischen Austauschdienstes

اهداء

إلى من ينبض قلبي بكل شرايينه ويهتف لساني بأعذب الكلمات وأجزل العبارات للقلبين الكبيرين ... إلى من كانت دعواتهما لي في السر والعلن خير زاد ... إلى والديّ الكريمين

إلى من فارقني جسده ولم تفارقني روحه ... أخي العزيز الشهيد أسامة طيب الله ثراه

إلى من تربيت معهم وسكنوا قلبي ووجداني ... إخوتي أحبتي

إلى التي عايشت معي تفاصيل هذا العمل آلامه وآماله ... زوجتي الفاضلة

إلى ضحكتي في هذه الدنيا، سعادتي ونور عيني ... أطفالي الأحباء

إلى فلسطين وشهدائها ... و إلى أولى القبلتين وثالث الحرمين الشريفين، المسجد الأقصى

إلى كل من أحببتهم بصدق وبقلب لا يعرف حقداً ولا ندماً

بكل الحب والتقدير والوفاء أهدي لهم هذا الجهد المتواضع .ولهم مني خالص الشكر وصادق الدعاء،،،

ACKNOWLEDGEMENTS

Firstly and always I thank Allah (God) for his endless bestowal in making me live these great moments. Without his support and mercy, I could never have finished this thesis without the faith I have in Him and depending on Him.

This thesis was written while the author was with the Institute of Digital Signal Processing (DSV), in the Faculty of Engineering at the University of Duisburg-Essen in Germany.

I would like to express my gratitude to my supervisor Prof. Dr.-Ing. Thomas Kaiser for his endless support, encouragement and understanding. He taught me how to think, how to be creative, and how to be in the right side of research. With every passing day, I realize how lucky I am to work with such a pleasant and positive supervisor. I am really proud to be one of his students.

I am also thankful to Ao.Univ.Prof. Dipl.-Ing. Dr.techn. Gerald Matz - Vienna University of Technology- for his interest in my work and for being my second supervisor.

I would like to thank all my colleagues in DSV for creating an inspiring, conducive, and friendly atmosphere for research. Many thanks for their recommendation and suggestion to present my thesis in the best form. Thanks also go to Dr.-Ing Mohamed El-Hadidy for his appreciated support and cooperation. I will not forget the nice person in DSV Rolf Küppers, special thanks to his memory.

I would also thank the German Academic Exchange Service – Deutscher Akademischer Austausch-Dienst – (DAAD) for their financial support to pursue my higher education, Master and PhD degree sequentially in Jordan and Germany.

My heartiest thanks go to all my friends who gave me the right diversion from this work, different perspectives, and many reasons to smile. Special thanks go to Mohammed Mushtaha for his support during the first period in Germany. I am also appreciated to all my friends in Duisburg with whom I spent very nice days in Germany.

Finally, I would like to express my greatest and deepest appreciation to my family. Thanks

to my parents and brothers whose endless love and sincere prayers have always been with me. I am truly indebted to their support, encouragement, prayers and unconditional love. Special thanks to my wife, Yasmeen, and my sons, Osama, Ahmed, Yusuf, for being a steadfast source of encouragement and inspiration to me. Thank you for being a wonderful family and going through the difficulties of having a student husband and father.

Last but not least, I would like to say: my parents, family, friends, I missed you too much. Without your encouragement, I would not have finished the degree. You have a special position in my heart.

Mohammed El-Absi
Duisburg, Germany
June, 2015

ABSTRACT

Interference alignment (IA) is a promising joint-transmission technology that essentially enables the maximum achievable degrees-of-freedom (DoF) in K-user interference channels. Fundamentally, wireless networks are interference-limited since the spectral efficiency of each user in the network is degraded with the increase of users. IA breaks through this barrier, that is caused by the traditional interference management techniques, and promises large gains in spectral efficiency and DoF, notably in interference limited environments.

This dissertation concentrates on overcoming the challenges as well as exploiting the opportunities of IA in K-user multiple-input multiple-output (MIMO) interference channels. In particular, we consider IA in K-user MIMO interference channels in three novel aspects.

In the first aspect, we develop a new IA solution by designing transmit precoding and interference suppression matrices through a novel iterative algorithm based on Min-Maxing strategy. Min-Maxing IA optimization problem is formulated such that each receiver maximizes the power of the desired signal, whereas it preserves the minimum leakage interference as a constraint. This optimization problem is solved by relaxing it into a standard semidefinite programming form, and additionally its convergence is proved. Furthermore, we propose a simplified Min-Maxing IA algorithm for rank-deficient interference channels to achieve the targeted performance with less complexity. Our numerical results show that Min-Maxing IA algorithm proffers significant sum-rate improvement in K-user MIMO interference channels compared to the existing algorithms in the literature at high signal-to-noise ratio (SNR) regime. Moreover, the simplified algorithm matches the optimal performance in the systems of rank-deficient channels.

In the second aspect, we deal with the practical challenges of IA under realistic channels, where IA is highly affected by the spatial correlation. Data sum-rate and symbol error-rate of IA are dramatically degraded in real-world scenarios since the correlation between channels decreases the SNR of the received signal after alignment. For this reason, an acceptable sum-rate of IA in MIMO orthogonal frequency-division-multiplexing (MIMO-OFDM) interference

channels was obtained in the literature by modifying the locations of network nodes and the separation between the antennas within each node in order to minimize the correlation between channels. In this regard, we apply transmit antenna selection to MIMO-OFDM IA systems either through bulk or per-subcarrier selection aiming at improving the sum-rate and/or error-rate performance under real-world channel circumstances while keeping the minimum spatial antenna separation of half-wavelengths. A constrained per-subcarrier antenna selection is performed to avoid subcarrier imbalance across the antennas of each user that is caused by per-subcarrier selection. Furthermore, we propose a sub-optimal antenna selection algorithm to reduce the computational complexity of the exhaustive search. An experimental testbed of MIMO-OFDM IA with antenna selection in indoor wireless network scenarios is implemented to collect measured channels. The performance of antenna selection in MIMO IA systems is evaluated using measured and deterministic channels, where antenna selection achieves considerable improvements in sum-rate and error-rate under real-world channels.

Third aspect of this work is exploiting the opportunity of IA in resource management problem in OFDM based MIMO cognitive radio systems that coexist with primary systems. We propose to perform IA based resource allocation to improve the spectral efficiency of cognitive systems without affecting the quality of service (QoS) of the primary system. IA plays a vital role in the proposed algorithm enabling the secondary users (SUs) to cooperate and share the available spectrum aiming at increasing the DoF of the cognitive system. Nevertheless, the number of SUs that can share a given subcarrier is restricted to the IA feasibility conditions, where this limitation is considered in problem formulation. As the optimal solution for resource allocation problem is mixed-integer, we propose a two-phases efficient sub-optimal algorithm to handle this problem. In the first phase, frequency-clustering with throughput fairness consideration among SUs is performed to tackle the IA feasibility conditions, where each subcarrier is assigned to a feasible number of SUs. In the second phase, the power is allocated among subcarriers and SUs without violating the interference constraint to the primary system. Simulation results show that IA with frequency-clustering achieves a significant sum-rate increase compared to cognitive radio systems with orthogonal multiple access transmission techniques.

The considered aspects with the corresponding achievements bring IA to have a powerful role in the future wireless communication systems. The contributions lead to significant improvements in the spectral efficiency of IA based wireless systems and the reliability of IA under real-world channels.

ZUSAMMENFASSUNG

Interference Alignment (IA) ist eine vielversprechende kooperative Übertragungstechnik, die die meisten Freiheitsgrade (engl. degrees-of-freedom, DoF) in Bezug auf Zeit, Frequenz und Ort in einem Mehrnutzer Überlagerungskanal bietet. Im Grunde sind Funksysteme Interferenz begrenzt, da die Spektraleffizienz jedes einzelnen Nutzers mit zunehmender Nutzerzahl sinkt. IA durchbricht die Schranke, die herkömmliches Interferenzmanagement errichtet und verspricht große Steigerungen der Spektraleffizienz und der Freiheitsgrade, besonders in Interferenzbegrenzter Umgebung.

Die vorliegende Dissertation betrachtet bisher noch unerforschte Möglichkeiten von IA in Mehrnutzerszenarien für Mehrantennen- (MIMO) Kanäle sowie deren Anwendung in einem kognitiven Kommunikationssystem.

Als erstes werden mit Hilfe eines effizienten iterativen Algorithmus, basierend auf der Min-Maxing Strategie, senderseitige Vorkodierungs- und Interferenzunterdrückungs Matrizen entwickelt. Das Min-Maxing Optimierungsproblem ist dadurch beschreiben, dass jeder Empfänger seine gewünschte Signalleistung maximiert, während das Minimum der Leck-Interferenz als Randbedingung beibehalten wird. Zur Lösung des Problems wird es in eine semidefinite Form überführt, zusätzlich wird deren Konvergenz nachgewiesen. Des Weiteren wird ein vereinfachter Algorithmus für nicht vollrangige Kanalmatrizen vorgeschlagen, um die Rechenkomplexität zu verringern. Wie numerische Ergebnisse belegen, bedeutet die Min-Maxing Strategie eine wesentliche Verbesserung des Systemdurchsatzes gegenüber den bisher in der Literatur beschriebenen Algorithmen für Mehrnutzer MIMO Szenarien im hohen Signal-Rausch-Verhältnis (engl. signal-to-noise ratio, SNR). Mehr noch, der vereinfachte Algorithmus zeigt das optimale Verhalten in einem System mit nicht vollrangigen Kanalmatrizen.

Als zweites werden die IA Herausforderungen an Hand von realistischen/realen Kanälen in der Praxis untersucht. Hierbei wird das System stark durch räumliche Korrelation beeinträchtigt. Der Datendurchsatz sinkt und die Symbolfehlerrate steigt dramatisch unter diesen Bedingungen, da korrelierte Kanäle den SNR des empfangenen Signals nach dem Alignment verschlechtern. Aus diesem Grund wurde in der Literatur für IA in MIMO-

OFDM Überlagerungskanälen sowohl die Position der einzelnen Netzwerkknoten als auch die Trennung zwischen den Antennen eines Knotens variiert, um so die Korrelierung der verschiedenen Kanäle zu minimieren. Das vorgeschlagene MIMO-OFDM IA System wählt unter mehreren Sendeantennen, entweder pro Unterträger oder für das komplette Signal, um so die Symbolfehlerrate und/oder die gesamt Datenrate zu verbessern, während die räumliche Trennung der Antennen auf die halbe Wellenlänge beschränkt bleiben soll. Bei der Auswahl pro Unterträger ist darauf zu achten, dass die Antennen gleichmäßig ausgelastet werden. Um die Rechenkomplexität für die vollständige Durchsuchung gering zu halten, wird ein suboptimaler Auswahlalgorithmus verwendet. Mit Hilfe einer Innenraummessanordnung werden reale Kanaldaten für die Simulationen gewonnen. Die Evaluierung des MIMO IA Systems mit Antennenauswahl für deterministische und gemessene Kanäle hat eine Verbesserung bei der Daten- und Fehlerrate unter realen Bedingungen ergeben.

Als drittes beschäftigt sich die vorliegende Arbeit mit den Möglichkeiten, die sich durch MIMO IA Systeme für das Ressourcenmanagementproblem bei kognitiven Funksystemen ergeben. In kognitiven Funksystemen müssen MIMO IA Systeme mit primären koexistieren. Es wird eine IA basierte Ressourcenzuteilung vorgeschlagen, um so die spektrale Effizienz des kognitiven Systems zu erhöhen ohne die Qualität (QoS) des primären Systems zu beeinträchtigen. Der vorgeschlagenen IA Algorithmus sorgt dafür, dass die Zweitnutzer (engl. secondary user, SU) untereinander kooperieren und sich das zur Verfügung stehende Spektrum teilen, um so die DoF des kognitiven Systems zu erhöhen. Die Anzahl der SUs, die sich eine Unterträgerfrequenz teilen, ist durch die IA Randbedingungen begrenzt. Die Suche nach der optimalen Ressourcenverteilung stellt ein gemischt-ganzzahliges Problem dar, zu dessen Lösung ein effizienter zweistufiger suboptimaler Algorithmus vorgeschlagen wird. Im ersten Schritt wird durch Frequenzzusammenlegung (Clusterbildung), unter Berücksichtigung einer fairen Durchsatzverteilung unter den SUs, die IA Anforderung erfüllt. Dazu wird jede Unterträgerfrequenz einer praktikablen Anzahl an SUs zugeteilt. Im zweiten Schritt wird die Sendeleistung für die einzelnen Unterträgerfrequenzen und SUs so festgelegt, dass die Interferenzbedingungen des Primärsystems nicht verletzt werden. Die Simulationsergebnisse für IA mit Frequenzzusammenlegung zeigen eine wesentliche Verbesserung der Datenrate verglichen mit kognitiven Systemen, die auf orthogonalen Mehrfachzugriffsverfahren beruhen.

Die in dieser Arbeit betrachteten Punkte und erzielten Lösungen führen zu einer wesentlichen Steigerung der spektralen Effizienz von IA Systemen und zeigen deren Zuverlässigkeit unter realen Bedingungen.

CONTENTS

LIST OF FIGURES

LIST OF ACRONYMS

AWGN	Additive White Gaussian Noise
CDMA	Code Division Multiple Access
CDF	Cumulative Distribution Function
CSI	Channel State Information
DoF	Degrees-of-Freedom
FBMC	Filter Bank MultiCarrier
FCC	Federal Communications Commission
FDMA	Frequency Division Multiple Access
FFT	Fast Fourier Transformation
IA	Interference Alignment
IC	Interference Channel
IoT	Internet of Things
Max-SINR	Maximum Signal-to-Interference-plus-Noise-Ratio
Max-SR	Maximum Sum-Rate
MB-UWB	Multiband Ultra Wide Band
MC	Multi-Carrier
MIMO	Multiple-Input-Multiple-Output
Min-ER	Minimum Error-Rate
Min-EG	Minimum Eigenvalue
MLI	Minimum Leakage Interference
MMSE	Minimum Mean Square Error
OFDM	Orthogonal Frequency Division Multiplexing
OQAM	Offset Quadrature Amplitude Modulated
PC	Personal Computer
PN	Pseudo Noise
PSD	Power Spectral Density

PU	Primary User
QoS	Quality-of-Service
RCRM	Rank Constrained Rank Minimization
RF	Radio Frequency
SDR	Software Defined Radio
SISO	Single-Input-Single-Output
SINR	Signal-to-Interference-plus-Noise-Ratio
SNR	Signal-to-Noise-Ratio
SU	Secondary User
TDMA	Time Division Multiple Access
USRP	Universal Software Radio Peripheral
USB	Universal Serial Bus

NOTATION

x	Scalar notation
$\mathbf{x}$	Vector notation
$\mathbf{X}$	Matrix notation
$\mathbf{X}^{-1}$	Inverse of matrix $\mathbf{X}$
$\mathbf{X}^{\mathrm{H}}$	Conjugate transpose (Hermitian) matrix of matrix $\mathbf{X}$
$\log_2(x)$	The base 2 logarithm of the element x
$\mathrm{rank}(\mathbf{X})$	Rank of matrix $\mathbf{X}$
$\mathrm{null}(\mathbf{X})$	Null of matrix $\mathbf{X}$
$\mathrm{diag}(\mathbf{x})$	makes a diagonal matrix whose diagonal elements are entries of vector $\mathbf{x}$
$\mathrm{span}(\mathbf{X})$	Subspace spanned by the column of matrix $\mathbf{X}$
$\dim(\mathbf{X})$	Dimensionality of matrix $\mathbf{X}$
$\mathrm{Tr}(\mathbf{X})$	Trace (sum of elements in the main diagonal) of matrix $\mathbf{X}$
$\mu(\mathbf{X})$	Singular values of matrix $\mathbf{X}$
$\mathrm{minEig}(\mathbf{X})$	The minimum eigenvalue of matrix $\mathbf{X}$
$\mid \mathbf{X} \mid$	Determinant of matrix $\mathbf{X}$
$\| \mathbf{X} \|$	Norm of matrix $\mathbf{X}$
$\| \mathbf{X} \|_F$	Frobenius norm of matrix $\mathbf{X}$
$\mathbf{I}_x$	Identity matrix of dimensions $x \times x$
$\nu_x(\mathbf{X})$	Eigenvectors corresponding to the x eigenvalues of matrix $\mathbf{X}$
$\nu^x_{min}(\mathbf{X})$	Eigenvectors corresponding to the x smallest eigenvalues of matrix $\mathbf{X}$
$\nu^x_{max}(\mathbf{X})$	Eigenvectors corresponding to the x largest eigenvalues of matrix $\mathbf{X}$
∇x	Gradient of x
$\nabla^{\mathrm{G}} x$	Grassmann tangent space of x
arg max	Maximization
arg min	Minimization
arg sel	Selection Cost

$\mathbb{E}[x]$	Mathematical expectation of random variable x
$\mathbb{C}$	Complex field
$\mathbb{R}$	Real field
$\mathbf{X} \succeq 0$	Matrix $\mathbf{X}$ is positive semidefinite and all its eigenvalues are nonnegative
$\mathbf{X} \prec \mathbf{Y}$	denotes that the column space of $\mathbf{X}$ is a subset of the column space of $\mathbf{Y}$
$[\mathbf{X}]_{\psi}$	The columns of matrix $\mathbf{X}$ corresponding to the set ψ
$\forall$	For all
$\lceil x \rceil$	Ceil Function
$\lfloor x \rfloor$	Floor Function
$[x]^{+}$	Equivalent to $\max(0, x)$
$\mathcal{O}(.)$	Order of the number of computation steps
s.t.	Subject to
$\frac{\partial f}{\partial x}$	Partial derivative of f with respect to x

1 INTRODUCTION

Right now, all over the world, mobile internet access is becoming wholly vital to provide flexible working practices. Moreover, mobile networks expand to accommodate wide-range of connected devices and corresponding services to achieve the Internet of Things (IoT) paradigm [1–3]. IoT is a new revolution that provides a variety of things or objects - such as environmental sensors, vehicles, medical devices, industrial equipment, surveillance cameras, etc. - to interact and communicate with each other. Forecasts predict 100 billion devices to be connected to the cloud by 2025, and all need to access and share data anywhere and anytime [4]. Moreover, it is forecasted that mobile data traffic reaches 18 exabytes (18 billion GB) per month by 2018 compared to 1.5 exabytes per month at the end of 2013 [5, 6]. Furthermore, total mobile subscriptions are expected to grow from 6.8 billion at the beginning of 2014 to 9.2 billion by the end of 2019. Additionally, mobile broadband subscriptions are expected to account for more than 80 percent of all mobile subscriptions, compared to around 30 percent in 2013 [6]. As predicted, this massive demand for wireless communications will lead to an exponential growth in network traffic.

In order to respond these ever-increasing demands, the future wireless communication systems have to support massive data-rate and high quality-of-service (QoS) by improving the spectral efficiency and spectrum utilization. Interference, which is caused when multiple users access simultaneously a common communication channel, is one of the most challenging phenomena that limits the spectral efficiency of wireless communication systems. Hence, there is a tremendous potential for efficient interference management to minimize interference effect and greatly improve the capacity of wireless networks. Conventional interference management strategies coordinate the users in a way that the channel access is orthogonalized. In orthogonal schemes such as time-division-multiple-access (TDMA) and frequency-division-multiple-access (FDMA), the resources of the system are distributed among the users aiming at that different interference signals are being orthogonal to that of the desired signal and also orthog-

onal to each other. Although the orthogonal schemes are able to avoid interference, they suffer from low spectral efficiency since the maximum data-rate per user is proportionally decreased with increasing number of users. Other interference management approaches were proposed like treating interference as noise or decoding a strong interference [7, 8]. However, they suffer from the complexity as well as the poor sum-rate at high signal-to-noise ratio (SNR) values [9]. Recently, a new sophisticated interference management technique, called interference alignment (IA), was proposed to optimally manage the interference in wireless systems [10].

1.1 Motivation and Scope

IA is a cooperative interference management technique that efficiently utilizes the signaling dimensions provided by the system resources such as time, frequency, antennas, or/and code [11–15]. IA technique is employed by designing transmit precoding matrices that are able to align interfering signals at each receiver in a lower-dimensional subspace, while the desired signal is to be aligned in the other orthogonal subspace, termed interference-free subspace [10]. Cadambe and Jafar proved in [10] that IA can provide each user in a K-user interference channel with half of the achievable rates for one user in an interference-free channel at high SNRs, regardless of the number of users. Therefore, the sum-rate of the network grows linearly with the number of users.

In this dissertation, we focus on IA through the spatial domain in K-user multiple-input multiple-output (MIMO) interference channels [14]. The K-user MIMO interference channel is an information-theoretical terminology that denotes a network that consists of K MIMO transmitter-receiver pairs, where each transmitter sends an independent stream of information to its paired receiver. The basic idea of IA in K-user MIMO interference channels is to use a combination of linear precoders at the transmitters and interference suppression decoders at the receivers [16–19]. In this regard, the dissertation aims to construct and devise novel IA algorithms within the following scopes:

1. **Computing IA Solutions:** IA closed-form solutions are properly well defined so far only for limited scenarios such as 3-user MIMO interference channels with $2 \times d$ number of antennas at each node and d data streams per user [17]. Therefore, iterative algorithmic approaches were proposed as an alternative to achieve IA [19]. In the literature, many iterative approaches were proposed as in [20–23]. However, robust data sum-rate performance has not been achieved among the different K-user MIMO interference channels

by the previous approaches. Instead, we propose a more robust IA solution that improves the sum-rate of K-user MIMO interference channels.

2. **Practical Reliability of IA in Real-World Environments:** The ideal data sum-rate performance of IA in K-user MIMO interference channels is achieved in the literature by considering ideal independent channels. In reality, this assumption is generally impossible to be observed since MIMO channels have considerable spatial correlation due to the clustering of scatterers in the propagation environment [24]. Moreover, indoor environments create challenging multipath propagation scenarios, which produce significant correlated channels [25]. Unfortunately, it was stated in the literature that the performance of MIMO IA interference channels is highly dependent on channel realizations, where spatial correlation generally has an adverse effect on sum-rate and error-rate performance. The correlation between channels degrades the SNR of the received signal in the interference-free subspace after alignment [26]. In this context, we deal with the problem by applying antenna selection aiming at increasing the practical feasibility of IA in K-user orthogonal frequency division multiplexing (OFDM) MIMO interference channels under real-world circumstances.

3. **IA in Cognitive Radio Systems:** Cognitive radio is proposed to improve the spectrum utilization by introducing a new licensing scheme which allows a group of users, non-licensed, to access the vacant portion of the spectrum left by the licensed users without affecting the QoS of the licensed system [27, 28]. In the literature, most of the resource allocation problems of cognitive systems are performed based on FDMA multiple access techniques, in which each frequency band or subcarrier can be accessed by one cognitive user [29]. Moreover, IA in cognitive radio systems is rarely addressed, where IA based resource management in multicarrier MIMO cognitive radio systems is not considered. Additionally, large cognitive radio networks with a large number of users, which is a challenge for IA, are not considered in the previous works. In this context, the opportunity of IA as an effective interference management technique is exploited by performing IA based resource management in order to improve the spectral efficiency of multicarrier MIMO cognitive radio systems without affecting the QoS of the primary system.

As we can see from the above, studying IA in the scopes of this dissertation is highly attractive since the considered issues promise to achieve significant spectral efficiency in the future communication systems.

1.2 Dissertation Contributions and Organization

In this dissertation, we develop IA strategies and algorithms in order to improve the spectral efficiency of wireless communication systems. The main contributions and chapters organization of this dissertation can be summarized as follows.

- **Chapter 2: Background of Interference Alignment**
  This chapter presents some relevant background on the fundamentals of IA. We begin by introducing the types of interference channels with more concentration on K-user interference channels. We briefly discuss interference management techniques in K-user interference channels. Then, IA is presented in K-user interference channels, where the solutions of IA in addition to the feasibility of IA is described.

- **Chapter 3: Iterative Interference Alignment Based on Min-Maxing Strategy**
  Chapter 3 proposes a new iterative IA solution based on Min-Maxing strategy in order to improve the data sum-rate of K-user MIMO interference channels, wherein the interference leakage is minimized and, simultaneously, the desired power is maximized. We reformulate and relax Min-Maxing IA solution into a standard semidefinite programming form. Moreover, the convergence of the proposed method is proven. We also propose a simplified Min-Maxing IA solution for rank-deficient interference channels to achieve the targeted performance with less complexity. Further, numerical results are presented to evaluate the proposed schemes compared to other algorithms.

  The contributions of this chapter originated one journal paper and one conference paper:

  – **M. El-Absi**, M. El-Hadidy, T. Kaiser, "A distributed Interference Alignment Algorithm using Min-Maxing Strategy," *Transactions on Emerging Telecommunications Technologies*, doi: 10.1002/ett.2897, 2014.

  – **M. El-Absi**, M. El-Hadidy, T. Kaiser, "Min-Maxing Interference Alignment Algorithm as a Semidefinite Programming Problem," *IEEE 14th Workshop on Signal Processing Advances in Wireless Communications (SPAWC)*, June 2013, pp. 290–294.

- **Chapter 4: Antenna Selection for MIMO-OFDM Interference Alignment Systems**
  In this chapter, we apply transmit antenna selection to MIMO-OFDM IA systems either through bulk or per-subcarrier selection, aiming at improving the data sum-rate and/or

error-rate performance under real-world channel circumstances while keeping the minimum spatial antenna separation of 0.5 wavelengths. In order to avoid subcarrier imbalance across the antennas of each user who is caused by per-subcarrier selection, a constrained per-subcarrier antenna selection is operated. Furthermore, we propose a sub-optimal antenna selection to reduce the computational complexity of the optimal antenna selection algorithm. We implement MIMO-OFDM IA testbed to present an experimental validation for IA with antenna selection in indoor wireless network scenarios. Furthermore, the experimental results are compared with deterministic channels that are synthesized using hybrid EM ray-tracing models.

The contributions of this chapter originated two conference papers and one journal paper (under second review at the time of this writing):

- **M. El-Absi**, S. Galih, M. Hoffmann, M. El-Hadidy, and T. Kaiser, "Antenna Selection for Reliable MIMO-OFDM Interference Alignment Systems: Measurement Based Evaluation," *IEEE Transactions on Vehicular Technology*, 2015.
- **M. El-Absi**, M. El-Hadidy, T. Kaiser, "Reliability of MIMO-OFDM Interference Alignment Systems with Antenna Selection under Real-World Environments," *IEEE Proceedings of the 20th European Wireless Conference*, 14-16 May 2014, pp.1-6.
- **M. El-Absi**, M. El-Hadidy, T. Kaiser, "Antenna selection for interference alignment based on subspace canonical correlation," *International Symposium on Communications and Information Technologies (ISCIT)*, 2012, pp. 423–427.

- **Chapter 5: Interference Alignment Based Resource Management in Cognitive Radio Networks**

  This chapter performs IA based resource allocation in multicarrier MIMO cognitive radio systems in order to improve their spectral efficiency. IA based problem formulation enables the cognitive users to share the available spectrum as well as guarantees QoS of the primary system. The resource allocation problem is formulated as a mixed-integer optimization problem, where the optimal solution is generally prohibitive. Therefore, we propose a two-phases efficient sub-optimal algorithm in order to reduce the computational complexity of the optimal solution. In the first phase, frequency-clustering is performed to schedule the subcarriers among the cognitive users, while the power is allocated among the subcarriers and cognitive users in the second phase.

The contributions of this chapter originated four conference papers and one journal paper (under second review at the time of this writing):

- **M. El-Absi**, M. Shaat, F. Bader, and T. Kaiser, "Interference Alignment with Frequency Clustering for Efficient Resource Allocation in Cognitive Radio Networks," *IEEE Transactions on Wireless Communications (Minor Revision round)*, May 2015.
- **M. El-Absi**, M. Shaat, F. Bader, and T. Kaiser, "Interference Alignment with Frequency Clustering for Efficient Resource Allocation in Cognitive Radio Networks," *IEEE Global Communications Conf. (Globecom)*, 8-12 Dec. 2014.
- **M. El-Absi**, M. Shaat, F. Bader, and T. Kaiser, "Power loading and spectral efficiency comparison of MIMO OFDM/FBMC for interference alignment based cognitive radio systems," *11th Int. Symp. Wireless Communication Systems (ISWCS)*, Aug. 2014, pp. 480–485.
- **M. El-Absi**, T. Kaiser, "Optimal Resource Allocation Based on Interference Alignment for OFDM and FBMC MIMO Cognitive Radio Systems," *Proceedings of 23rd European Conference on Networks and Communications (EuCNC)*, 23-25 June 2014, pp. 1–5.
- **M. El-Absi**, M. Shaat, F. Bader, T. Kaiser, "Interference Alignment Based Resource Management in MIMO Cognitive Radio Systems," *IEEE Proceedings of the 20th European Wireless Conference*, 14-16 May 2014, pp. 1-6.

- **Chapter 6: Conclusions and Future Work**
  This chapter summarizes the main research challenges and highlights the achieved results. Moreover, it gives constructive guidelines and recommendations for future extension to this work.

For convenience, a schematic diagram showing the contributions within the chapters is presented in Fig. 1.1.

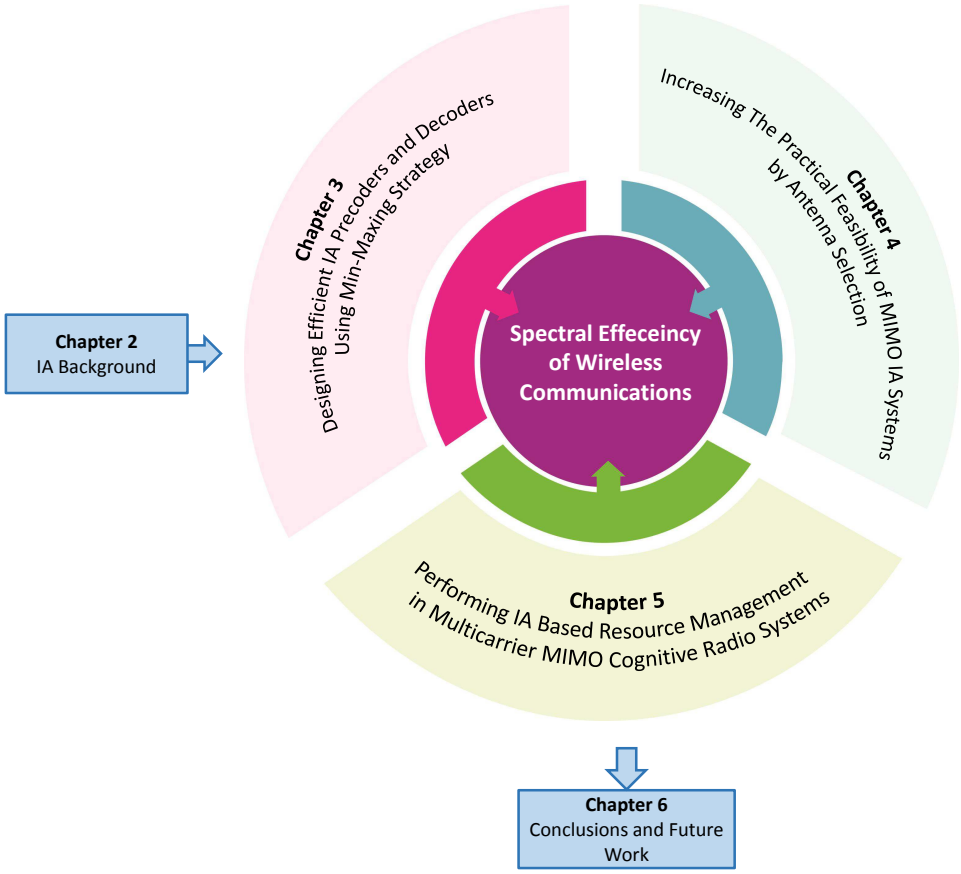

Figure 1.1: Schematic representation of the contributions and the chapters.

2 BACKGROUND OF INTERFERENCE ALIGNMENT

This chapter presents the background and the basics of IA in K-user MIMO interference channels that are required through the dissertation. An overview of K-user interference channels is presented. Additionally, interference management techniques that are used for interference channels are introduced. Afterwards, the basic concept of IA in K-user interference channels is briefly illustrated, where IA in K-user SISO and MIMO interference channels are described. Finally, IA solutions through closed-form and iterative methods are presented.

2.1 Introduction

Wireless communication systems often have multiple transmitters and receivers sharing the same transmission medium, which causes mutual interference into each other [30–32]. Therefore, the characterization of the capacity of multiuser systems is more difficult than single-user systems, where multiuser systems are considered interference-limited since the spectral efficiency of the system is restricted by the interference. Referring to information-theoretical terminologies, multiuser channels are classified into different models such as broadcast channels, multiple access channels and interference channels, as shown in Fig. 2.1 [33–37]. In broadcast channels, one transmitter transmits multiple independent messages to multiple independent receivers [33, 34]. Therefore, the transmission from the transmitter to each receiver is considered as an interference to other receivers. In multiple access channels, the situation is reversed, where multiple independent transmitters send multiple independent information to a common receiver [35, 36]. Accordingly, the communication from each transmitter to the common receiver interferes the communications of other transmitters. Whereas the interference channel models the communication of a transmitter-receiver pair in the presence of interference from all other pairs, where each transmitter sends an independent stream of information to its paired receiver causing interference to other receivers [37]. In the rest of this chapter, interference channels are considered in more details.

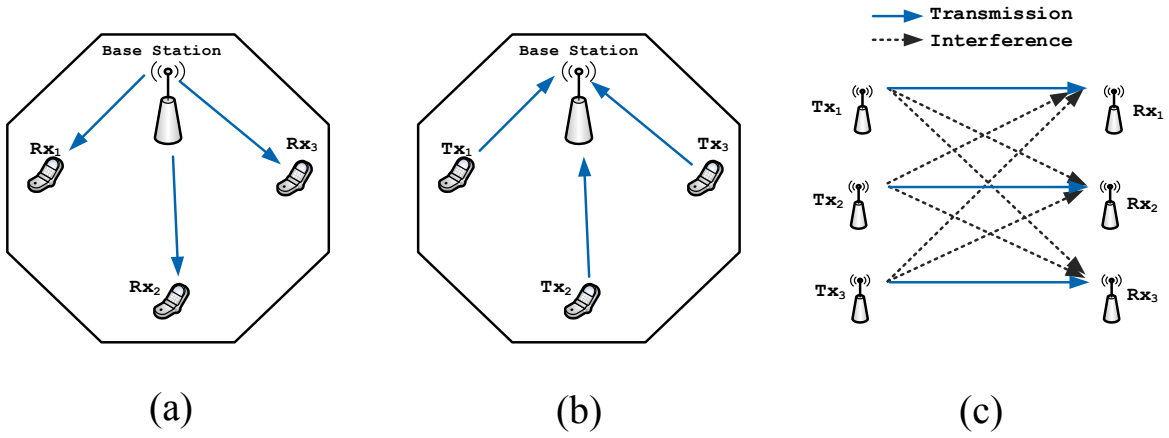

Figure 2.1: a) Broadcast channels, b) Multiple access channel, c) K-user interference channel.

2.2 Interference Channels

In the interference channel framework, each transmitter sends an independent stream of information to its paired receiver. As the transmission medium is shared by a number of multiple transmitter-receiver pairs, the communications between each transmitter and its corresponding receiver interfere with the communications of other transmitter-receiver pairs [37]. This interference is considered as a major limiting factor for the capacity of interference channels. Characterizing the capacity region of interference channels is generally an open problem in information theory [38–40]. It was shown that in Gaussian interference networks when the interference is very strong, the capacity region would not be affected by interference [37,41]. This can be achieved when each receiver can first decode the message of the unintended source and subtract it from the received signal before decoding its own message. The scheme was extended to the "strong interference", and the capacity region was established in [8, 42]. Moreover, some outer bounds were further proposed for moderate and weak interference in [37, 43–45], where the characterization of the capacity region is more challenging compared to the "very strong and strong interference scenario". However, exact channel capacity characterization in general interference channels is still unknown.

The concept of "degrees-of-freedom (DoF)" was appeared as an approximation for the behavior of the channel capacity when the SNR approaches to infinity [46,47], which is defined as

$$d = \lim_{SNR\to\infty} \frac{R(\text{SNR})}{\log_2(\text{SNR})}, \tag{2.1}$$

where d is the DoF metric and $R(\text{SNR})$ is the sum-rate with respect to SNR. Equivalently,

sum-rate can be expressed as

$$R(\text{SNR}) = d \log_2(\text{SNR}) + o(\log_2(\text{SNR})), \tag{2.2}$$

where $o(\log_2(\text{SNR}))$ is a term that vanishes as SNR goes to infinity. Based on this definition, DoF can be interpreted as the number of achievable independent data streams at each user. Additionally, DoF is also known as the multiplexing gain or capacity pre-log factor as well [48, 49].

2.3 Interference Management in K-user Interference Channels

Multi-user wireless systems have to employ interference management in order to achieve a high system capacity. Accordingly, interference management in K-user interference channels have received much attention in order to propose approaches deal with interference in shared medium. These approaches can be categorized as follows [10]

- **Treat interference as noise**: This scheme ignores the structure of interference and simply treats it as noise [7]. This scheme is optimal whenever the interference power is much less than the desired signal power [50]. Therefore, it is considered one of the low complex strategies.

- **Interference decoding**: Interference decoding is introduced when interference is strong or very strong and originates from a single source [8]. In this scheme, each receiver first decodes the message of the unintended source and subtracts it from the received signal before decoding the desired message. However, this approach is quite complex and limits other users' data-rates. Moreover, generalizing this method to K-user interference channel is not straightforward in general.

- **Orthogonalization**: This approach is used when the interference is being strong as the desired signal. In this approach, the transmissions of different users are orthogonalized in a way that each transmitter-receiver pair has access to only a portion of the available resources. Traditional schemes based on user access orthogonalization are TDMA, FDMA and code division multiple access (CDMA). Although this approach is widely used in multiuser communication systems, the spectral efficiency of each pair degrades as the number of users increases [51].

Generally, the aforementioned interference management strategies may not be spectrally efficient. Interference decoding and treating interference as noise are limited for specific scenarios and for a limited number of users (e.g. two-user scenario for interference decoding approach). Furthermore, they perform well only at low SNR regime, while the sum-rate saturates at high SNRs. Orthogonal schemes exhibit the better sum-rate at medium and high SNR, since their sum-rate is scaled linearly as a function of the SNR. However, the linear scaling is limited by the fact that the K users have to share the resource [10]. As a result of that, each user only gets $1/K$ fraction of the resource and, hence, achieves $1/K$ DoF. Although signal reception at each receiver does not directly suffer from interference, this scheme is not optimal in terms of spectral efficiency. This results from that the interference spans a large dimension of the received signal space at each receiver. Accordingly, the capacity per user, i.e. k^{th} user, in a K-user interference channel that uses orthogonal schemes, is

$$R_k(\text{SNR}) = \frac{1}{K}\log_2(\text{SNR}) + o(\log_2(\text{SNR})), \tag{2.3}$$

and the total sum-rate of the K-user interference channel is

$$R(\text{SNR}) = \log_2(\text{SNR}) + o(\log_2(\text{SNR})). \tag{2.4}$$

As an example, consider such a 3-user interference channel, where each transmitter wishes to communicate only with its corresponding receiver. Hence, each user receives two interfering signals in addition to the desired signal. By assuming that all propagation delays are equal, the interference is managed using TDMA as depicted in Fig. 2.2. In this example, each user can transmit upon $1/3$ portion of the time dimension. At the receive side, the signals can be perfectly separated. However, a fraction $2/3$ of the time dimension is spanned by the interference signals. Therefore, if the dimensionality of the interference subspace is minimized, a larger interference-free subspace would be left for desired transmission. In fact, this is the concept of "Interference Alignment (IA)" [10].

2.4 The Concept of Interference Alignment

IA is a cooperative interference management strategy that aligns interfering signals at each receiver in one subspace, while the desired signal is to be aligned in another orthogonal subspace, termed interference-free subspace [10]. This alignment can exploit the available signaling di-

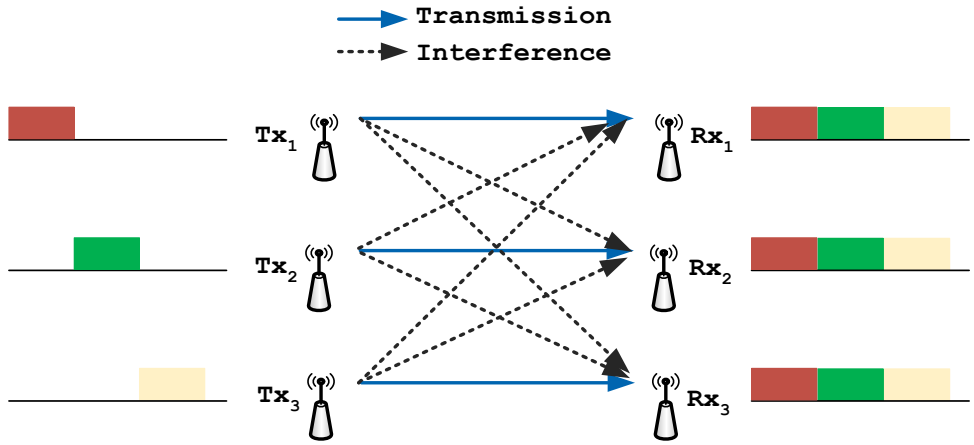

Figure 2.2: An illustrative representation of TDMA concept for 3-user interference channel.

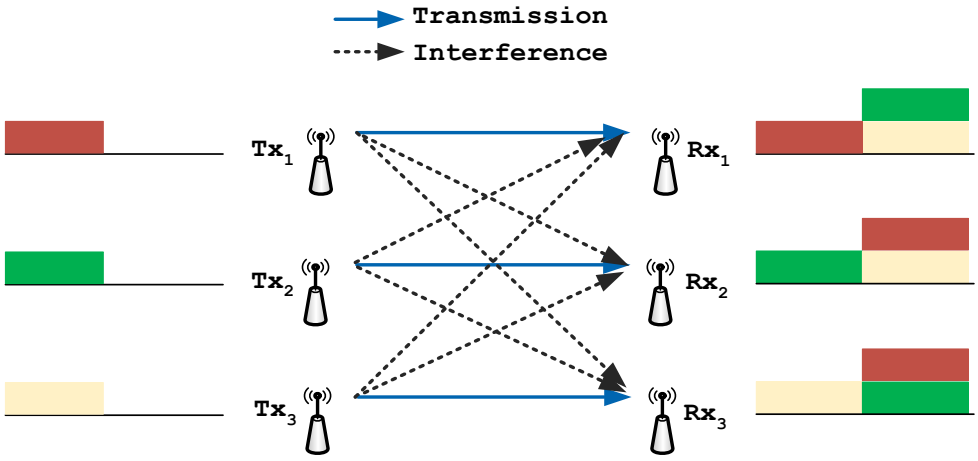

Figure 2.3: An illustrative representation of IA concept for 3-user interference channel.

mensions in time [11, 12], frequency [13], space [11, 14], or/and code [15]. IA is employed by designing transmit precoding matrices and receive decoding matrices that are able to distinguish between interference signals and desired signal at the receiver side. Cadambe and Jafar proved in [10] that IA can optimally manage the interference aiming at providing the K users in an interference channel with half of the achievable capacity of one user in an interference-free channel at high SNRs, regardless of the number of users. Therefore, the capacity per user, i.e. k^{th} user, in a K-user interference channel is

$$R_k(\text{SNR}) = \frac{1}{2}\log_2(\text{SNR}) + o(\log_2(\text{SNR})), \tag{2.5}$$

and the total sum-rate of the K-user interference channel is

$$R(\text{SNR}) = \frac{K}{2}\log_2(\text{SNR}) + o(\log_2(\text{SNR})). \tag{2.6}$$

This result is achieved in [10] when the channel coefficients change in every time slot. The DoF per user in (2.5) is $1/2$ and, hence, all users get half the communication resources. Consequently, the total achievable DoF of the K-user interference channel is $K/2$. Unlike orthogonal schemes, IA can achieve a linear increase of DoF with the number of users as seen in (2.6). Considering the illustrated example in the previous section, if IA is used instead of TDMA, each user can get a fraction $1/2$ of the time dimension as shown in Fig. 2.3, regardless of the number of users. This means that the DoF per user is increased, and the total DoF of the system is $3/2$. It is clear in this example that the interference subspace is reduced to $1/2$ portion of the time dimension.

In [10], two types of interference channel settings are evaluated: K-user single-input single-output (SISO) interference channel with time varying channel coefficients and the K-user MIMO interference channel with constant channel coefficients.

2.5 IA in K-user SISO Interference Channels

In this section, we will briefly review IA in K-user SISO interference channels. Two system models are considered in this section: 1) K-user SISO interference channels with time extension, 2) K-user SISO multicarrier interference channels.

2.5.1 K-user SISO Interference Channels with Time Extension

We consider a 3-user SISO interference channel to reveal the basic idea of IA in time-varying SISO interference networks, where each node in the network is equipped with single antenna. In this network, at each time slot there is not enough space dimension to apply IA because each node has only one antenna. Therefore, the symbol extension is proposed in [10] to overcome this limitation. We denote the symbol extension of the transmitted symbol x_k from the k^{th} transmitter over τ time slots as

$$\mathbf{x}_k(t) = [x_k(\tau(t-1)+1) \;\; x_k(\tau(t-1)+2) \;\; \dots \;\; x_k(\tau t)]\,, \tag{2.7}$$

and the symbol extension of the received symbol y_k at the k^{th} receiver over τ time slots as

$$\mathbf{y}_k(t) = [y_k(\tau(t-1)+1) \;\; y_k(\tau(t-1)+2) \;\; \dots \;\; y_k(\tau t)]\,. \tag{2.8}$$

Thus, the received signal at the k^{th} receiver can be expressed as

$$\mathbf{y}_k(t) = \mathbf{H}_{k1}(t)\mathbf{x}_1(t) + \mathbf{H}_{k2}(t)\mathbf{x}_2(t) + \mathbf{H}_{k3}(t)\mathbf{x}_3(t) + \mathbf{z}_k(t), \tag{2.9}$$

where $\mathbf{z}_k(t)$ represents the expansion of additive white Gaussian noise (AWGN) over τ time symbols, and $\mathbf{H}_{kj}(t)$ represents the diagonal extended channel matrix between the k^{th} receiver and the j^{th} transmitter expressed as

$$\mathbf{H}_{kj}(t) = \begin{bmatrix} h_{kj}(\tau(t-1)+1) & 0 & \cdots & 0 \\ 0 & h_{kj}(\tau(t-1)+2) & \cdots & 0 \\ \vdots & \vdots & \ddots & \vdots \\ 0 & 0 & \cdots & h_{kj}(\tau t) \end{bmatrix}, \tag{2.10}$$

where $h_{kj}(t)$ is the channel coefficient between the k^{th} receiver and the j^{th} transmitter at time t. Perfect global channel state information (CSI) is assumed to be known at all nodes. Moreover, it is assumed that the channel coherence time is one, where channel gains remain constant within one time slot, but change independently across different time slots.

IA aims to construct the precoding and decoding matrices in a way that the interferences from different transmitters are aligned together at each receiver within one-half of the total received signal space, keeping the other half for the desired signal. It is found in [10] that, using IA with symbol extension of $\tau = 2m + 1$ time slots, a 3-user SISO interference channel can obtain $3m + 1$ DoF, where m is a non-negative integer. Assume Transmitter 1 encodes its message into $m + 1$ independent data streams $x_1^l(t)$ and transmits them using $\tau \times 1$ precoder vectors $\mathbf{v}_1^l$, where $l = 1, 2, \ldots, m+1$. Therefore, the transmitted signal $\mathbf{s}_1(t)$ can be represented as

$$\hat{\mathbf{s}}_1(t) = \sum_{l=1}^{m+1} x_1^l(t)\mathbf{v}_1^l = \mathbf{V}_1\mathbf{x}_1(t), \tag{2.11}$$

where $\mathbf{V}_1 = \begin{bmatrix} \mathbf{v}_1^1 & \mathbf{v}_1^2 & \cdots & \mathbf{v}_1^{m+1} \end{bmatrix}$ represents the $(2m+1)\times(m+1)$ precoding matrix. Similarly, Transmitters 2 and 3 encode their messages into m independent data streams as

$$\hat{\mathbf{s}}_2(t) = \sum_{i=1}^{m} x_2^i(t)\mathbf{v}_2^i = \mathbf{V}_2\mathbf{x}_2(t) \tag{2.12}$$

$$\hat{\mathbf{s}}_3(t) = \sum_{i=1}^{m} x_3^i(t)\mathbf{v}_3^i = \mathbf{V}_3\mathbf{x}_3(t). \tag{2.13}$$

Therefore, the received signal at the k^{th} receiver can be represented as

$$\mathbf{y}_k(t) = \sum_{j=1}^{3} \mathbf{H}_{kj}\mathbf{V}_j\mathbf{x}_j(t) + \mathbf{z}_k(t). \tag{2.14}$$

User 1 can achieve $\frac{m+1}{2m+1}$ DoF using IA by aligning the interfering signals from Transmitter 2 and 3 in a subspace with dimension smaller than m as follows

$$\text{rank}\left([\mathbf{H}_{12}\mathbf{V}_2 \quad \mathbf{H}_{13}\mathbf{V}_3]\right) \leq m, \tag{2.15}$$

where rank$(\mathbf{A})$ represents the rank of matrix $\mathbf{A}$. This condition can be achieved by properly designing the precoding matrices at transmitters 2 and 3 as follows

$$\mathbf{H}_{12}\mathbf{V}_2 = \mathbf{H}_{13}\mathbf{V}_3. \tag{2.16}$$

$\frac{m}{2m+1}$ DoF can be obtained for User 2 when interference subspace has a dimension not greater than $m+1$, which can be described as

$$\text{rank}\left([\mathbf{H}_{21}\mathbf{V}_1 \quad \mathbf{H}_{23}\mathbf{V}_3]\right) \leq m+1. \tag{2.17}$$

The constraint in (2.17) can be satisfied when

$$\mathbf{H}_{23}\mathbf{V}_3 \prec \mathbf{H}_{21}\mathbf{V}_1, \tag{2.18}$$

where $\mathbf{E} \prec \mathbf{F}$ denotes that the column space of $\mathbf{E}$ is a subset of the column space of $\mathbf{F}$. Similarly to User 2, User 3 requires that the interference subspace dimension should satisfy

$$\text{rank}\left([\mathbf{H}_{31}\mathbf{V}_1 \quad \mathbf{H}_{32}\mathbf{V}_2]\right) \leq m+1, \tag{2.19}$$

and

$$\mathbf{H}_{32}\mathbf{V}_2 \prec \mathbf{H}_{31}\mathbf{V}_1. \tag{2.20}$$

One of the solutions that can satisfy the previous equation sets is

$$\mathbf{V}_1 = \left[\mathbf{w} \quad \hat{\mathbf{T}}\mathbf{w} \quad \cdots \quad \hat{\mathbf{T}}^m\mathbf{w}\right] \tag{2.21}$$

$$\mathbf{V}_2 = \mathbf{H}_{32}^{-1}\mathbf{H}_{31}\left[\mathbf{w} \quad \hat{\mathbf{T}}\mathbf{w} \quad \cdots \quad \hat{\mathbf{T}}^{m-1}\mathbf{w}\right] \tag{2.22}$$

$$\mathbf{V}_3 = \mathbf{H}_{23}^{-1}\mathbf{H}_{21}\left[\hat{\mathbf{T}}\mathbf{w} \quad \hat{\mathbf{T}}^2\mathbf{w} \quad \cdots \quad \hat{\mathbf{T}}^m\mathbf{w}\right], \tag{2.23}$$

where $\mathbf{A}^{-1}$ denotes the inverse of matrix $\mathbf{A}$. $\mathbf{w}$ is a $(2m+1)\times 1$ vector that all its elements are 1, and

$$\hat{\mathbf{T}} = \mathbf{H}_{12}\mathbf{H}_{21}^{-1}\mathbf{H}_{23}\mathbf{H}_{32}^{-1}\mathbf{H}_{31}\mathbf{H}_{13}^{-1}. \tag{2.24}$$

To guarantee each receiver can decode its own message, it was verified in [10] that the columns of $[\mathbf{H}_{11}\mathbf{V}_1 \ \ \mathbf{H}_{12}\mathbf{V}_2]$, $[\mathbf{H}_{22}\mathbf{V}_2 \ \ \mathbf{H}_{21}\mathbf{V}_1]$, and $[\mathbf{H}_{33}\mathbf{V}_3 \ \ \mathbf{H}_{31}\mathbf{V}_1]$ are linearly independent. Therefore, the desired and interference subspaces can be almost surly separated.

As a conclusion, the pairs $1, 2$ and 3 achieve DoF $= \langle \frac{m+1}{2m+1}, \frac{m}{2m+1}, \frac{m}{2m+1}\rangle$ per symbol, respectively. Asymptotically, DoF $= \langle \frac{1}{2}, \frac{1}{2}, \frac{1}{2}\rangle$ are achievable when $m \to \infty$. In other words, each pair can get half of the cake at high SNRs.

2.5.2 K-user Multicarrier Interference Channels

We consider another example for K-user SISO interference channels, which is the K-user multicarrier interference channel [23, 52, 53]. We assume that a K-user multicarrier interference channel consisting of N bands for K transmitters and receivers. Each node has a single antenna, and each user transmits d data streams.

The channel between the j^{th} transmitter and the k^{th} receiver is diagonal such that

$$\mathbf{H}_{kj} = \begin{bmatrix} h_{kj}(0) & 0 & \cdots & 0 \\ 0 & h_{kj}(1) & \cdots & 0 \\ \vdots & \vdots & \ddots & \vdots \\ 0 & 0 & \cdots & h_{kj}(N-1) \end{bmatrix}, \tag{2.25}$$

where $h_{kj}(n) \in \mathbb{C}$ is the frequency domain channel coefficient of band n. The received signal at receiver k is

$$\mathbf{y}_k = \underbrace{\mathbf{U}_k{}^{\mathrm{H}}\mathbf{H}_{kk}\mathbf{V}_k\mathbf{x}_k}_{\text{Desired Signal}} + \underbrace{\sum_{j=1, j\neq k}^{K} \mathbf{U}_k{}^{\mathrm{H}}\mathbf{H}_{kj}\mathbf{V}_j x_j}_{\text{Interference Signals}} + \mathbf{U}_k{}^{\mathrm{H}}\mathbf{z}_k, \tag{2.26}$$

where $\mathbf{A}^{\mathrm{H}}$ is the conjugate transpose (Hermitian) matrix of matrix $\mathbf{A}$. $\mathbf{V}_k,\ \mathbf{U}_k \in \mathbb{C}^{N\times d}$ are the precoder and interference suppression matrix for the k^{th} user in the multicarrier interference channel, respectively. Finding the decoders and precoders can be proceeded as in Section 2.5.1.

2.6 IA in K-user MIMO Interference Channels

IA using time-extension requires a fast fading and large number of time slots in order to reach the promised DoF. Therefore, this approach is considered impractical. In this context, alignment in spatial dimension through MIMO system, which is the focus of the thesis, is more practical than alignment in time or frequency dimensions [14]. The key idea of IA in MIMO interference channels is to use a combination of linear precoders at the transmitters and interference suppression decoders at the receivers in order to align the interference signals at half of the spatial subspaces at the receiver side. This increases the interference-free spatial dimension and, consequentially, the DoF of the system [16–18].

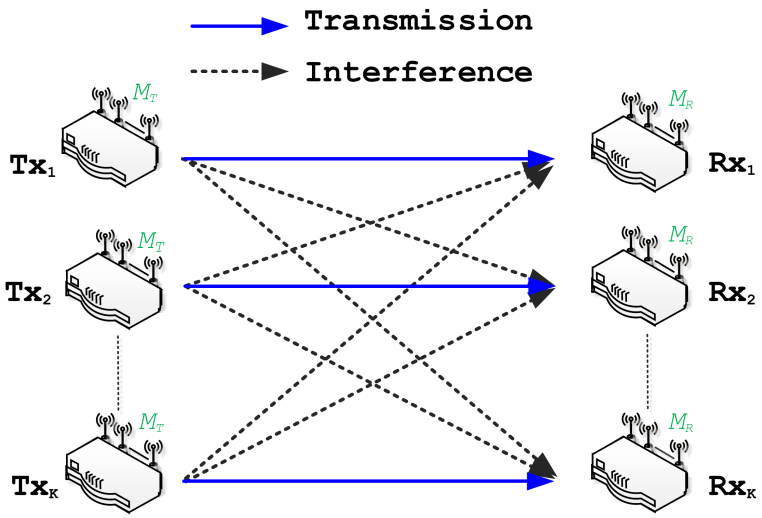

Figure 2.4: K-user MIMO interference channel.

In this regards, we consider a *K*-user MIMO interference channel with IA (MIMO IA) equipped with M_T transmit antennas at each transmitter and M_R receive antennas at each receiver as seen in Fig. 2.4. In this system, each user wishes to transmit d data streams to its desired receiver causing interference to all the other receivers. This interference channel is expressed as $(M_R \times M_T, d)^K$. It is assumed that the K-user MIMO interference channel is static during the transmission time. Accordingly, the transmitted signal $\hat{\mathbf{s}}_k \in \mathbb{C}^{M_T\times 1}$ from the k^{th}

node is given by

$$\hat{\mathbf{s}}_k = \mathbf{V}_k \mathbf{x}_k, \tag{2.27}$$

where $\mathbf{V}_k \in \mathbb{C}^{M_T \times d}$ is the precoding matrix applied at the k^{th} user to the symbol vector $\mathbf{x}_k \in \mathbb{C}^{d \times 1}$. For practical purposes, $\mathbf{V}_k$ is considered orthonormal such that [19]

$$\mathbf{V}_k^{\mathrm{H}} \mathbf{V}_k = \mathbf{I}_d, \tag{2.28}$$

where $\mathbf{I}_d$ denotes an identity matrix of dimensions $d \times d$. The discrete-time complex received signal at the k^{th} receiver $\widehat{\mathbf{y}}_k \in \mathbb{C}^{M_R \times 1}$ is represented as

$$\begin{aligned} \widehat{\mathbf{y}}_k &= \sum_{j=1}^{K} \mathbf{H}_{kj} \mathbf{V}_j \mathbf{x}_j + \mathbf{z}_k \\ &= \mathbf{H}_{kk} \mathbf{V}_k \mathbf{x}_k + \sum_{j=1, j \neq k}^{K} \mathbf{H}_{kj} \mathbf{V}_j \mathbf{x}_j + \mathbf{z}_k, \end{aligned} \tag{2.29}$$

where $\mathbf{H}_{kj} \in \mathbb{C}^{M_R \times M_T}$ is the flat frequency domain channel matrix between the j^{th} transmitter and the k^{th} receiver, and $\mathbf{z}_k \in \mathbb{C}^{M_R \times 1}$ is the zero mean unit variance circularly symmetric AWGN vector at the k^{th} receiver. It is assumed in this work that the CSI is perfectly known at each node. To reconstruct the transmitted signal at the k^{th} receiver, the received signal is decoded using an orthonormal linear interference suppression matrix $\mathbf{U}_k \in \mathbb{C}^{M_R \times d}$ such that

$$\mathbf{U}_k^{\mathrm{H}} \mathbf{U}_k = \mathbf{I}_d. \tag{2.30}$$

The reconstructed data $\mathbf{y}$ at the k^{th} receiver is defined as

$$\mathbf{y}_k = \underbrace{\mathbf{U}_k^{\mathrm{H}} \mathbf{H}_{kk} \mathbf{V}_k \mathbf{x}_k}_{\text{Desired Signal}} + \underbrace{\sum_{j=1, j \neq k}^{K} \mathbf{U}_k^{\mathrm{H}} \mathbf{H}_{kj} \mathbf{V}_j x_j}_{\text{Interference Signals}} + \mathbf{U}_k^{\mathrm{H}} \mathbf{z}_k. \tag{2.31}$$

The precoding matrices and interference suppression matrices are jointly designed to mitigate the interference term in (2.31). The role of precoding matrices is to align the interference signals at the minimum subspace dimension at each receiver, while ensuring that the desired signal at each receiver is linearly independent of the interference subspace [17]. In order to

achieve that, the following two conditions have to be fulfilled

$$\mathbf{U}_k^{\mathrm{H}}\mathbf{H}_{kj}\mathbf{V}_j = 0, \ \forall j \neq k \text{ and} \tag{2.32}$$

$$\text{rank}\left(\mathbf{U}_k^{\mathrm{H}}\mathbf{H}_{kk}\mathbf{V}_k\right) = d_k, \ \forall k \in \{1, 2, \cdots, K\}. \tag{2.33}$$

The condition in (2.32) ensures that all interference signals $\mathbf{H}_{kj}\mathbf{V}_j$ are perfectly aligned into $N_R - d$ dimensions for the interference subspace, while the second condition in (2.33) ensures that the received desired signal has full-rank effective channel matrix of d. The feasibility of achieving MIMO IA conditions in (2.32) and (2.33) will be discussed in the following section.

The achieved sum-rate in bits per second per hertz of K-user MIMO interference channels using zero-forcing receivers is calculated as [26]

$$R = \sum_{k=1}^{K} \log_2 \left| \mathbf{I}_d + \frac{\mathbf{U}_k^{\mathrm{H}}\mathbf{H}_{kk}\mathbf{V}_k\mathbf{S}_k\mathbf{V}_k^{\mathrm{H}}\mathbf{H}_{kk}^{\mathrm{H}}\mathbf{U}_k}{\sigma^2\mathbf{I}_d + \mathbf{U}_k^{\mathrm{H}}\mathbf{Q}_k\mathbf{U}_k} \right|, \tag{2.34}$$

where σ^2 is the variance of the AWGN, and $\mathbf{S}_k = \mathbb{E}\left[\mathbf{x}_k\mathbf{x}_k^{\mathrm{H}}\right] \in \mathbb{R}^{d\times d}$ is the input covariance matrix of the k^{th} user. $\mathbf{Q}_k$ is the interference covariance matrix at the k^{th} receiver, which can be expressed as

$$\mathbf{Q}_k = \sum_{j=1, j\neq k}^{K} \mathbf{H}_{kj}\mathbf{V}_j\mathbf{S}_j\mathbf{V}_j^{\mathrm{H}}\mathbf{H}_{kj}^{\mathrm{H}}. \tag{2.35}$$

Therefore, the transmitted power by the k^{th} user is $P_k = \text{Tr}\left(\mathbf{S}_k\right)$. If the IA feasibility conditions in (2.32) and (2.33) are achieved, the interference can be completely eliminated at each receiver. Assuming perfect IA is achieved, the received signal in (2.31) becomes

$$\mathbf{y}_k = \mathbf{U}_k^{\mathrm{H}}\mathbf{H}_{kk}\mathbf{V}_k\mathbf{x}_k + \mathbf{U}_k^{\mathrm{H}}\mathbf{z}_k, \tag{2.36}$$

and, consequentially, the sum-rate is

$$R = \sum_{k=1}^{K} \log_2 \left| \mathbf{I}_d + \frac{1}{\sigma^2}\mathbf{U}_k^{\mathrm{H}}\mathbf{H}_{kk}\mathbf{V}_k\mathbf{S}_k\mathbf{V}_k^{\mathrm{H}}\mathbf{H}_{kk}^{\mathrm{H}}\mathbf{U}_k \right|. \tag{2.37}$$

2.6.1 Feasibility of MIMO IA Systems

The feasibility of linear MIMO IA systems was investigated in [18], where the solvability of the IA polynomial equation is analyzed based on algebraic geometry. The authors of [10] claimed

that for randomly generated channel matrices, that lack any special structure, the condition in (2.33) is almost surly satisfied if the condition in (2.32) is satisfied. Therefore, finding the feasibility of MIMO IA systems is mainly dependent on achieving the condition in (2.32) [18]. It is verified that IA is surely feasible if a system is proper [18, 54]. Based on Bezout's theorem, MIMO IA system is considered proper if the number of equations is not larger than the number of variables. The number of equations generated from (2.32) is $N_e = (K+1)d$ and the number of variables equals $N_v = M_T + M_R$. Therefore, the interference channel $(M_R \times M_T, d)^K$ is feasible if and only if [18]

$$M_T + M_R - (K+1)d \geq 0. \tag{2.38}$$

2.6.2 IA in K-user MIMO-OFDM Interference Channels

IA can be applied to K-user MIMO-OFDM interference channels independently on each subcarrier, thanks to the frequency orthogonality introduced by the multicarrier techniques. For a K-user MIMO-OFDM IA system with M_T transmit antennas, M_R receive antennas and *N* subcarriers, the transmitted d data streams over the n^{th} subcarrier $\mathbf{x}_k^n \in \mathbb{C}^{d\times 1}$ is multiplied by the precoding matrix $\mathbf{V}_k^n \in \mathbb{C}^{M_T\times d}$. Using this precoding over the n^{th} subcarrier, the desired data is aligned at its own receiver in the interference-free subspace, while the interference signals from the other transmitters are aligned at the interference subspace [10, 17]. By assuming perfect knowledge of the CSI at each node, the discrete-time complex received signal at the k^{th} receiver over the n^{th} subcarrier is represented as

$$\mathbf{y}_k^n = \mathbf{U}_k^{n\mathrm{H}}\mathbf{H}_k^n\mathbf{V}_k^n\mathbf{x}_k^n + \sum_{j=1,j\neq k}^{K} \mathbf{U}_k^{n\mathrm{H}}\mathbf{H}_{kj}^n\mathbf{V}_j^n\mathbf{x}_j^n + \mathbf{U}_k^{n\mathrm{H}}\mathbf{z}_k^n, \tag{2.39}$$

where $\mathbf{U}_k^n \in \mathbb{C}^{M_R\times d}$ is an orthonormal linear interference suppression matrix applied at the k^{th} receiver over the n^{th} subcarrier, $\mathbf{H}_{kj}^n \in \mathbb{C}^{M_R\times M_T}$ denotes the channel frequency response between the j^{th} transmitter and the k^{th} receiver over the n^{th} subcarrier, and $\mathbf{z}_k^n \in \mathbb{C}^{M_R\times 1}$ is the zero mean unit variance circularly symmetric AWGN vector at the k^{th} receiver over the n^{th} subcarrier.

In MIMO-OFDM IA systems, IA feasibility conditions in (2.32) and (2.33) should be independently achieved upon each subcarrier. That is [26]

$$\text{rank}\,(\mathbf{U}_k^{n\mathrm{H}}\mathbf{H}_{kk}^n\mathbf{V}_n^n) = d \qquad \forall k \quad \text{and} \quad \forall n, \tag{2.40}$$

and

$$\mathbf{U}_k^{n\mathrm{H}}\mathbf{H}_{kj}^n\mathbf{V}_j^n = 0 \qquad \forall j \neq k \quad \text{and} \quad \forall n. \tag{2.41}$$

Moreover, the sum-rate of MIMO-OFDM IA systems is calculated in terms of the achieved sum-rate in bits per second per hertz averaged over all subcarriers as follows

$$R = \frac{1}{N}\sum_{k=1}^{K}\sum_{n=1}^{N}\log_2\left|\mathbf{I}_d + \frac{\mathbf{U}_k^{n\mathrm{H}}\mathbf{H}_{kk}^n\mathbf{V}_k^n\mathbf{S}_k^n\mathbf{V}_k^{n\mathrm{H}}\mathbf{H}_{kk}^{n\ \mathrm{H}}\mathbf{U}_k^n}{\sigma^2\mathbf{I}_d + \mathbf{U}_k^{n\mathrm{H}}\mathbf{Q}_k^n\mathbf{U}_k^n}\right|, \tag{2.42}$$

where $\mathbf{Q}_k^n$ is the interference covariance matrix at the k^{th} receiver over the n^{th} subcarrier, which is

$$\mathbf{Q}_k^n = \sum_{j=1,j\neq k}^{K}\mathbf{H}_{kj}^n\mathbf{V}_j^n\mathbf{S}_k^n\mathbf{V}_j^{n\mathbf{H}}\mathbf{H}_{kj}^{n\ \mathbf{H}}. \tag{2.43}$$

$\mathbf{S}_k^n = \mathbb{E}\left[\mathbf{x}_k^n\mathbf{x}_k^{n\mathrm{H}}\right] \in \mathbb{R}^{d\times d}$ is the input covariance matrix of the k^{th} user over the n^{th} subcarrier, where the transmitted power by the k^{th} user over the n^{th} subcarrier is $P_k^n = \mathrm{Tr}\left(\mathbf{S}_k^n\right)$. If perfect IA is achieved upon all subcarriers, the received signal in (2.39) becomes

$$\mathbf{y}_k^n = \mathbf{U}_k^{n\mathrm{H}}\mathbf{H}_k^n\mathbf{V}_k^n\mathbf{x}_k^n + \mathbf{U}_k^{n\mathrm{H}}\mathbf{z}_k^n, \tag{2.44}$$

and, consequentially, the sum-rate is

$$R = \frac{1}{N}\sum_{k=1}^{K}\sum_{n=1}^{N}\log_2\left|\mathbf{I}_d + \frac{1}{\sigma^2}\mathbf{U}_k^{n\mathrm{H}}\mathbf{H}_{kk}^n\mathbf{V}_k^n\mathbf{S}_k^n\mathbf{V}_k^{n\mathrm{H}}\mathbf{H}_{kk}^{n\ \mathrm{H}}\mathbf{U}_k\right|. \tag{2.45}$$

Next, we overview the methods of designing MIMO IA precoders and decoders for feasible systems.

2.7 Interference Alignment Solutions

Designing IA solution, the precoding matrices and interference suppression matrices, is considered essential to achieve the promised performance of IA. Recently, closed-form and iterative methods have gained much of interest. In this section, we present an overview for closed-form and iterative methods.

2.7.1 Closed-Form Solution

Closed-form solution exists for limited scenarios of K-user MIMO interference channels as in [9, 10, 55]. In this section, a 3-user MIMO interference channel with $M_T = M_R = M$ is considered, where each user wishes to achieve $d = \frac{M}{2}$ DoF. For the simplicity, M is assumed to be even. The closed-form solution of such system can achieve $\frac{3M}{2}$ DoF without time extension as presented in [10]. According to (2.31), the received signal at the k^{th} receiver is

$$\mathbf{y}_k = \mathbf{U}_k^{\mathrm{H}}\mathbf{H}_{k1}\mathbf{V}_1\mathbf{x}_1 + \mathbf{U}_k^{\mathrm{H}}\mathbf{H}_{k2}\mathbf{V}_2\mathbf{x}_2 + \mathbf{U}_k^{\mathrm{H}}\mathbf{H}_{k3}\mathbf{V}_3\mathbf{x}_3 + \mathbf{U}_k^{\mathrm{H}}\mathbf{z}_k. \tag{2.46}$$

In order to decode the d transmitted data streams at each receiver without interference, interference signals from all unintended transmitters should be aligned into $M/2$ dimensional subspace leaving the other half free from interference. To this end, the following constraints should be considered while designing the precoders $\mathbf{V}_1$, $\mathbf{V}_2$ and $\mathbf{V}_3$

$$\begin{aligned} \text{span}(\mathbf{H}_{12}\mathbf{V}_2) &= \text{span}(\mathbf{H}_{13}\mathbf{V}_3) && (2.47)\\ \mathbf{H}_{21}\mathbf{V}_1 &= \mathbf{H}_{23}\mathbf{V}_3 && (2.48)\\ \mathbf{H}_{31}\mathbf{V}_1 &= \mathbf{H}_{32}\mathbf{V}_2, && (2.49) \end{aligned}$$

where span$(\mathbf{A})$ represents the space spanned by the column vectors of matrix $\mathbf{A}$. Since all the channel matrices, $\mathbf{H}_{kj}\ \forall k, j \in \{1, 2, 3\}$, are full-rank of M, thus the above equations can be reformulated as follows

$$\begin{aligned} \text{span}(\mathbf{V}_1) &= \text{span}(\mathbf{E}\mathbf{V}_1) && (2.50)\\ \mathbf{V}_2 &= (\mathbf{H}_{32})^{-1}\mathbf{H}_{31}\mathbf{V}_1 && (2.51)\\ \mathbf{V}_3 &= (\mathbf{H}_{23})^{-1}\mathbf{H}_{21}\mathbf{V}_1, && (2.52) \end{aligned}$$

where

$$\mathbf{E} = (\mathbf{H}_{31})^{-1}\mathbf{H}_{32}(\mathbf{H}_{12})^{-1}\mathbf{H}_{13}(\mathbf{H}_{23})^{-1}\mathbf{H}_{21}. \tag{2.53}$$

Consequently, one possible design of $\mathbf{V}_1$ can be as follows

$$\mathbf{V}_1 = [\mathbf{e}_1, \mathbf{e}_2, \cdots, \mathbf{e}_{M/2}], \tag{2.54}$$

where $\mathbf{e}_1, \mathbf{e}_2, \cdots, \mathbf{e}_M$ denote M eigenvectors of $\mathbf{E}$. $\mathbf{V}_2$ and $\mathbf{V}_3$ can be designed by substituting the value of $\mathbf{V}_1$ in (2.51 and 2.52), respectively. Accordingly, the suppression matrices at the receivers can be easily designed as follows

$$\mathbf{U}_1 = \text{null}([\mathbf{H}_{12}\mathbf{V}_2]^{\text{H}}) = \text{null}([\mathbf{H}_{13}\mathbf{V}_3]^{\text{H}}) \quad (2.55)$$

$$\mathbf{U}_2 = \text{null}([\mathbf{H}_{21}\mathbf{V}_1]^{\text{H}}) = \text{null}([\mathbf{H}_{23}\mathbf{V}_3]^{\text{H}}) \quad (2.56)$$

$$\mathbf{U}_3 = \text{null}([\mathbf{H}_{31}\mathbf{V}_1]^{\text{H}}) = \text{null}([\mathbf{H}_{32}\mathbf{V}_2]^{\text{H}}) \quad (2.57)$$

where null$(\mathbf{A})$ represents the null space of matrix $\mathbf{A}$. So far, the precoders $\mathbf{V}_1, \mathbf{V}_2$ and $\mathbf{V}_3$ are designed in a away that guarantees the dimension of interference subspace is $M/2$, which satisfies IA condition in (2.32). Then, in order to satisfy the second condition in (2.33) where the desired signal subspace and the interference subspace should be linearly independent, the following constraints should be satisfied

$$\text{rank}\left([\mathbf{H}_{11}\mathbf{V}_1 \;\; \mathbf{H}_{12}\mathbf{V}_2]\right) = M \quad (2.58)$$

$$\text{rank}\left([\mathbf{H}_{22}\mathbf{V}_2 \;\; \mathbf{H}_{21}\mathbf{V}_1]\right) = M \quad (2.59)$$

$$\text{rank}\left([\mathbf{H}_{33}\mathbf{V}_3 \;\; \mathbf{H}_{31}\mathbf{V}_1]\right) = M. \quad (2.60)$$

The authors of [10] have shown that the above constraints are satisfied with probability of 1 when the condition in (2.32) is achieved. This solution requires a global channel knowledge at all the nodes of the system.

2.7.2 Iterative Interference Alignment Solutions

Iterative IA has been suggested as an alternative to achieve IA solution in MIMO interference channels because closed-form solution is still not feasible in general [19, 54]. Unlike closed-form solutions, iterative IA approach requires only local channel knowledge, which is considered more practical to be realized. The concept of iterative IA is different from other iterative algorithms such as interference avoidance in [56] or iterative waterfilling in [57]. In iterative waterfilling/interference avoidance algorithms, each transmitter tries to do the best for his own receiver. Therefore, they follow a selfish approach. While in iterative IA, the nodes decide to cooperate and follow an unselfish approach in order to improve the total sum-rate of the system. As an example, each transmitter tries to minimize the interference he causes to other receivers.

The iterative approaches mainly depend on the channel reciprocity concept, where channel

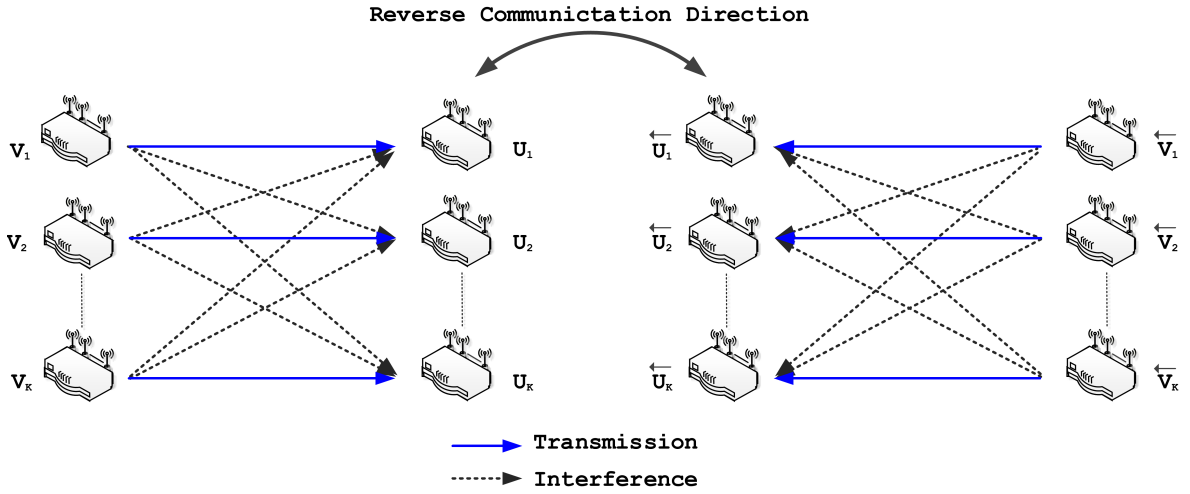

Figure 2.5: K-user MIMO interference channels with reciprocity.

conditions in one direction can be completely known from the other direction even there is a non-negligible difference in their transmission time. However, if the difference is small relative to the coherence time, the reciprocity can be a useful feature to utilize [58, 59]. The reciprocal network is simply obtained by diverting the role of transmitters and receivers as seen in Fig. 2.5. This can be described using the left arrow notation as

$$\overleftarrow{\mathbf{y}}_k = \overleftarrow{\mathbf{U}}_k^{\mathrm{H}} \overleftarrow{\mathbf{H}}_{kk} \overleftarrow{\mathbf{V}}_k \overleftarrow{\mathbf{x}}_k + \sum_{j=1, j\neq k}^{K} \overleftarrow{\mathbf{U}}_k^{\mathrm{H}} \overleftarrow{\mathbf{H}}_{kj} \overleftarrow{\mathbf{V}}_j \overleftarrow{\mathbf{x}}_j + \overleftarrow{\mathbf{U}}_k^{\mathrm{H}} \overleftarrow{\mathbf{z}}_k, \tag{2.61}$$

where $\overleftarrow{\mathbf{y}}_k$ is the reconstructed data at the k^{th} receiver in the reciprocal system, $\overleftarrow{\mathbf{U}}_k \in \mathbb{C}^{M_T \times d}$ is the orthonormal linear interference suppression matrix applied at the k^{th} receiver, and $\overleftarrow{\mathbf{H}}_{kj} = \mathbf{H}_{jk}^{\mathrm{H}}$ is the channel between the j^{th} transmitter and the k^{th} receiver in the reciprocal system. $\overleftarrow{\mathbf{V}}_j \in \mathbb{C}^{M_R \times d}$ is the orthonormal precoding matrix applied to the symbol vector $\overleftarrow{\mathbf{x}}_j \in \mathbb{C}^{d \times 1}$ that is transmitted from the j^{th} node, and $\overleftarrow{\mathbf{z}}_k \in \mathbb{C}^{M_T \times 1}$ is the zero mean unit variance circularly symmetric AWGN vector at the k^{th} receiver.

Minimum leakage interference (MLI), maximum signal-to-interference-plus-noise-ratio (Max-SINR), and maximum sum-rate (Max-SR) were proposed as iterative IA algorithms [19, 21]. These algorithms utilize wireless channels reciprocity to achieve IA with local channel knowledge at each node. Next, these algorithms are described in more details.

MLI Algorithm

MLI is a distributed IA algorithm that iteratively adjusts its precoders and decoders over the reciprocal network until convergence [19]. The objective of MLI algorithm is to minimize the total leakage interference experienced by all receivers. MLI algorithm can perfectly align the leakage interference if the IA problem is feasible. However, MLI algorithm achieves non-optimal sum-rate performance since it discards the power of the desired signal in the useful subspace. To design MLI precoders and decoders, each receiver computes its interference covariance matrix and identifies the interference at each receiver. Assuming equal power allocation among data streams where P is the transmitted power by each user, the interference covariance matrix is calculated at the k^{th} receiver as

$$\mathbf{Q}_k = \sum_{j=1, j\neq k}^{K} \frac{P}{d} \mathbf{H}_{kj} \mathbf{V}_j \mathbf{V}_j^{\mathrm{H}} \mathbf{H}_{kj}^{\mathrm{H}}, \tag{2.62}$$

where the total leakage interference at the k^{th} receiver is defined as

$$L_k = \mathrm{Tr}\left(\mathbf{U}_k^{\mathrm{H}} \mathbf{Q}_k \mathbf{U}_k\right). \tag{2.63}$$

Afterwards, the interference suppression matrix is corresponding to d eigenvectors of the least interference subspace as

$$\mathbf{U}_k = \nu_{min}^{d}\left(\mathbf{Q}_k\right) \qquad \forall k, \tag{2.64}$$

where $\nu_{min}^{d}\left(\mathbf{Q}_k\right)$ is the d columns that are corresponding to the d smallest eigenvalues of the interference matrix $\mathbf{Q}_k$. Accordingly, the total leakage interference of the K-user interference channel is reduced [19]. Afterwards, the previous steps are performed in the reciprocal network. Hence, by reversing the roles of the transmitters and the receivers, the precoding matrices $\overleftarrow{\mathbf{V}}_k$ in the the reciprocal network are the decoders of the direct channel $\mathbf{U}_k$. Therefore, $\overleftarrow{\mathbf{U}}_k$ can be computed as

$$\overleftarrow{\mathbf{U}}_k = \nu_{min}^{d}\left(\overleftarrow{\mathbf{Q}}_k\right) \qquad \forall k, \tag{2.65}$$

where $\overleftarrow{\mathbf{Q}}_k$ is

$$\overleftarrow{\mathbf{Q}}_k = \sum_{j=1, j\neq k}^{K} \frac{P}{d} \overleftarrow{\mathbf{H}}_{kj} \overleftarrow{\mathbf{V}}_j \overleftarrow{\mathbf{V}}_j^{\mathrm{H}} \overleftarrow{\mathbf{H}}_{kj}^{\mathrm{H}}. \tag{2.66}$$

The adjustment of the precoders and decoders over the reciprocal network is iteratively repeated until convergence. MLI method is detailed in Algorithm 2.1.

Algorithm 2.1 MLI Iterative Interference Alignment

1: Initialize precoders $\mathbf{V}_1, \mathbf{V}_2, ..., \mathbf{V}_K$ arbitrarily such that $\mathbf{V}_k^{\mathrm{H}}\mathbf{V}_k = \mathbf{I}_d \quad \forall k$.
2: For each receiver, compute $\mathbf{Q}_k$ according to (2.62);
3: Compute decoders $\mathbf{U}_k$ according to (2.64);
4: Exchange the roles of the precoders and decoders and set $\overleftarrow{\mathbf{V}}_k = \mathbf{U}_k$;
5: For each receiver, compute $\overleftarrow{\mathbf{Q}}_k$ in the reverse channel according to (2.66);
6: Compute decoders $\overleftarrow{\mathbf{U}}_k$ according to (2.65);
7: Reverse the communication link as $\mathbf{V}_k = \overleftarrow{\mathbf{U}}_k$;
8: Repeat the steps (2)-(7) until convergence.

Max-SINR Algorithm

The objective of Max-SINR algorithm is to maximize the SINR of each stream instead of minimizing the leakage interference. Therefore, the precoders and decoders are adjusted iteratively over the reciprocal network to maximize the SINR of each stream [19]. SINR of the i^{th} stream at the k^{th} receiver is defined as [19]

$$\mathrm{SINR}_{ki} = \frac{P}{d}\frac{\mathbf{U}_k(i)^{\mathrm{H}}\mathbf{H}_{kk}\mathbf{V}_k(i)\mathbf{V}_k(i)^{\mathrm{H}}\mathbf{H}_{kk}^{\mathrm{H}}\mathbf{U}_k(i)}{\mathbf{U}_k(i)^{\mathrm{H}}\mathbf{B}_{ki}\mathbf{U}_k(i)} \quad \forall i \text{ and } \forall k, \tag{2.67}$$

where $\mathbf{V}_k(i)$ and $\mathbf{U}_k(i)$ denote the i^{th} column of the precoding and decoding matrices of the k^{th} user, respectively. The matrix $\mathbf{B}_{ik}$ is the interference plus noise covariance matrix for the considered stream at the k^{th} receiver, which is defined as

$$\mathbf{B}_{ki} = \frac{P}{d}\sum_{j=1}^{K}\sum_{l=1}^{d}\mathbf{H}_{kj}\mathbf{V}_j(l)\mathbf{V}_j(l)^{\mathrm{H}}\mathbf{H}_{kj}^{\mathrm{H}} - \frac{P}{d}\mathbf{H}_{kk}\mathbf{V}_k(i)\mathbf{V}_k(i)^{\mathrm{H}}\mathbf{H}_{kk}^{\mathrm{H}} + \mathbf{I}_{M_R} \quad \forall i \text{ and } \forall k. \tag{2.68}$$

The column vectors of the receiving interference suppression matrix that maximizes the SINR of the i^{th} stream at the k^{th} receiver are given by

$$\mathbf{U}_k(i) = \frac{\mathbf{B}_{ki}^{-1}\mathbf{H}_{kk}\mathbf{V}_k(i)}{\left\|\mathbf{B}_{ki}^{-1}\mathbf{H}_{kk}\mathbf{V}_k(i)\right\|}. \tag{2.69}$$

These steps of adjustment of the precoders and decoders over the reciprocal network are iteratively repeated until convergence. This method is summarized in Algorithm 2.2.

Algorithm 2.2 Max-SINR Iterative Interference Alignment

1: Initialize precoders $\mathbf{V}_1, \mathbf{V}_2, ..., \mathbf{V}_K$ arbitrarily such that $\mathbf{V}_k^{\mathrm{H}}\mathbf{V}_k = \mathbf{I}_d \quad \forall k$.
2: For each receiver and each stream, compute $\mathbf{B}_{ki}$ according to (2.68);
3: Compute the i^{th} column of the k^{th} decoder $\mathbf{U}_k(i)$ according to (2.69);
4: Exchange the roles of the precoders and decoders and set $\overleftarrow{\mathbf{V}}_k = \overline{\mathbf{U}}_k$;
5: For each receiver and each stream, compute $\overleftarrow{\mathbf{B}}_{ki}$ in the reverse channel;
6: Compute the i^{th} column of the k^{th} decoder $\overleftarrow{\mathbf{U}}_k(i)$;
7: Reverse the communication link as $\mathbf{V}_k = \overleftarrow{\mathbf{U}}_k$;
8: Repeat the steps (2)-(7) until convergence.

Max-SR Algorithm

In Max-SR algorithm, a gradient descent approach combined with MLI is used in order to move the solution obtained at each step of MLI in the direction of increasing the sum-rate [21]. After finding $\mathbf{U}_k$ as in MLI algorithm, the gradient of the sum-rate with respect to $\mathbf{U}_k$ is calculated as [21]

$$\begin{aligned}\nabla_k R = &\sum_{j=1}^{K} \left(\mathbf{H}_{jk}\mathbf{C}_j^{-1}\mathbf{H}_{jk} - \mathrm{Tr}\left(\mathbf{V}_k^{\mathrm{H}}\mathbf{H}_{jk}\mathbf{C}_j^{-1}\mathbf{H}_{jk}\mathbf{V}_k\right)\right)\mathbf{V}_k \\ &+ \sum_{j\neq k}\left(\mathrm{Tr}\left(\mathbf{V}_k^{\mathrm{H}}\mathbf{H}_{jk}\overline{\mathbf{C}}_j^{-1}\mathbf{H}_{jk}\mathbf{V}_k\right) - \mathbf{H}_{jk}\overline{\mathbf{C}}_j^{-1}\mathbf{H}_{jk}\right)\mathbf{V}_k,\end{aligned} \tag{2.70}$$

where

$$\mathbf{C}_j = \sum_{l=1}^{K}\mathbf{Q}_{jl} + \sigma^2\mathbf{I}_{M_R}$$

and

$$\overline{\mathbf{C}_j} = \sum_{l\neq k}\mathbf{Q}_{jl} + \sigma^2\mathbf{I}_{M_R}.$$

Afterwards, the Grassmann tangent space $\nabla_k^{\hat{G}} R$ is obtained as

$$\nabla_k^{\hat{G}} R = \left(\mathbf{I}_{M_R} - \mathbf{U}_k\mathbf{U}_k^{\mathrm{H}}\right)\nabla_k R. \tag{2.71}$$

The solution is obtained at each step by moving the geodesic on the Grassmann manifold according to

$$\mathbf{U}_k = \left(\mathbf{U}_k\hat{\mathbf{F}}\left(\cos\Sigma t\right)\hat{\mathbf{F}}^{\mathrm{H}}\right) + \left(\hat{\mathbf{G}}\left(\sin\Sigma t\right)\hat{\mathbf{F}}^{\mathrm{H}}\right), \tag{2.72}$$

where $\nabla_k^{\hat{G}} \mathrm{R} = \hat{\mathbf{G}}\Sigma\hat{\mathbf{F}}^{\mathrm{H}}$ is the compact singular value decomposition of the $(M_R \times d)$ gradient matrix. This approach is summarized in Algorithm 2.3.

Algorithm 2.3 Max-SR Iterative Interference Alignment

1: Initialize precoders $\mathbf{V}_1, \mathbf{V}_2, ..., \mathbf{V}_K$ arbitrarily such that $\mathbf{V}_k^{\mathrm{H}}\mathbf{V}_k = \mathbf{I}_d \quad \forall k$.
2: For each receiver, compute $\mathbf{Q}_k$ according to (2.62);
3: Compute decoders $\mathbf{U}_k$ according to (2.64);
4: Compute the gradient of the sum-rate with respect to $\mathbf{U}_k$ as in (2.70);
5: Obtain the Grassmann tangent space $\nabla_k^{\hat{G}} \mathbf{R}$ as in (2.71);
6: Find the modified decoder $\mathbf{U}_k$ by moving the geodesic on the Grassmann manifold according to (2.72);
7: Exchange the roles of the precoders and decoders and set $\overleftarrow{\mathbf{V}}_k = \mathbf{U}_k$;
8: Perform the steps in (2)-(6) for the reverse link to find $\overleftarrow{\mathbf{U}}_k$;
9: Repeat the steps (2)-(7) until convergence.

3 ITERATIVE INTERFERENCE ALIGNMENT BASED ON MIN-MAXING STRATEGY

Chapter 3 presents a new iterative IA algorithm based on Min-Maxing strategy aiming at improving the sum-rate of K-user MIMO interference channels. We formulate Min-Maxing IA method by maximizing the power of the desired signal and, concurrently, minimizing the leakage interference. Min-Maxing method is handled by convex optimization after reformulating and relaxing the optimization problem into a standard semidefinite programming approximation. Moreover, a simplified version of the optimal Min-Maxing method is proposed for rank-deficient interference channels. The proposed scheme is evaluated by numerical simulation and compared to the previous iterative IA algorithms. This chapter encompasses research published in [60, 61].

3.1 Introduction

Iterative algorithmic approaches are proposed as an alternative to find IA solutions in K-user MIMO interference channels since closed-form solution for proper IA problems is still not feasible in general [19, 54]. Moreover, iterative IA approach requires only local channel knowledge, which is considered more practical to be realized. Recently, many iterative IA methods were proposed in the literature [19–21, 62, 63]. In [19], MLI and Max-SINR were proposed as iterative IA algorithms, where both are described in Section 2.7.2. MLI and Max-SINR utilize wireless channel reciprocity to achieve IA with local channel knowledge at each node. MLI and Max-SINR iteratively adjust their precoders and decoders over the reciprocal network until convergence. MLI algorithm can perfectly align the leakage interference if the IA problem is feasible. Nevertheless, MLI algorithm achieves non-optimal sum-rate performance since it discards the power of the desired signal in the useful subspace. On the other side, in spite of Max-SINR can often achieve the best sum-rate performance of all the proposed strategies in

most of the cases (not all cases), it loses some of its DoF at high SNRs and requires high implementation complexity due to the non-orthogonal precoders and decoders that are generated from this algorithm [62]. The authors of [21] proposed Max-SR iterative method in order to maximize the sum-rate of K-user interference channels by moving the precoders obtained at each step of MLI procedure along the direction given by the gradient of the sum-rate. However, this method converges very slowly as well as the optimal sum-rate and the convergence are not guaranteed [21]. Furthermore, two new approaches were proposed to modify the performance of Max-SINR algorithm, where the authors of [64] proposed a new convergent version of the Max-SINR algorithm and the authors of [65] presented two algorithms to jointly design sub-streams instead of independently as max-SINR did.

Moreover, several studies used convex optimization approach to propose iterative IA methods [22, 53, 66–69]. In [22], IA problem is reformulated into a relaxed convex of a rank constrained rank minimization (RCRM) problem, which improves the sum-rate performance when the system is proper and infeasible. IA solution is found in [66, 67] based on minimum mean square error (MMSE). Moreover, the authors of [53, 68] designed a linear transceiver based on optimizing transmit covariance matrices for all transmitters and MMSE for all receivers. In [69], maximization of the weighted sum-rate is addressed since it allows the system to cover all the rate tuples on the Pareto-optimal rate region boundary. However, robust sum-rate performance has not been achieved among the different K-user MIMO interference channels by all the previous approaches.

In this chapter, we propose a new iterative IA algorithm for K-user MIMO interference channels based on Min-Maxing strategy. Min-Maxing strategy tends to maximize the desired character (power of the desired signal) and minimize the undesired one (leakage interference) at the same time. Therefore, the proposed method maximizes the power of the desired signal and keeps the minimum leakage interference, where those factors are the main effective factors affecting the sum-rate performance of IA systems. We formulate Min-Maxing iterative IA as an optimization problem by maximizing the desired signal power while setting the minimum leakage interference obtained from MLI algorithm as a constraint. We approach such a non-convex problem by reformulating and relaxing the cost function and the constrains as a standard semidefinite programming problem. This formulation can attain the minimum aggregated interference from non-intended users and maximize the signal from the intended user concurrently. We address the convergent of Min-Maxing IA method in K-user MIMO interference channels. Furthermore, a simplified Min-Maxing algorithm is proposed for the MIMO

interference channels of rank-deficient channels with less complexity. Min-Maxing algorithm is extended to be applied for interference channels with diagonal structure as K-user multicarrier interference channels.

This chapter is organized as follows: Section 3.2 formulates and solves the new iterative IA algorithm. Section 3.3 presents the convergence proof of this method. Furthermore, the simplified min-maxing algorithm is presented in this Section 3.4. Sum-rate simulation results are illustrated and discussed for different interference channels in Section 3.5.

3.2 Min-Maxing Interference Alignment

In this section, we formulate IA problem based on Min-Maxing strategy in a distributed way in order to improve the sum-rate performance of K-user MIMO interference channels. We consider a $(M_R \times M_T, d)^K$ interference channel, which was discussed briefly in Section 2.6. Accordingly, the discrete-time complex received signal at the k^{th} receiver $\mathbf{y}_k \in \mathbb{C}^{M_R \times 1}$ is represented as

$$\mathbf{y}_k = \mathbf{U}_k^{\mathrm{H}} \mathbf{H}_{kk} \mathbf{V}_k \mathbf{x}_k + \sum_{j=1, j \neq k}^{K} \mathbf{U}_k^{\mathrm{H}} \mathbf{H}_{kj} \mathbf{V}_j \mathbf{x}_j + \mathbf{U}_k^{\mathrm{H}} \mathbf{z}_k, \tag{3.1}$$

Therefore, our aim is to design the matrices $\mathbf{V}_k$ and $\mathbf{U}_k$ for the K users in order to achieve the goal of IA and improve the sum-rate of MIMO IA systems.

Basically, Min-Maxing IA algorithm maximizes the intended signal power, while it keeps the minimum leakage interference at each receiver. In feasible IA systems, MLI technique can typically align the leakage interference. However, MLI sum-rate performance is not optimal since it does not consider the power of the desired signal in the interference-free subspace. Therefore, in the proposed algorithm, we utilize MLI algorithm to find the minimum interference leakage that can be achieved at the receiver side. This problem is formulated and solved in Section 3.2, and described in Section 3.2.2.

3.2.1 Problem Formulation

We formulate Min-Maxing problem by maximizing the power of the desired signal in the interference-free subspace at each receiver while we keep the minimum leakage interference obtained by MLI algorithm. The interference leakage is obtained at each receiver as in MLI

algorithm as follows

$$\mathbf{U}_k = \nu_{min}^d \left(\mathbf{Q}_k\right) \qquad \forall k, \tag{3.2}$$

where

$$\mathbf{Q}_k = \sum_{j=1, j\neq k}^{K} \frac{P}{d} \mathbf{H}_{kj} \mathbf{V}_j \mathbf{V}_j^{\mathbf{H}} \mathbf{H}_{kj}^{\mathbf{H}}. \tag{3.3}$$

Hence, the minimum leakage interference can be computed as

$$L_{\min}^k = \mathrm{Tr}\left(\mathbf{U}_k^{\mathrm{H}} \mathbf{Q}_k \mathbf{U}_k\right). \tag{3.4}$$

After that, we can formulate these multiple requirements at the k^{th} receiver in the following trace maximization problem

$$P1: \ \arg\max_{\bar{\mathbf{U}}_k} \mathrm{Tr}\left(\bar{\mathbf{U}}_k^{\mathrm{H}} \mathbf{H}_{kk} \mathbf{V}_k \mathbf{V}_k^{\mathrm{H}} \mathbf{H}_{kk}^{\mathrm{H}} \bar{\mathbf{U}}_k\right) \tag{3.5a}$$

$$\text{s.t.}: \ \mathrm{Tr}\left(\bar{\mathbf{U}}_k^{\mathrm{H}} \mathbf{Q}_k \bar{\mathbf{U}}_k\right) = L_{\min}^k \tag{3.5b}$$

$$\bar{\mathbf{U}}_k^{\mathrm{H}} \bar{\mathbf{U}}_k = \mathbf{I}_d \tag{3.5c}$$

$$\bar{\mathbf{U}}_k \in \mathbb{C}^{M_R \times d}, \tag{3.5d}$$

where $\overline{\mathbf{U}}_k$ is the re-designed $\mathbf{U}_k$ in order to achieve the optimization goal in Problem $P1$. This optimization problem is non-convex because the constraint (3.5c) is a non-convex rank constraint. Therefore, we aim to reformulate Problem $P1$ into a convex problem in the form of a semidefinite programming problem. Let

$$\mathbf{W}_k = \mathbf{H}_{kk} \mathbf{V}_k \mathbf{V}_k^{\mathrm{H}} \mathbf{H}_{kk}^{\mathrm{H}},$$

where $\mathbf{W}_k \in \mathbb{C}^{M_R \times M_R}$ is a positive semidefinite matrices $(\mathbf{W}_k \succeq 0)$. Problem $P1$ can be re-written as

$$P2: \ \arg\max_{\bar{\mathbf{U}}_k} \mathrm{Tr}\left(\bar{\mathbf{U}}_k^{\mathrm{H}} \mathbf{W}_{kk} \bar{\mathbf{U}}_k\right) \tag{3.6a}$$

$$\text{s.t.}: \ \mathrm{Tr}\left(\bar{\mathbf{U}}_k^{\mathrm{H}} \mathbf{Q}_k \bar{\mathbf{U}}_k\right) = L_{\min}^k \tag{3.6b}$$

$$\bar{\mathbf{U}}_k^{\mathrm{H}} \bar{\mathbf{U}}_k = \mathbf{I}_d \tag{3.6c}$$

$$\bar{\mathbf{U}}_k \in \mathbb{C}^{M_R \times d}. \tag{3.6d}$$

Then, we define

$$\mathbf{Z}_k = \bar{\mathbf{U}}_k \bar{\mathbf{U}}_k^{\mathrm{H}}, \qquad \mathbf{Z}_k \in \mathbb{C}^{M_R \times M_R}.$$

It was shown in [70] that the set of $\Psi_1 = \{\bar{\mathbf{U}}_k \bar{\mathbf{U}}_k^{\mathrm{H}} : \bar{\mathbf{U}}_k^{\mathrm{H}} \bar{\mathbf{U}}_k = \mathbf{I}_d\}$ is the set of extreme points of $\Psi_2 = \{\mathbf{Z}_k : \mathbf{Z}_k = \mathbf{Z}_k^{\mathrm{H}}, \mathrm{Tr}\,(\mathbf{Z}_k) = d, 0 \preceq \mathbf{Z} \preceq \mathbf{I}\}$. Let

$$\Psi_1 = \{\bar{\mathbf{U}}_k \bar{\mathbf{U}}_k^{\mathrm{H}} : \bar{\mathbf{U}}_k^{\mathrm{H}} \bar{\mathbf{U}}_k = \mathbf{I}_d\}$$

and

$$\Psi_2 = \{\mathbf{Z}_k : \mathbf{Z}_k = \mathbf{Z}_k^{\mathrm{H}}, \mathrm{Tr}\,(\mathbf{Z}_k) = d, 0 \preceq \mathbf{Z} \preceq \mathbf{I}\}.$$

$\mathbf{Z}_k$ has a dimension of M_R by M_R where $\bar{\mathbf{U}}_k \bar{\mathbf{U}}_k^{\mathrm{H}}$ is a projection matrix of order M_R and rank d. This means that $\mathbf{Z}_k$ and $\mathbf{I}_{M_R} - \mathbf{Z}_k$ are both positive semi-definite. Therefore, Ψ_2 is the convex hult of Ψ_1, and Ψ_1 is the set of extreme points of Ψ_2. The fact that any convex combination of elements of Ψ_1 lies in Ψ_2 is immediate. Furthermore, since the spectral decomposition of $\mathbf{Z}_k$ has eigenvalues lying between 0 and 1 and their sum is d, it is clear that any element of Ψ_2 with rank greater than d is not an extreme point. The only candidates for extreme points, then, are those with rank d, i.e. the elements of Ψ_1. But it is not possible that some rank d elements are extreme points and others not, since the definition of Ψ_2 does not in any way distinguishes between different rank d elements. Since a compact convex set must have extreme points and is the convex hull of its extreme points, the constraint Ψ_1 is stricter than Ψ_2. According to the fact that $\mathrm{Tr}\left(\bar{\mathbf{U}}_k^{\mathrm{H}} \mathbf{W}_{kk} \bar{\mathbf{U}}_k\right) = \mathrm{Tr}\left(\mathbf{W}_{kk} \bar{\mathbf{U}}_k \bar{\mathbf{U}}_k^{\mathrm{H}}\right)$, constraints (3.6c) and (3.6d) can be relaxed into $\mathrm{Tr}\,(\mathbf{Z}_k) = d \quad \text{and} \quad 0 \preceq \mathbf{Z}_k \preceq \mathbf{I}$, which are both convex. Therefore, maximizing the cost function over $\bar{\mathbf{U}}_k \bar{\mathbf{U}}_k^{\mathrm{H}} \in \Psi_1$ is equivalent to maximizing it over $\mathbf{Z}_k \in \Psi_2$. When the cost function is linear and subject to Ψ_2, the solution will be at one of the extreme points [71]. Consequently, for linear cost functions, the optimization problems subject to Ψ_1 and Ψ_2 are exactly equivalent. After including the above steps, problem $P2$ can be written as

$$P3: \ \arg\max_{\mathbf{Z}_k} \ \mathrm{Tr}\,(\mathbf{W}_k \mathbf{Z}_k) \tag{3.7a}$$

$$\text{s.t.}: \ \mathrm{Tr}\,(\mathbf{Q}_k \mathbf{Z}_k) \leq L_{\min}^k \tag{3.7b}$$

$$\mathrm{Tr}\,(\mathbf{Z}_k) = d \tag{3.7c}$$

$$0 \preceq \mathbf{Z}_k \preceq \mathbf{I}. \tag{3.7d}$$

The constrain (3.7d) can be written into a standard semidefinite programming form as

$$\begin{bmatrix} \mathbf{Z}_k & \mathbf{0} \\ \mathbf{0} & \mathbf{G} \end{bmatrix} \succeq 0 \tag{3.8a}$$

$$\mathbf{Z}_k + \mathbf{G} = \mathbf{I}, \tag{3.8b}$$

where $\mathbf{G}$ is a slack variable. Finally, the optimization problem has been formulated into a standard semidefinite programming form.

From the matrix $\mathbf{Z}_k$ obtained by the semidefinite programming, we can recover the output $\bar{\mathbf{U}}_k$ by eigen-decomposition, where $\bar{\mathbf{U}}_k$ is eigenvectors corresponding to the d largest eigenvalues of the $\mathbf{Z}_k$. It is clear that Min-Maxing algorithm generates orthogonal precoders and decoders.

3.2.2 Algorithm Description

Min-Maxing iterative algorithm alternates between the original and reciprocal networks in order to update its precoders and interference suppression decoders according to Problem $P3$. Algorithm 3.1 describes the procedures of the algorithm where the following steps are performed:

- *Step I:* In the original network, each receiver solves the following optimization problem

$$P4: \ \arg\max_{\mathbf{Z}_k} \ \mathrm{Tr}\left(\mathbf{W}_k \mathbf{Z}_k\right) \tag{3.9a}$$

$$\text{s.t.}: \ \mathrm{Tr}\left(\mathbf{Q}_k \mathbf{Z}_k\right) \leq L_{\min}^k \tag{3.9b}$$

$$\mathrm{Tr}\left(\mathbf{Z}_k\right) = d \tag{3.9c}$$

$$\begin{bmatrix} \mathbf{Z}_k & \mathbf{0} \\ \mathbf{0} & \mathbf{G} \end{bmatrix} \succeq 0 \tag{3.9d}$$

$$\mathbf{Z}_k + \mathbf{G} = \mathbf{I}, \tag{3.9e}$$

  After finding $\mathbf{Z}_k$, $\bar{\mathbf{U}}_k$ can be extracted from $\mathbf{Z}_k$ by eigen-decomposition as discussed in the last section.

- *Step II:* In the reciprocal channel, the roles of the transmitters and the receivers are ex-

changed. Therefore, $\overleftarrow{\mathbf{V}}_k = \bar{\mathbf{U}}_k$. $\overleftarrow{\mathbf{U}}_k$ is computed in the reciprocal network as

$$\overleftarrow{\mathbf{U}}_k = \nu_{min}^d \left(\overleftarrow{\mathbf{Q}}_k \right) \qquad \forall k, \tag{3.10}$$

where

$$\overleftarrow{\mathbf{Q}}_k = \sum_{j=1, j\neq k}^{K} \frac{P}{d} \mathbf{H}_{kj} \overleftarrow{\mathbf{V}}_j \overleftarrow{\mathbf{V}}_j^{\mathbf{H}} \mathbf{H}_{kj}^{\mathbf{H}}. \tag{3.11}$$

Hence, the minimum leakage that is observed from MLI is

$$\overleftarrow{L}_{\min}^k = \mathrm{Tr} \left(\overleftarrow{\mathbf{U}}_k^{\mathrm{H}} \overleftarrow{\mathbf{Q}}_k \overleftarrow{\mathbf{U}}_k \right). \tag{3.12}$$

By defining $\overleftarrow{\mathbf{W}}_k = \overleftarrow{\mathbf{H}}_{kk} \overleftarrow{\mathbf{V}}_k \overleftarrow{\mathbf{V}}_k^{\mathrm{H}} \overleftarrow{\mathbf{H}}_{kk}^{\mathrm{H}}$, each receiver in the reciprocal network solves the following optimization problem

$$P5: \ \arg\max_{\overleftarrow{\mathbf{Z}}_k} \mathrm{Tr} \left(\overleftarrow{\mathbf{W}}_k \overleftarrow{\mathbf{Z}}_k \right) \tag{3.13a}$$

$$\text{s.t.}: \ \mathrm{Tr} \left(\overleftarrow{\mathbf{Q}}_k \overleftarrow{\mathbf{Z}} \right) \leq \overleftarrow{L}_{\min}^k \tag{3.13b}$$

$$\mathrm{Tr} \left(\overleftarrow{\mathbf{Z}} \right) = d \tag{3.13c}$$

$$\begin{bmatrix} \overleftarrow{\mathbf{Z}} & \mathbf{0} \\ \mathbf{0} & \mathbf{G} \end{bmatrix} \succeq 0 \tag{3.13d}$$

$$\overleftarrow{\mathbf{Z}} + \mathbf{G} = \mathbf{I}, \tag{3.13e}$$

After finding $\overleftarrow{\mathbf{Z}}$, $\overleftarrow{\mathbf{U}}_k$ can be extracted from $\overleftarrow{\mathbf{Z}}$ by eigen-decomposition.

Step I and II are repeated in this manner until the algorithm converges.

3.3 Convergence of Min-Maxing Algorithm

In the following, we prove that the convergence of Min-Maxing algorithm is guaranteed. It was proven in [19] that computing $\mathbf{U}_k$ according to step 3 and 8 in algorithm 3.1 minimizes the leakage interference at each iteration. Therefore, it is stated for the given $\mathbf{V}_k$ of the user k at iteration $t+1$ that

$$L_k(\mathbf{U}_k(t+1), \mathbf{V}_k(t)) \leq L_k(\mathbf{U}_k(t), \mathbf{V}_k(t)).$$

Algorithm 3.1 Min-Maxing Iterative Interference Alignment

1: Initialize precoders $\mathbf{V}_1, \mathbf{V}_2, ..., \mathbf{V}_K$ arbitrarily such that $\mathbf{V}_k^{\mathrm{H}}\mathbf{V}_k = \mathbf{I}_d \quad \forall k$.
2: For each receiver, compute $\mathbf{Q}_k$ according to (3.3);
3: Compute decoders $\mathbf{U}_k$ according to (3.2);
4: Calculate L_{min}^k according to (3.4);
5: Optimize $\overline{\mathbf{U}}_k$ according to (3.9);
6: Exchange the roles of the precoders and decoders and set $\overleftarrow{\mathbf{V}}_k = \overline{\mathbf{U}}_k$;
7: For each receiver, compute $\overleftarrow{\mathbf{Q}}_k$ according to (3.11);
8: Compute decoders $\overleftarrow{\mathbf{U}}_k$ according to (3.10);
9: Calculate $\overleftarrow{L}_{min}^k$;
10: Optimize $\overleftarrow{\mathbf{U}}_k$ according to (3.13);
11: Repeat the steps (2)-(10) until convergence.

Then, $\mathbf{U}_k$ is re-designed to $\overline{\mathbf{U}}_k$ in order to maximize the power of the desired signal while keeping the minimum leakage interference. Therefore

$$L_k(\overline{\mathbf{U}}_k(t+1), \mathbf{V}_k(t)) \leq L_k(\mathbf{U}_k(t), \mathbf{V}_k(t)).$$

Likewise in the reciprocal channel, for the given $\overline{\mathbf{U}}_k(t+1)$, $\mathbf{V}_k(t+1)$ is computed to minimize the leakage interference. Then

$$\overleftarrow{L}_k(\overline{\mathbf{U}}_k(t+1), \mathbf{V}_k(t+1)) \leq \overleftarrow{L}_k(\overline{\mathbf{U}}_k(t+1), \mathbf{V}_k(t)).$$

After that, $\mathbf{V}_k(t+1)$ is re-designed to $\overline{\mathbf{V}}_k(t+1)$ in order to maximize the power of the desired signal while keeping the minimum leakage interference. Therefore

$$\overleftarrow{L}_k(\overline{\mathbf{U}}_k(t+1), \overline{\mathbf{V}}_k(t+1)) \leq \overleftarrow{L}_k(\overline{\mathbf{U}}_k(t+1), \mathbf{V}_k(t)).$$

Since the total leakage interference is lower bounded by zero and because the total leakage interference is minimized by each update for the decoders and precoders of the system at each iteration, Min-Maxing algorithm is convergent.

3.4 Simplified Min-Maxing Interference Alignment

For rank-deficient channels, we propose a simplified algorithm to solve the optimization problem $P1$ with less computational complexity. This simplified method is sufficient when M_R and M_T are not symmetric, and d is smaller than the dimensionality of null($\mathbf{Q}_k$), i.e $c = \dim(\text{null}(\mathbf{Q}_k))$. For this case, a simpler solution for problem $P1$ can be found.

By parameterizing $\bar{\mathbf{U}}_k$ to be as follows

$$\bar{\mathbf{U}}_k = \mathbf{A}_k \mathbf{T}_k, \tag{3.14}$$

where $\mathbf{A}_k = \nu^c_{min}(\mathbf{Q}_k)$, $\mathbf{A}_k^{\mathrm{H}}\mathbf{A}_k = \mathbf{I}_c$, and $\mathbf{T}_k \in \mathbb{C}^{c\times d}$ is an orthonormal matrix such that $\mathbf{T}_k^{\mathrm{H}}\mathbf{T}_k = \mathbf{I}_d$, Problem $P2$ can be written as

$$P6: \ \arg\max_{\bar{\mathbf{U}}_k} \mathrm{Tr}\left(\bar{\mathbf{U}}_k^{\mathrm{H}}\mathbf{W}_{kk}\bar{\mathbf{U}}_k\right) \tag{3.15a}$$

$$\text{s.t.}: \ \bar{\mathbf{U}}_k = \mathbf{A}_k\mathbf{T}_k \tag{3.15b}$$

$$\mathbf{T}_k^{\mathrm{H}}\mathbf{T}_k = \mathbf{I}_d \tag{3.15c}$$

$$\mathbf{T}_k \in \mathbb{C}^{c\times d}. \tag{3.15d}$$

Problem $P6$ can be re-written by moving the constraint (3.15b) into the cost function (3.15a) to be as

$$P7: \ \arg\max_{\mathbf{T}_k} \mathrm{Tr}\left(\mathbf{T}_k^{\mathrm{H}}\mathbf{A}_k^{\mathrm{H}}\mathbf{W}_{kk}\mathbf{A}_k\mathbf{T}_k\right) \tag{3.16a}$$

$$\text{s.t.}: \ \mathbf{T}_k^{\mathrm{H}}\mathbf{T}_k = \mathbf{I}_d \tag{3.16b}$$

$$\mathbf{T}_k \in \mathbb{C}^{c\times d}. \tag{3.16c}$$

Problem $P7$ can be solved as $\mathbf{T}_k = \nu^c_{max}\left(\mathbf{A}_k^{\mathrm{H}}\mathbf{W}_{kk}\mathbf{A}_k\right)$ [72].

In reciprocal network, the roles of the transmitters and the receivers are exchanged. $\overleftarrow{\bar{\mathbf{U}}}_k$ is defined as

$$\overleftarrow{\bar{\mathbf{U}}}_k = \overleftarrow{\mathbf{A}}_k \overleftarrow{\mathbf{T}}_k. \tag{3.17}$$

Therefore, Problem $P7$ is formulated as

$$P8: \ \underset{\overleftarrow{\mathbf{T}}_k}{\arg\max}\ \mathrm{Tr}\left(\overleftarrow{\mathbf{T}}_k^{\mathrm{H}}\overleftarrow{\mathbf{A}}_k^{\mathrm{H}}\overleftarrow{\mathbf{W}}_{kk}\overleftarrow{\mathbf{A}}_k\overleftarrow{\mathbf{T}}_k\right) \tag{3.18a}$$

$$\text{s.t.}: \ \overleftarrow{\mathbf{T}}_k^{\mathrm{H}}\overleftarrow{\mathbf{T}}_k = \mathbf{I}_d \tag{3.18b}$$

$$\overleftarrow{\mathbf{T}}_k \in \mathbb{C}^{c\times d}, \tag{3.18c}$$

where $\overleftarrow{\mathbf{A}}_k = \nu_{min}^{\overleftarrow{c}}\left(\overleftarrow{\mathbf{Q}}_k\right)$, $\overleftarrow{\mathbf{A}}_k^{\mathrm{H}}\overleftarrow{\mathbf{A}}_k = \mathbf{I}_{\overleftarrow{c}}$, and $\overleftarrow{c} = \dim\left(\mathrm{null}(\overleftarrow{\mathbf{Q}}_k)\right)$. Hence, $\overleftarrow{\mathbf{T}}_k$ is found as $\nu_{max}^{\overleftarrow{c}}\left(\overleftarrow{\mathbf{A}}_k^{\mathrm{H}}\overleftarrow{\mathbf{W}}_{kk}\overleftarrow{\mathbf{A}}_k\right)$. The simplified algorithm is executed through the following

- *Step I:* In the original network, each receiver finds $\mathbf{T}_k$ to be $\nu_{max}^{c}\left(\mathbf{A}_k^{\mathrm{H}}\mathbf{W}_{kk}\mathbf{A}_k\right)$. Then $\bar{\mathbf{U}}_k$ can be extracted according to (3.14).
- *Step II:* In the reciprocal network, each receiver finds $\overleftarrow{\mathbf{T}}_k$ to be $\nu_{max}^{\overleftarrow{c}}\left(\overleftarrow{\mathbf{A}}_k^{\mathrm{H}}\overleftarrow{\mathbf{W}}_{kk}\overleftarrow{\mathbf{A}}_k\right)$. Then $\overleftarrow{\bar{\mathbf{U}}}_k$ can be extracted according to (3.17).

Step I and II are repeated in this manner until the algorithm converges. This algorithm is detailed in Algorithm 3.2.

3.5 Simulation Results

In this section, we evaluate the performance of the proposed IA algorithm in comparison with Max-SINR, MLI and Max-SR iterative IA techniques by means of numerical simulations in K-user MIMO and multicarrier interference channels. Specifically, we choose Max-SINR technique since it has the best sum-rate of all previous techniques in most cases [62]. Besides, MLI technique in some cases outperforms Max-SINR, and Max-SR offers better performance compared to MLI and Max-SINR in other cases. Since Max-SR requires a large number of iterations to converge, we consider different numbers of iterations in our simulation. The simulation has been performed for 1000 channel realizations where each channel element is drawn from independent and identically distributed real Gaussian distribution with zero mean and unit variance. CVX toolbox was used in the simulation [73].

3.5.1 Results of K-user MIMO Interference Channels

In this part of simulations, three regimes are considered:

Algorithm 3.2 Simplified Min-Maxing Interference Alignment

1: Initialize precoders $\mathbf{V}_1, \mathbf{V}_2, ..., \mathbf{V}_K$ arbitrarily such that $\mathbf{V}_k^{\mathrm{H}}\mathbf{V}_k = \mathbf{I}_d \quad \forall k$.
2: For each receiver, compute $\mathbf{Q}_k$ according to (3.3);
3: **if** $c \geq d$ **then**
4: Find $\mathbf{A}_k = \nu_{min}^{c}\left(\mathbf{Q}_k\right)$;
5: Find $\mathbf{T}_k = \nu_{max}^{c}\left(\mathbf{A}_k^{\mathrm{H}}\mathbf{W}_{kk}\mathbf{A}_k\right)$;
6: Optimize $\overline{\mathbf{U}}_k = \mathbf{A}_k\mathbf{T}_k$;
7: **else if**
8: $\overline{\mathbf{U}}_k = \nu_{min}^{d}\left(\mathbf{Q}_k\right)$;
9: **end if**
10: Exchange the roles of the precoders and decoders and set $\overleftarrow{\mathbf{V}}_k = \overline{\mathbf{U}}_k$;
11: For each receiver, compute $\overleftarrow{\mathbf{Q}}_k$ according to (3.11);
12: **if** $\overleftarrow{c} \geq d$ **then**
13: Find $\overleftarrow{\mathbf{A}}_k = \nu_{min}^{\overleftarrow{c}}\left(\overleftarrow{\mathbf{Q}}_k\right)$;
14: Find $\overleftarrow{\mathbf{T}}_k = \nu_{max}^{\overleftarrow{c}}\left(\overleftarrow{\mathbf{A}}_k^{\mathrm{H}}\overleftarrow{\mathbf{W}}_{kk}\overleftarrow{\mathbf{A}}_k\right)$;
15: Optimize $\overleftarrow{\overline{\mathbf{U}}}_k = \overleftarrow{\mathbf{A}}_k\overleftarrow{\mathbf{T}}_k$;
16: **else if**
17: $\overleftarrow{\overline{\mathbf{U}}}_k = \nu_{min}^{d}\left(\overleftarrow{\mathbf{Q}}_k\right)$;
18: **end if**
19: Repeat the steps (2)-(18) until convergence.

1. $d < \frac{M_T+M_R}{K+1}$, where the unknowns are more than the equations in the IA conditions as: $(4\times 8, d=1,2)^3$, $(5\times 2, 1)^3$ and $(8\times 8, 2)^{K=4,5}$ interference channels.

2. $d = \frac{M_T+M_R}{K+1}$, where it is marginal proper as: $(6\times 6, 3)^3$ and $(5\times 3, 2)^3$ interference channels.

3. $d > \frac{M_T+M_R}{K+1}$ improper systems as $(5\times 2, 2)^3$ interference channel.

Firstly, we present the sum-rate performance of iterative IA methods under $d < \frac{M_T+M_R}{K+1}$ regime. Fig. 3.1 shows the sum-rate performance of the different iterative IA approaches for $(4\times 8, 2)^3$ interference channel. It is notable that Min-Maxing, MLI and Max-SINR mostly converge after 100 iterations, while Max-SR presents a significant poor sum-rate at this iteration number. It is noted in this figure that Max-SINR loses some of its DoF at high SNRs because it optimizes SINR stream-by-stream without considering orthogonal precoder constraint [21], [22].

Moreover, MLI performance is worse than Max-SINR even if it gives the minimum interference leakage. However, Min-Maxing offers the best sum-rate performance at high SNRs in this case. Furthermore, the simplified Min-Maxing is presented in this figure with 100 iterations, which gives very close performance to the optimal Min-Maxing method since the channel is rank-deficient and, hence, the optimal solution can be found using Algorithm 3.2. Sum-rate performance of Max-SR is going to be better when the number of iterations is increased to 1000, but it is still worse than all other approaches. Although, Max-SR converges after 3000 iterations, and it gives better sum-rate performance than MLI and Max-SINR at high SNRs, Min-Maxing performance with 100 iterations introduces the best sum-rate, and it is slightly better at 3000 iterations. As a result of that, Min-Maxing, MLI and Max-SINR need significant fewer number of iterations than Max-SR to achieve acceptable sum-rate performance in this regime. Additionally, Min-Maxing achieves the best sum-rate with 100 iterations compared to all simulated methods at high SNRs. Therefore, we proceed the comparison in this regime using MLI and Max-SINR with 100 iterations.

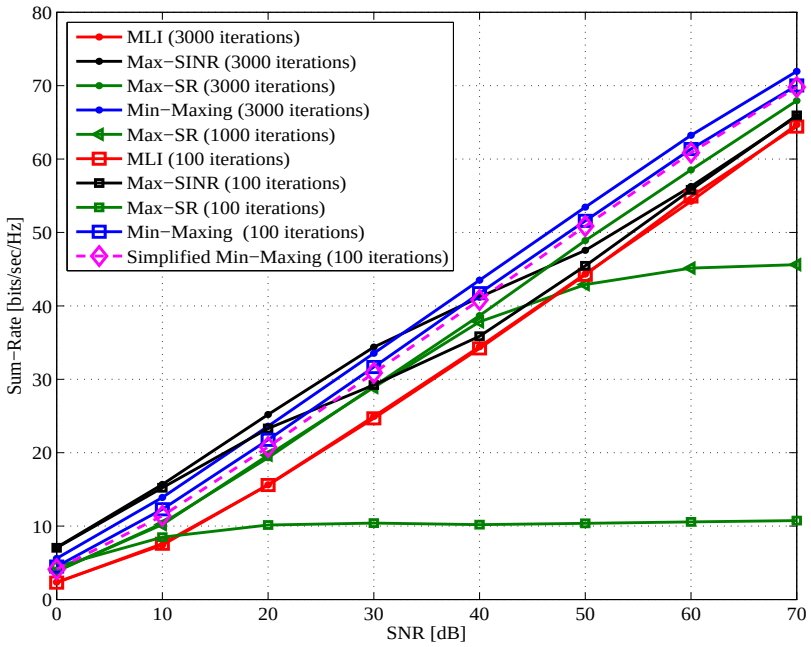

Figure 3.1: MIMO IC: Sum-rate performance comparison for $(4 \times 8, 2)^3$ system.

Fig. 3.2 presents the convergence behavior of the considered IA methods for $(4 \times 8, 2)^3$ interference channel when SNR=50 dB. Min-Maxing algorithm converges fast as MLI method to the best sum-rate value. While Max-SINR presents the fastest convergence, but the sum-rate convergence value is lower than Min-Maxing method. Whereas Max-SR method converges very slowly compared to the other methods.

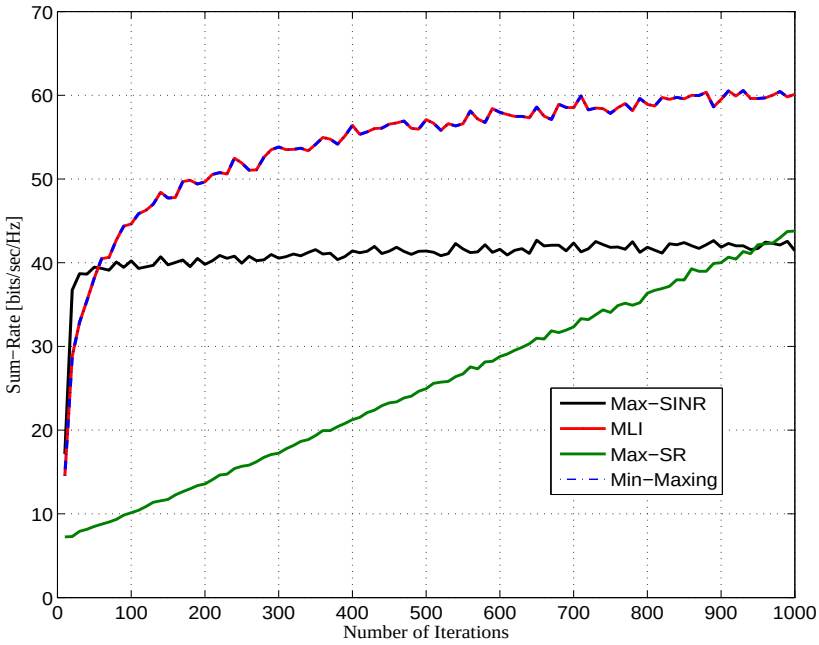

Figure 3.2: MIMO IC: Convergence behaviour comparison for $(4 \times 8, 2)^3$ system at 50 dBm.

Fig. 3.3 compares the performance of the $(4\times8, 2)^3$ interference channel with the $(4\times8, 1)^3$ interference channel. As expected, with $d = 2$, the sum-rate is improved for all IA methods since more data streams are sent. Max-SINR and Min-Maxing algorithm behaviors are identical, and better than MLI algorithm.

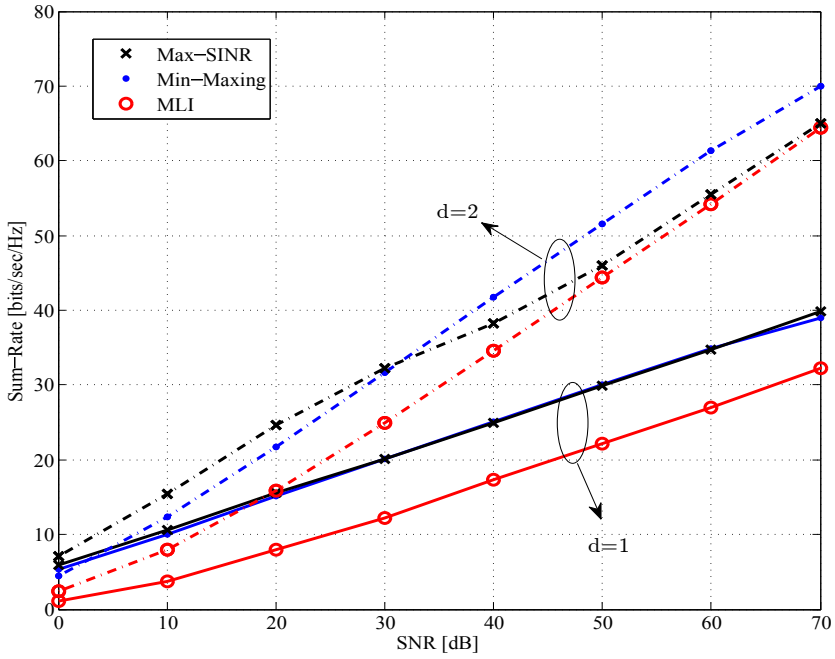

Figure 3.3: MIMO IC: Sum-rate performance comparison for $(4 \times 8, d = 1, 2)^3$ system.

Fig. 3.4 shows the sum-rate performance of $(5 \times 2, 1)^3$ interference channel, where Max-SINR can achieve the optimal DoF because it optimizes the SINR only for one data stream. In this case, Min-Maxing algorithm achieves the optimal sum-rate as max-SINR at high SNRs while it exhibits a small loss sum-rate compared to Max-SINR algorithm at low SNRs. Furthermore, both are better than MLI for all SNRs, where MLI can achieve the minimum leakage interference. As the case in the previous interference channel, the simplified Min-Maxing method approaches the optimal Min-Maxing sum-rate with the same number of iterations.

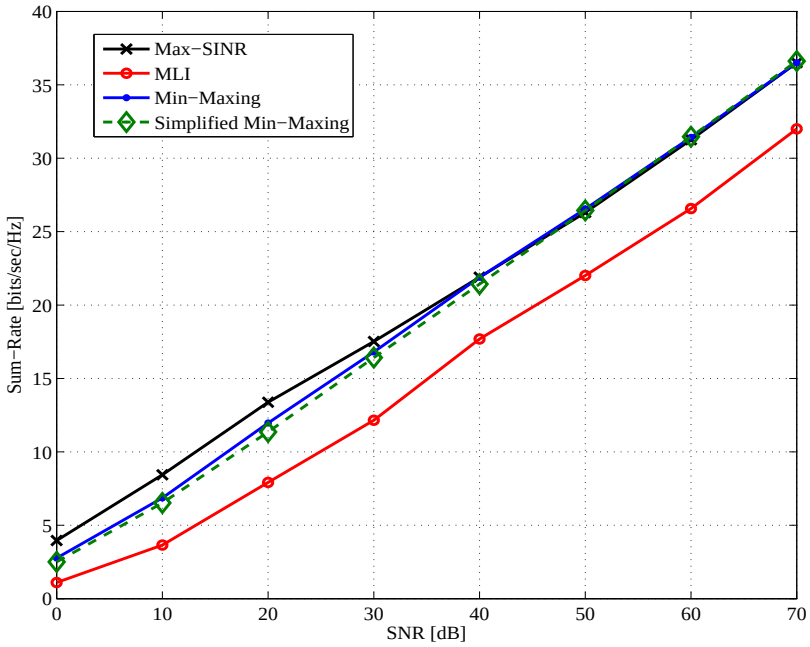

Figure 3.4: MIMO IC: Sum-rate performance comparison for $(5 \times 2, 1)^3$ system.

In Fig. 3.5 and Fig. 3.6, we compare Min-Maxing algorithm to MLI and Max-SINR using $(8 \times 8, 2)^4$ and $(8 \times 8, 2)^5$ interference channels, respectively. For both systems, Max-SINR technique outperforms both our proposed algorithm and MLI algorithm in terms of achievable throughput at low SNRs, while our algorithm achieves the best performance compared to all other techniques at high SNRs. In those interference channels, as seen in Fig. 3.5 and Fig. 3.6, the simplified Min-Maxing method fails to approach the optimal method since the channel is full-rank and Algorithm 3.2 is not efficient in this case.

We conclude for $d < \frac{M_T+M_R}{K+1}$ regime that although the systems in this regime have more DoF to reach the optimal sum-rate, Max-SINR and MLI fail to achieve that. Whereas Min-Maxing achieves the optimal sum-rate among these types of systems at high SNRs.

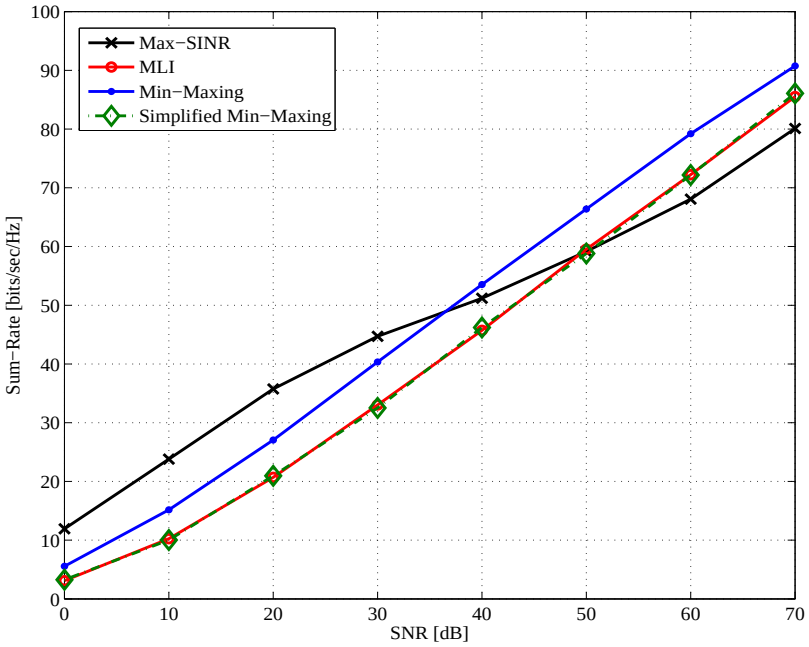

Figure 3.5: MIMO IC: Sum-rate performance comparison for $(8 \times 8, 2)^4$ system.

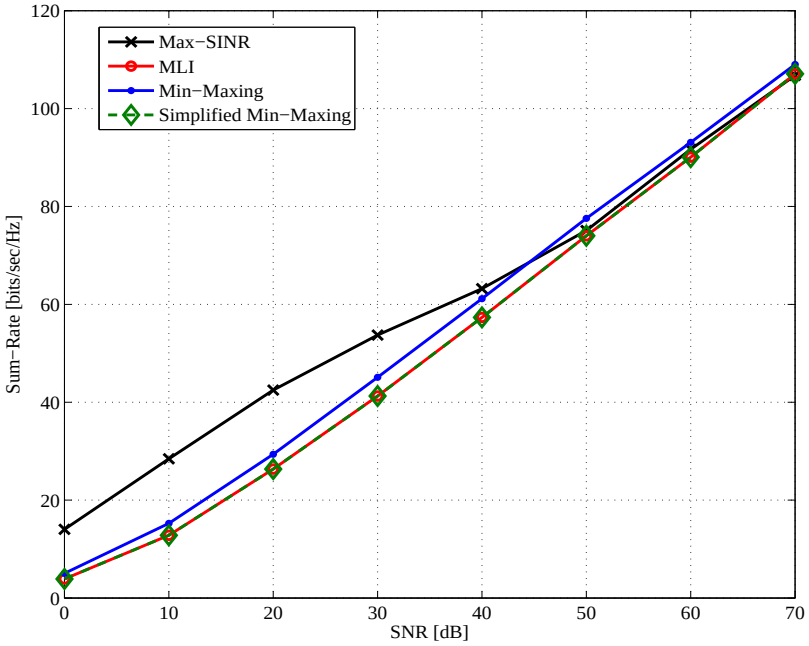

Figure 3.6: MIMO IC: Sum-rate performance comparison for $(8 \times 8, 2)^5$ system.

Next, we present the performance of Min-Maxing IA for marginal proper systems. Fig. 3.7 exhibits the sum-rate performance of the different iterative IA approaches for $(6 \times 6, 3)^3$ interference channel. In this regime, Min-Maxing, MLI and Max-SINR demand 500 iterations to present acceptable sum-rate performances, while Max-SR fails to achieve that. As the number of iterations increases, all the sum-rate performances are enhanced. At 3000 iterations, Min-

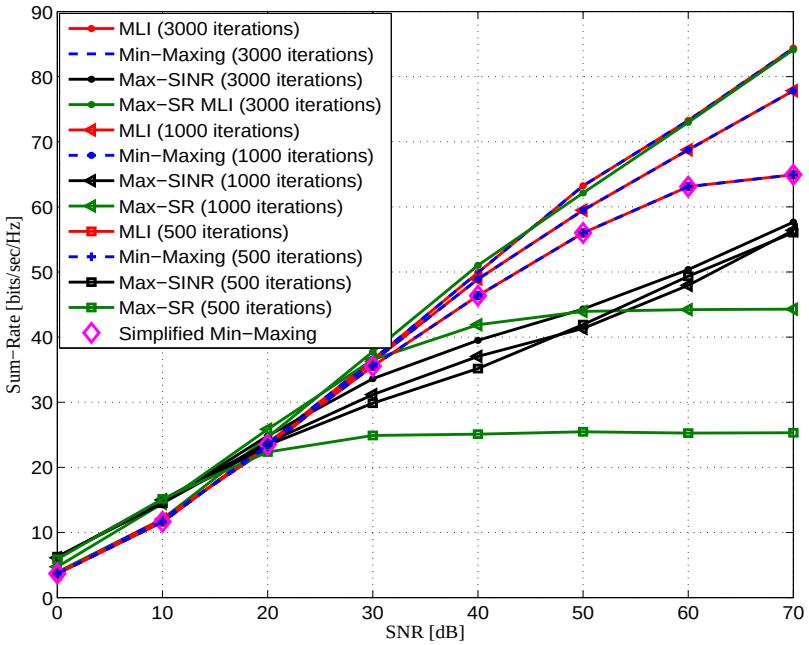

Figure 3.7: MIMO IC: Sum-rate performance comparison for $(6 \times 6, 3)^3$ system.

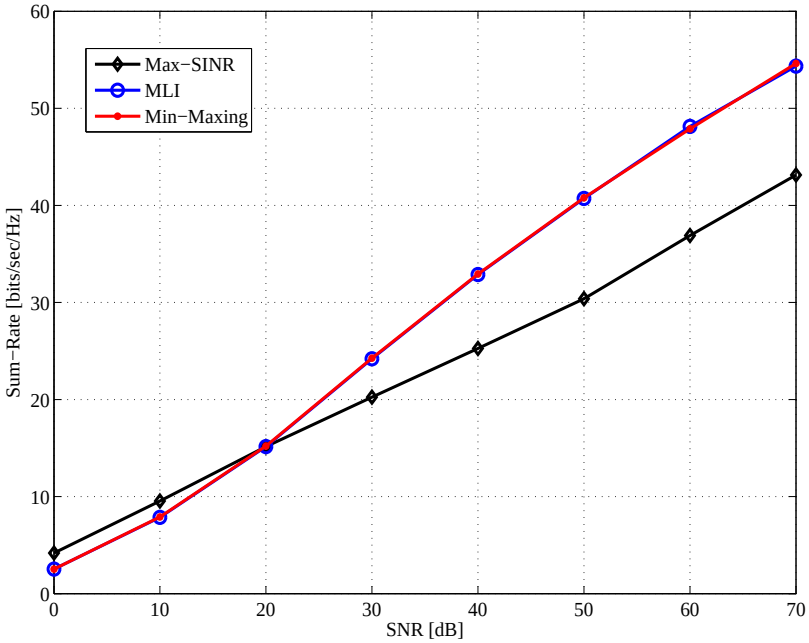

Figure 3.8: MIMO IC: Sum-rate performance comparison for $(5 \times 3, 2)^3$ system.

Maxing, Max-SR and MLI converge to the identical solution since the IA problem is tightly proper in this regime. It is noted also that Min-Maxing gives always the same performance as MLI regardless of the number of iterations. We further proceed our comparison in this regime with only 500 iterations using MLI and Max-SINR approaches, where Fig. 3.8 exhibits the sum-rate performance of $(5 \times 3, 2)^3$ interference channel. The behavior in this system is the

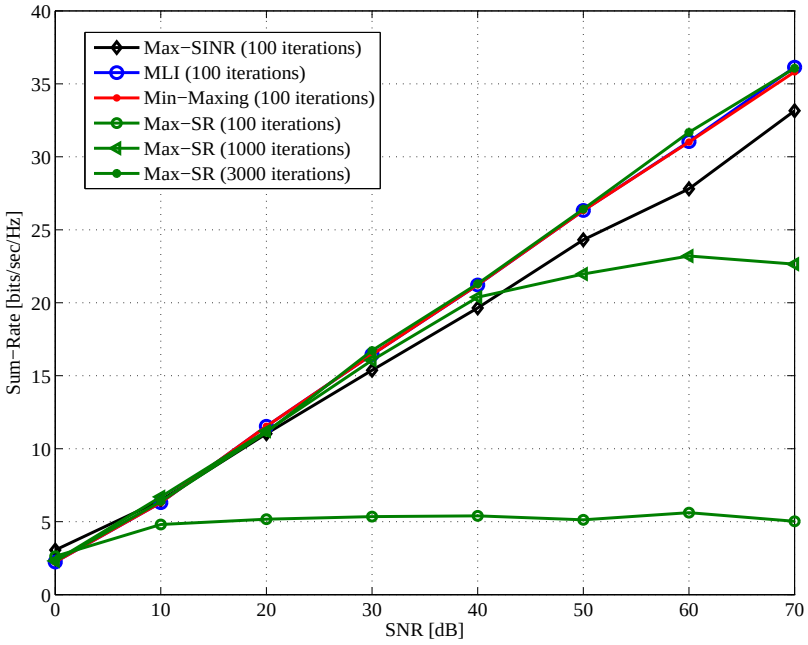

Figure 3.9: MIMO IC: Sum-rate performance comparison for $(5 \times 2, 2)^3$ system.

same as $(6 \times 6, 3)^3$ interference channel, where Max-SINR technique gives small improvement compared to both our proposed algorithm and MLI approach with respect to the achievable sum-rate at low SNRs, while our proposed algorithm exactly matches the sum-rate performance of MLI, and both schemes are much better than Max-SINR technique at high SNRs. For marginal proper systems, the simplified Min-Maxing algorithm presents the same performance as the optimal Min-Maxing and MLI algorithms since there is only one solution is existed in this case, which can be seen in Fig. 3.7.

In a case of improper systems, we show the sum-rate behavior of Min-Maxing algorithm in such systems using $(5 \times 2, 2)^3$ interference channel as seen in Fig. 3.9. In this regime, the unknowns are less than the equations for the IA conditions; therefore, the performance of Min-Maxing algorithm matches MLI algorithm, and both achieve sum-rate performance better than Max-SINR method. It is noted that Min-Maxing, MLI and Max-SINR reach the convergence point after 100 iterations, while Max-SR requires 3000 iterations to converge, which is the same as the previous systems. The simplified Min-Maxing approach gives the same solution as MLI and optimal Min-Maxing approaches.

It is concluded from the simulation above that Min-Maxing method is the only method can guarantee the best sum-rate performance among all the simulated interference channels at high SNR values, while MLI, Max-SINR and Max-SR are incapable of achieving a robust sum-rate

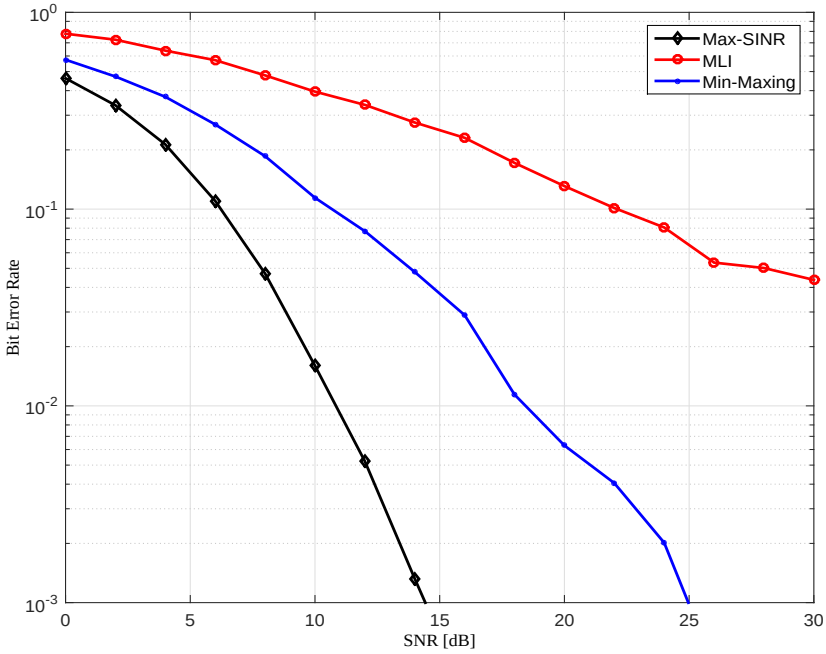

Figure 3.10: Bit error-rate performance comparison for $(4 \times 8, 2)^3$ system.

performance at high SNRs for the different regimes.

In Fig. 3.10, we simulate the error-rate performance for the iterative IA methods. As expected, Max-SINR presents the best error-rate since SINR has the direct effect on the error rate as seen in Fig.3.10. However, we note that Min-Maxing method improves the error-rate compared to MLI method, which is an extra advantage achieved by Min-maxing method compared to MLI.

3.5.2 Results of K-user Multicarrier Interference Channels

We extend the evaluation of Min-Maxing IA in a K-user multicarrier interference channel (MC IC) that is presented in Section 2.5.2. We consider $K = 3$ users multicarrier interference channel, where each user transmits $d = 3$ streams using $L = 7$ and 8 bands. For the first interference channel with $L = 7$, 3 data streams are sent by each user. Therefore, 9 data streams are transmitted over the 7 bands. Fig. 3.11 shows the sum-rate performance of the multicarrier interference channel with $L = 7$. At high SNRs, Min-Maxing method outperforms other methods in terms of sum-rate by more than 2 bits/s/Hz. Furthermore, Fig. 3.12 shows the sum-rate performance of $L = 8$ interference channel for the different IA techniques, where each user sends 3 data streams. In this system, Min-Maxing method also exhibits the best sum-rate performance at high SNRs. We conclude for diagonal channels that the conditions (2.32) and

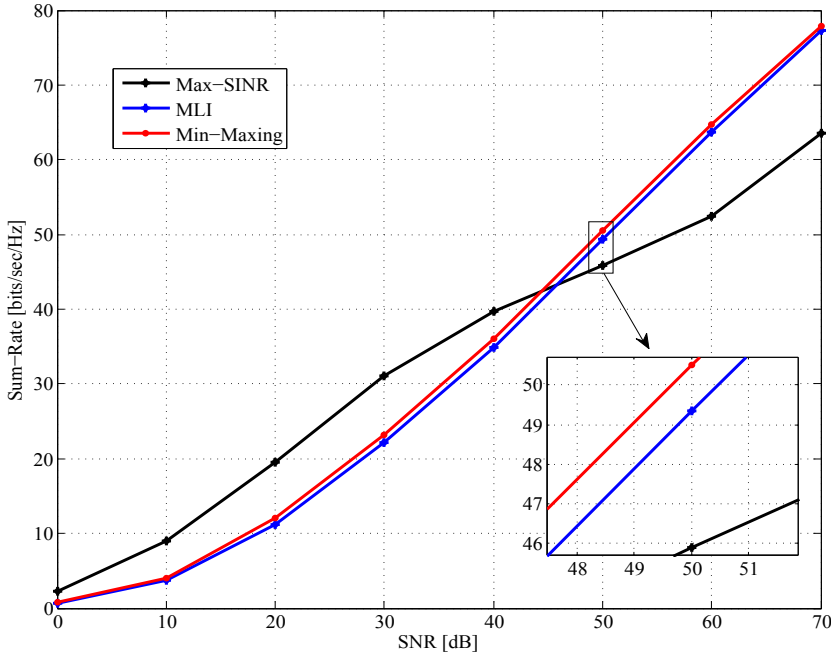

Figure 3.11: MC IC: Sum-rate performance comparison for $L = 7$, $K = 3$ and $d = 3$ system.

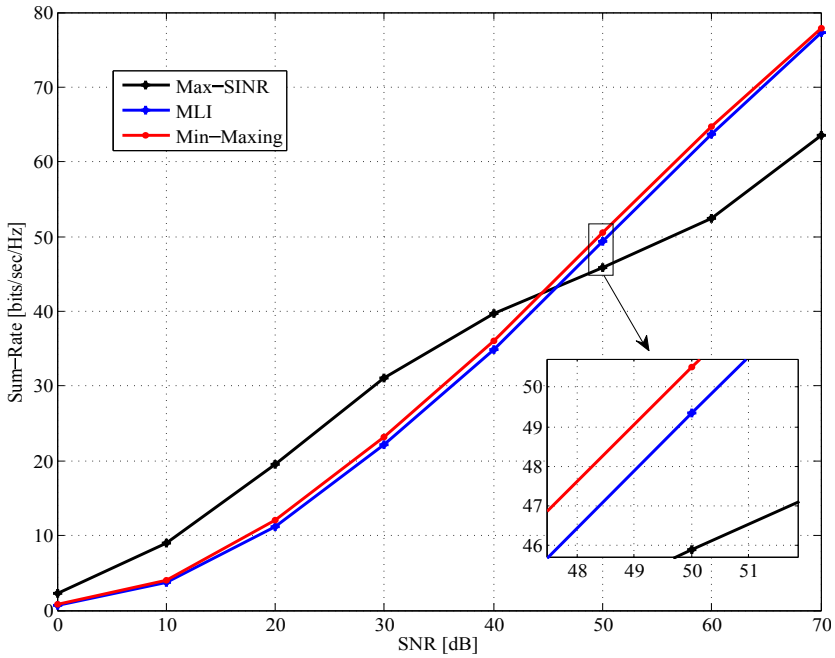

Figure 3.12: MC IC: Sum-rate performance comparison for $L = 8$, $K = 3$ and $d = 3$ system.

(2.33) are non-trivial to be achieved [19], [74]. However, Min-Maxing through its formulation considers doing the best for both conditions. Accordingly, it always achieves the best sum-rate at high SNRs.

Our investigation for Min-Maxing IA performance proves that this scheme achieves a considerable sum-rate improvement compared to the previous schemes.

4 Antenna Selection for MIMO-OFDM Interference Alignment Systems

This chapter proposes to apply antenna selection to MIMO-OFDM IA interference channels through bulk selection and per-subcarrier selection to effectively improve the practical reliability of IA in real-world environments. Moreover, a constrained per-subcarrier selection is developed to attain power balancing among the antennas of each node. Furthermore, a sub-optimal antenna selection algorithm is proposed to reduce the computational complexity of the optimal selection. MIMO-OFDM IA testbed is implemented to collect measured channels and present a realistic performance evaluation for the proposed method. The contents of this chapter have been partially published in references [75–77].

4.1 Introduction

The ideal sum-rate performance of MIMO IA interference channels is achieved in the literature by considering independent channels from a continuous distribution, which is predictable under sufficient rich scattered environments (e.g. [10, 17–19, 60] and references therein). In reality, this assumption is generally impossible to be observed since MIMO channels have spatial correlation due to the clustering of scatterers in the propagation environment [24]. Moreover, indoor environments create challenging multipath propagation scenarios, which produce significant correlated channels [25]. Unfortunately, it was claimed in the literature that the performance of MIMO IA interference channels is highly dependent on channel realizations, where spatial correlation generally has an adverse effect on sum-rate and error-rate performance since the correlation between channels decreases the SNR of the received signal after alignment [26].

Recently, the performance of IA was evaluated experimentally in [26, 78–82]. In this regard, MIMO-OFDM IA testbed was established in [26] to collect measured channels, where the practical feasibility of MIMO IA in slowly time-varying real-world channels with no fre-

quency or time extensions was evaluated. It was shown in this work that IA can achieve better DoF as the channels are less correlated. In order to overcome the effect of spatial correlation, the authors modified the separation between the antennas within each node to be in average 2 wavelengths (2λ), which is considered not practical to be implemented in reality. In [78–80], real-time MIMO IA testbeds were implemented to provide the actual performance of MIMO IA in realistic scenarios. These works considered some practical issues that affect IA performance such as spatial correlation, channel estimation errors and radio frequency (RF) impairments. Consequently, these practical studies claimed that the performance of IA using the theoretical channels are significantly overrated especially in indoor environments. Moreover, they concluded that in the absence of other issues such as channel estimation errors and channel time-variations, collinearity between the desired signal and interference subspaces causes significant degradation in IA performance.

Antenna selection is a powerful technique for enhancing the capacity and reliability of reception compared to open loop MIMO techniques [83–86]. Antenna selection technique was studied rarely in the literature to improve sum-rate and error-rate performance of IA [87, 88]. The authors of [87] suggested to apply different antenna selection criteria on single carrier MIMO IA systems in order to improve the sum-rate of IA using linear receivers, while an antenna selection criterion for maximum-likelihood receivers was considered in [88]. The authors of [87] and [88] assessed their techniques using theoretical channels. In this framework, antenna switching strategies were also suggested as in [89–91]. However, to the best of our knowledge, MIMO-OFDM IA interference channels with antenna selection have not been considered.

Motivated by the potential of combining IA and antenna selection, we consider in this chapter improving the practical feasibility of MIMO-OFDM IA systems in real-world environments by means of antenna selection. Therefore, we propose to apply transmit antenna selection to MIMO-OFDM IA systems either through bulk or per-subcarrier selection aiming at improving the sum-rate and/or error-rate performance under real-world channel circumstances while keeping the minimum spatial antenna separation of 0.5 wavelengths. Three selection criteria are considered, where the first criterion is the maximum sum-rate (Max-SR), in which we aim to improve the sum-rate of MIMO-OFDM IA systems. The second and third criteria are respectively the minimum error-rate (Min-ER) and minimum eigenvalue (Min-EG), in which we aim to improve the quality of the reception. A constrained per-subcarrier selection is considered to overcome the power imbalance between the antennas of each node by allocating the same number of subcarriers to all antennas with minimum rate loss. Moreover, we propose a sub-optimal

antenna selection algorithm to avoid the exhaustive search and reduce the computational complexity. Inspired by providing realistic performance evaluation, MIMO-OFDM IA testbed with antenna selection is established in order to collect measured channels.

In the following section, antenna selection approaches and MIMO-OFDM IA system model with antenna selection are presented. Section 4.3 shows the three transmit antenna selection criteria for MIMO-OFDM IA systems. The constrained per-subcarrier antenna selection is discussed in Section 4.4. Further, the sub-optimal antenna selection is presented in Section 4.5 in order to reduce computational complexity. Section 4.6 shows system implementation and simulation setup that are used in the performance evaluation. Finally, simulation results are illustrated and discussed in Section 4.7.

4.2 MIMO-OFDM IA System Model with Antenna Selection

4.2.1 Antenna Selection

MIMO technique is originally proposed to improve the performance of wireless communication systems in terms of diversity [92] and spatial multiplexing [46]. However, this improvement is achieved at the price of complexity and thus cost [83]. In order to reduce the complexity and the cost, antenna selection technique is proposed, where the best set of antennas out of the overall available antennas are selected at the transmitting or/and receiving side depending upon the selection strategy and the available RF chains [83, 93–95]. The low complexity comes through reducing the number of RF chains, which is considerably cheaper than introducing complete RF chains.

In this context, antenna selection can be employed to improve the capacity and reliability of reception depending on the used selection criterion [83–86, 96]. The selection criteria can be classified into two tracks: One is maximizing the capacity of the system; and the other is to minimize the error-rate. Moreover, transmit antenna selection is very similar to receive antenna selection except that little feedback is required for the case of transmit antenna selection [83]. Furthermore, antenna selection was proposed in the literature for point-to-point MIMO-OFDM systems to be handled through bulk selection [97] or per-subcarrier selection [98], [99]. In bulk selection, one transmit antenna subset is selected for all subcarriers at each transmit node. This strategy is considered cost efficient since only the active antennas require RF chains. In per-subcarrier selection strategy, each subcarrier at each transmit node has its own transmit antenna

subset. Per-subcarrier selection has a remarkable performance gain especially in high frequency selective channels, since the selection optimization is performed subcarrier-by-subcarrier [99]. Nevertheless, it requires more RF chains compared to bulk selection. Furthermore, it has the disadvantage of creating power imbalance across the transmit antennas. This occurs if one antenna is selected for a large number of subcarriers. As a result of that, the power amplifier works in the saturation region leading to performance degradation [98].

Next, we present the system model of MIMO-OFDM IA system with antenna selection through bulk and per-subcarrier selection.

4.2.2 System Model

A *K*-user MIMO-OFDM IA interference channel with M_T transmit antennas, M_R receive antennas, and *N* subcarriers is considered as seen in Fig. 4.1, where each user wishes to achieve d DoF. The details of this interference channel was described in Section 2.6.2.

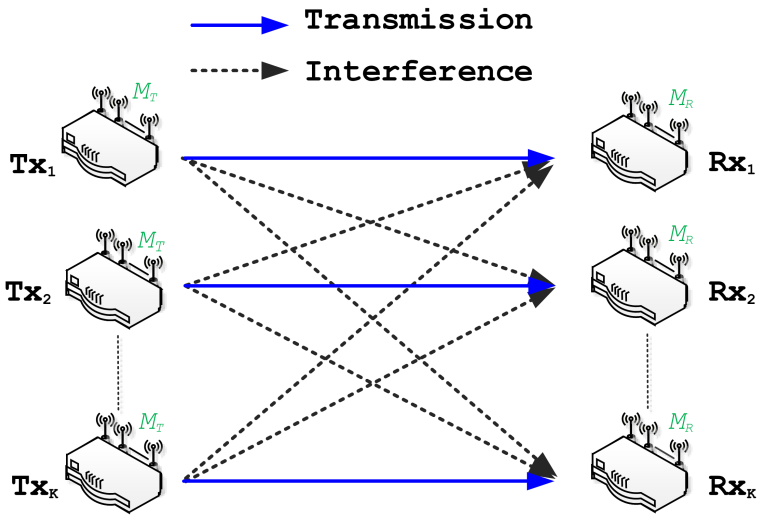

Figure 4.1: K-user interference channel system model.

In antenna selection strategy, a subset of transmit antennas M_s is selected out of M_T. Define ψ_i^k to be the i^{th} subset of all $A = \binom{M_T}{M_s}$ possible combinations of the antennas at the k^{th} transmitter, where ψ_i^k can be described as

$$\psi_i^k = \{I_m\}_{m=1}^{M}, \quad \{I_m\} \in \{0,1\}; i = 1,2,....,A, \tag{4.1}$$

where I_m is the indicator for the m^{th} transmit antenna. Therefore, I_m is set to 1 if and only if the m^{th} transmit antenna is active and 0 implies otherwise.

In IA, all users cooperate in order to achieve antenna selection criterion goal. Hence, we describe the indicator function for one possible subset of transmit antennas among all users, i.e the s^{th} subset, as $\gamma_s = \{\psi_i^k\}_{k=1}^K,\ \ i \in \{1, 2, .., A\}$. Therefore, the set that contains all the possible combinations $S = A^K$ of the transmit antennas among all users is written as $\chi = \{\gamma_1, \gamma_2, .., \gamma_S\}$.

In per-subcarrier selection, selection process is performed independently subcarrier-by-subcarrier among all users to choose the subset that achieves the selection goal, which can be described for the n^{th} subcarrier as

$$\gamma_{\text{opt}}^n = \underset{\gamma_s \in \chi}{\arg\,\text{sel}} \left\{ \sum_{k=1}^{K} \Delta_s^{k,n},\ s = 1, 2, .., S \right\} = \{\psi_{\text{o}}^{k,n}\}_{k=1}^K, \tag{4.2}$$

where arg sel$\{\}$ denotes the selection objective, $\Delta_s^{k,n}$ is the cost function of the k^{th} user over the n^{th} subcarrier for the γ_s subset, and $\psi_{\text{o}}^{k,n}$ is the chosen set for the k^{th} transmitter over the n^{th} subcarrier that achieves the selection criterion.

In bulk selection, the process is executed among all users and subcarriers cooperatively, which can be formulated as

$$\gamma_{\text{opt}} = \underset{\gamma_s \in \chi}{\arg\,\text{sel}} \left\{ \sum_{k=1}^{K} \sum_{n=1}^{N} \Delta_s^{k,n},\ s = 1, 2, .., S \right\} = \{\psi_{\text{o}}^{k}\}_{k=1}^K, \tag{4.3}$$

where ψ_{o}^k is the chosen set for the k^{th} transmitter over all the subcarriers that achieving the selection criterion. For the further description, we mention here that $\gamma_{\text{opt}}^n = \gamma_{\text{opt}}$ for all the subcarriers in bulk selection.

As an example for transmit antenna selection in MIMO-OFDM IA systems, consider 3 users each has $M_T = 3$ antennas to select $M_S = 2$ and $M_R = 2$ receive antennas. Accordingly, any user, i.e. the k^{th} user, has the following possibilities of subsets $\psi_1^k = \{1, 1, 0\}, \psi_2^k = \{1, 0, 1\}, \psi_3^k = \{0, 1, 1\}$. Hence, a possible subset among all users, i.e. the s^{th} subset, can be described as $\gamma_s = \{\psi_1^1, \psi_3^2, \psi_2^3\} = \{\{1, 1, 0\}, \{0, 1, 1\}, \{1, 0, 1\}\}$. Moreover, the set χ has 27 possible subsets from the transmit antennas among all users. Assuming that the per-subcarrier selection is performed using (4.2) over the n^{th} subcarrier and, then, the criterion selects $\gamma_{\text{opt}}^n = \{\{1, 0, 1\}, \{1, 1, 0\}, \{1, 0, 1\}\}$, this means that the selection criterion chooses at the n^{th} subcarrier the following subsets to communicate: $\psi_o^{1,n} = \{1, 0, 1\}, \psi_o^{2,n} = \{1, 1, 0\}, \psi_o^{3,n} = \{1, 0, 1\}$. Assuming again the bulk selection is executed through (4.3), and the output is $\gamma_{\text{opt}} = \{\{1, 0, 1\}, \{1, 1, 0\}, \{1, 0, 1\}\}$. This means that the selection criterion chooses for all subcarrier

the following subsets to communicate: $\psi_o^1 = \{1, 0, 1\}, \psi_o^2 = \{1, 1, 0\}, \psi_o^3 = \{1, 0, 1\}$.

After finding γ_{opt}^n using antenna selection technique, the discrete-time complex received signal over the n^{th} subcarrier at the k^{th} receiver after the fast Fourier transformation (FFT) is represented as

$$\mathbf{y}_k^n = \mathbf{U}_k^{n\text{H}}[\mathbf{H}_{kk}^n]_{\psi_{\text{o}}^{k,n}}\mathbf{V}_k^n\mathbf{x}_k^n + \sum_{j=1,j\neq k}^{K}\mathbf{U}_k^{n\text{H}}[\mathbf{H}_{kj}^n]_{\psi_{\text{o}}^{j,n}}\mathbf{V}_j^n x_j^n + \mathbf{U}_k^{n\text{H}}\mathbf{z}_k^n, \tag{4.4}$$

where $\mathbf{U}_k^n \in \mathbb{C}^{M_R\times d}$ is an orthonormal linear interference suppression matrix and $[\mathbf{H}_{kj}^n]_{\psi_{\text{o}}^{j,n}} \in \mathbb{C}^{M_R\times M_s}$ denotes the channel frequency response of the selected antennas in the subset $\psi_{\text{o}}^{j,n}$. $\mathbf{V}_k^n \in \mathbb{C}^{M_s\times d}$ is the orthonormal precoding matrix which is applied for the transmitted data $\mathbf{x}_k^n \in \mathbb{C}^{d\times 1}$ from the k^{th} node at the n^{th} subcarrier.

In this algorithm, uniform power allocation is assumed. Therefore, the sum-rate over the n^{th} subcarrier can be written as [26]

$$R^n(\gamma_{\text{opt}}^n) = \sum_{k=1}^{K}\log_2\left|\mathbf{I}_d + \frac{\mathbf{U}_k^{n\text{H}}[\mathbf{H}_{kk}^n]_{\psi_{\text{o}}^{k,n}}\mathbf{V}_k^n\mathbf{V}_k^{n\text{H}}[\mathbf{H}_{kk}^n]_{\psi_{\text{o}}^{k,n}}^{\text{H}}\mathbf{U}_k^n}{\sigma^2\mathbf{I}_d + \mathbf{U}_k^{n\text{H}}\mathbf{Q}_k^n\mathbf{U}_k^n}\right|, \tag{4.5}$$

where $\mathbf{Q}_k^n$ is the interference covariance matrix at the k^{th} receiver over the n^{th} subcarrier, which is written as

$$\mathbf{Q}_k^n = \sum_{k\neq j}\mathbf{U}_k^{n\text{H}}[\mathbf{H}_{kj}^n]_{\psi_{\text{o}}^{j,n}}\mathbf{V}_j^n\mathbf{V}_j^{n\text{H}}[\mathbf{H}_{kj}^n]_{\psi_{\text{o}}^{j,n}}^{\text{H}}\mathbf{U}_k^n. \tag{4.6}$$

Assuming perfect IA is achieved, the sum-rate becomes

$$R^n(\gamma_{\text{opt}}^n) = \sum_{k=1}^{K}\log_2\left|\mathbf{I}_d + \frac{1}{\sigma^2}\mathbf{U}_k^{n\text{H}}[\mathbf{H}_{kk}^n]_{\psi_{\text{o}}^{k,n}}\mathbf{V}_k^n\mathbf{V}_k^{n\text{H}}[\mathbf{H}_{kk}^n]_{\psi_{\text{o}}^{k,n}}^{\text{H}}\mathbf{U}_k^n\right|. \tag{4.7}$$

Therefore, the achieved sum-rate in bits per second per hertz averaged over all subcarriers can be expressed as

$$R(\gamma_{\text{opt}}) = \frac{1}{N}\sum_{n=1}^{N}R^n. \tag{4.8}$$

4.3 Antenna Selection Criteria for MIMO-OFDM IA Systems

The selection criteria can be categorized according to the goal of the selection into two groups: sum-rate and error-rate based criteria. In this work, we consider linear receivers since they are

more practical in spatial multiplexing systems. Without loss of generality and according to the practical implementation feasibility, perfect IA is assumed in this work, which is a general assumption for IA in practical implementation [26, 78–80].

4.3.1 The Relation between IA Performance and Canonical Correlations

In IA systems, the decoding process is carried out depending upon the components of the desired signal that are projected into the interference-free subspace. When the components of the desired signal in the interference-free space increase, the SNR at the receiver correspondingly increases, and the system error-rate and sum-rate performance consequentially are improved. Therefore, IA performance is highly dependent on the principal angles between the received signals and interference suppression matrices. The cosine of these principal angles is called canonical correlation. As seen in Fig. 4.2, for the same received signal power, the power of the decoded signals after the suppression matrix changes according to the principal angle. In the case of Θ_1, the power of the decoded signal is larger than the case of Θ_2 even if the power of $\mathbf{H}_{kk}\mathbf{V}_k$ is equal since $\Theta_1 < \Theta_2$. As a result of that, the orthogonality between the channels is extremely required to produce high-level of orthogonality between the desired subspace and the interference subspace in order to reduce the loss of SNR after the alignment. Therefore, high spatial correlation is translated into a large aligned signal at interference subspaces and, consequently, lower SNR after alignment [26].

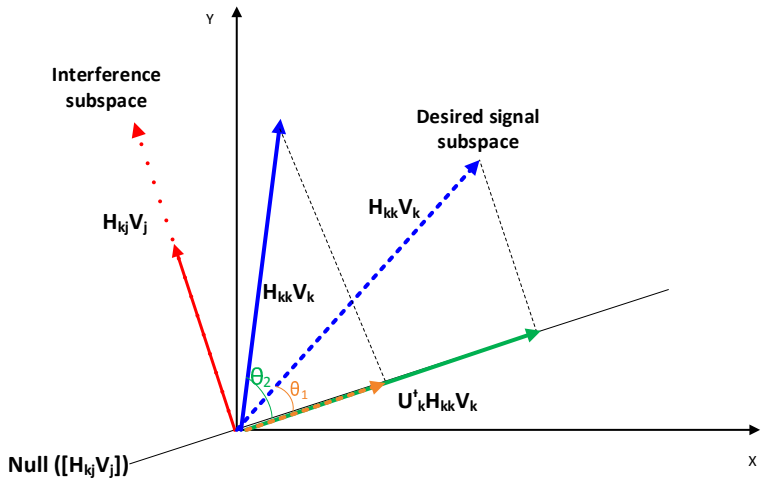

Figure 4.2: IA and principal angles representation.

Further, we present the impact of the canonical correlations, which are the cosine of the principal angles, on sum-rate of the K-user MIMO-OFDM IA system. The starting point for

the derivation is (4.8). At high SNRs, (4.8) can be approximated as

$$R(\gamma_s) \simeq \frac{1}{N}\sum_{k=1}^{K}\sum_{n=1}^{N}\log_2\left|\frac{1}{\sigma^2}\mathbf{U}_k^{n\mathrm{H}}[\mathbf{H}_{kk}^n]_{\psi_i^{k,n}}\mathbf{V}_k^n\mathbf{V}_k^{n\mathrm{H}}[\mathbf{H}_{kk}^n]_{\psi_i^{k,n}}^{\mathrm{H}}\mathbf{U}_k^n\right|. \tag{4.9}$$

According to thin QR decomposition, we can write

$$\mathbf{U}_k^n = \mathbf{F}_{U_k^n}\mathbf{J}_{U_k^n} \tag{4.10}$$

and

$$[\mathbf{H}_{kk}^n]_{\psi_i^{k,n}}\mathbf{V}_k^n = \mathbf{F}_{V_k^n}\mathbf{J}_{V_k^n}, \tag{4.11}$$

where $\mathbf{F}_{U_k^n}$, $\mathbf{F}_{V_k^n}$ are orthonormal $M_R \times d$ matrix and $\mathbf{J}_{U_k^n}$, $\mathbf{J}_{V_k^n}$ are $d \times d$ upper triangle matrix.

Under the above factorization, (4.9) is written as

$$R(\gamma_s) = \frac{1}{N}\sum_{k=1}^{K}\sum_{n=1}^{N}\log_2\left|\frac{1}{\sigma^2}\left(\mathbf{F}_{U_k^n}\mathbf{J}_{U_k^n}\right)^{\mathrm{H}}\left(\mathbf{F}_{V_k^n}\mathbf{J}_{V_k^n}\right)\left(\mathbf{F}_{V_k^n}\mathbf{J}_{V_k^n}\right)^{\mathrm{H}}\left(\mathbf{F}_{U_k^n}\mathbf{J}_{U_k^n}\right)\right|. \tag{4.12}$$

Since $\mathbf{U}_k^n$ is a unitary matrix, this leads to $\left|\mathbf{J}_{U_k^n}\mathbf{J}_{U_k^n}^{\mathrm{H}}\right| = 1$. Therefore, (4.12) can be simplified as

$$R(\gamma_s) = \frac{1}{N}\sum_{k=1}^{K}\sum_{n=1}^{N}\log_2\left(\left(\frac{1}{\sigma^2}\right)^2\left|\mathbf{F}_{U_k^n}^{\mathrm{H}}\mathbf{F}_{V_k^n}\right|\left|\mathbf{F}_{V_k^n}^{\mathrm{H}}\mathbf{F}_{U_k^n}\right|\left|\mathbf{J}_{V_k^n}\mathbf{J}_{V_k^n}^{\mathrm{H}}\right|\right). \tag{4.13}$$

The canonical correlations are obtained as singular values of $\mathbf{F}_{V_k^n}^{\mathrm{H}}\mathbf{F}_{U_k^n}$ as follows [100]

$$\mathbf{F}_{V_k^n}^{\mathrm{H}}\mathbf{F}_{U_k^n} = \bar{\mathbf{T}}_{k1}^n\Lambda\left(\bar{\mathbf{T}}_{k2}^n\right)^{\mathrm{H}}, \tag{4.14}$$

where $\bar{\mathbf{T}}_{k1}^n$ and $\bar{\mathbf{T}}_{k2}^n$ are $d \times d$ unitary matrices, Λ is $d \times d$ diagonal matrix equals diag$(\alpha_1^n, .., \alpha_d^n)$ and $(\alpha_1^n, ..., \alpha_d^n)$ are the canonical correlations between the subspace $\mathbf{U}_k^n$ and the subspace $[\mathbf{H}_{kk}^n]_{\psi_i^{k,n}}\mathbf{V}_k^n$.

Therefore, (4.13) can be written as

$$R(\gamma_s) = \frac{1}{N}\sum_{k=1}^{K}\sum_{n=1}^{N}\log_2\left(\left(\frac{1}{\sigma^2}\right)^2\left|\bar{\mathbf{T}}_{k1}^n\Lambda\left(\bar{\mathbf{T}}_{k2}^n\right)^{\mathrm{H}}\right|\left|\bar{\mathbf{T}}_{k2}^n\Lambda\left(\bar{\mathbf{T}}_{k1}^n\right)^{\mathrm{H}}\right|\left|\mathbf{J}_{V_k^n}\mathbf{J}_{V_k^n}^{\mathrm{H}}\right|\right). \tag{4.15}$$

Thereafter, (4.15) can be formulated

$$R(\gamma_s) = \frac{1}{N}\sum_{k=1}^{K}\sum_{n=1}^{N}\log_2\left(\frac{1}{\sigma^2}\prod_{a=1}^{d}\left([\alpha_a^n]_{\psi_i^{k,n}} \times \mu_a\left([\mathbf{H}_{kk}^n]_{\psi_i^{k,n}}\mathbf{V}_k^n\right)\right)\right)^2, \tag{4.16}$$

where $\mu_a\left([\mathbf{H}_{kk}^n]_{\psi_i^{k,n}}\mathbf{V}_k^n\right)$ is the a^{th} singular value of matrix $\left([\mathbf{H}_{kk}^n]_{\psi_i^{k,n}}\mathbf{V}_k^n\right)$. It is clear that as the canonical correlation increases, the desired signal and the interference spaces are less aligned, and the received signal SNR and sum-rate of the system increase.

4.3.2 Maximum Sum-Rate Selection Criterion (Max-SR)

In Max-SR criterion, antenna selection is performed to maximize the sum-rate of MIMO-OFDM IA systems. Max-SR through bulk selection can be formulated as

$$\gamma_{opt} = \arg\max_{\gamma_s\in\chi} R(\gamma_s). \tag{4.17}$$

We mention again here that γ_s and ψ_i^k are the same for all subcarriers in bulk selection. Sum-rate in (4.8) can be written as discussed in the previous section as

$$R(\gamma_s) = \frac{1}{N}\sum_{k=1}^{K}\sum_{n=1}^{N}\log_2\left(\frac{1}{\sigma^2}\prod_{a=1}^{d}\left([\alpha_a^n]_{\psi_i^{k,n}} \times \mu_a\left([\mathbf{H}_{kk}^n]_{\psi_i^{k,n}}\mathbf{V}_k^n\right)\right)\right)^2. \tag{4.18}$$

Therefore, (4.17) can be rewritten as

$$\gamma_{opt} = \arg\max_{\gamma_s\in\chi} \Theta(\gamma_s), \tag{4.19}$$

where

$$\Theta(\gamma_s) = \sum_{k=1}^{K}\sum_{n=1}^{N}\left(\prod_{a=1}^{d}\left([\alpha_a^n]_{\psi_i^{k,n}} \times \mu_a\left([\mathbf{H}_{kk}^n]_{\psi_i^{k,n}}\mathbf{V}_k^n\right)\right)\right)^2. \tag{4.20}$$

In per-subcarrier selection, the selection is performed subcarrier-by-subcarrier as follows

$$\gamma_{opt}^n = \arg\max_{\gamma_s\in\chi} R^n(\gamma_s) \qquad \forall n. \tag{4.21}$$

Correspondingly, the selection can be reformulated into

$$\gamma_{opt}^n = \arg\max_{\gamma_s\in\chi} \Theta^n(\gamma_s) \qquad \forall n, \tag{4.22}$$

where $\Theta^n(\gamma_s^n)$ is defined as

$$\Theta^n(\gamma_s^n) = \sum_{k=1}^{K} \left(\prod_{a=1}^{d} \left([\alpha_a^n]_{\psi_i^{k,n}} \times \mu_a \left([\mathbf{H}_{kk}^n]_{\psi_i^{k,n}} \mathbf{V}_k^n \right) \right) \right)^2 . \tag{4.23}$$

Max-SR bulk selection and per-subcarrier selection are described generally in Algorithms 4.1 and 4.2, respectively.

Algorithm 4.1 Bulk transmit antenna selection

1: Find χ;
2: **for** $s = 1$ to S **do**
3: Choose $\gamma_s \in \chi$;
4: **for** $n = 1$ to N **do**
5: Compute $\mathbf{V}_k^n$ and $\mathbf{U}_k^n$; $\forall k$ that are related to γ_s;
6: **end for**
7: Compute the cost function of the selection criterion using γ_s as in (4.20), (4.24), or (4.26);
8: **end for**
9: Choose the set γ_{opt} that optimize the selection criterion as in (4.3). Then compute the related coders $\mathbf{V}_k^n$ and $\mathbf{U}_k^n$ $\forall n$, where this set is used for all subcarriers.

4.3.3 Minimum Error-Rate Selection Criteria (Min-ER)

It was shown that maximizing the post processing SNR leads to minimization of the error-rate [101], [102]. Therefore, it is aimed in this selection criterion to maximize the SNR of the received signals by minimizing the lost energy of the received signal after alignment that results from spatial collinearity between the desired signal and interference subspaces. This can be achieved by selecting the subsets that have the maximum canonical correlation between the desired received signal subspace and the interference-free subspace [75]. For bulk selection, the optimization is

$$\gamma_{opt} = \underset{\gamma_s \in \chi}{\arg\max} \sum_{k=1}^{K} \sum_{n=1}^{N} \left(\prod_{a=1}^{d} [\alpha_a^n]_{\psi_i^{k,n}} \right)^2 , \tag{4.24}$$

while in per-subcarrier criterion, the selection is performed subcarrier-by-subcarrier as follows

$$\gamma_{opt}^{n} = \arg\max_{\gamma_s \in \chi} \sum_{k=1}^{K} \left(\prod_{a=1}^{d} [\alpha_a^n]_{\psi_i^{k,n}} \right)^2 . \tag{4.25}$$

Min-ER bulk selection and per-subcarrier selection are described generally in Algorithms 4.1 and 4.2, respectively.

Algorithm 4.2 Per-subcarrier transmit antenna selection

1: **for** $n = 1$ to N **do**
2: Find χ;
3: **for** $s = 1$ to S **do**
4: Choose $\gamma_s \in \chi$;
5: Compute $\mathbf{V}_k^n$ and $\mathbf{U}_k^n$; $\forall k$ for $\gamma_s \in \chi$;
6: Compute the cost function of the selection criterion using γ_s as in (4.23), (4.25), or (4.27);
7: **end for**
8: Choose the set γ_{opt}^n that optimize the selection criterion as in (4.2). Then compute the related coders $\mathbf{V}_k^n$ and $\mathbf{U}_k^n$, where this set is used for only this subcarrier.
9: **end for**

4.3.4 Minimum Eigenvalue Selection Criterion (Min-EG)

It was exposed that the postprocessing SNR of the k^{th} user at the n^{th} subcarrier is lower bounded by minEig $\left(\mathbf{U}_k^{n\mathrm{H}} [\mathbf{H}_{kk}^n]_{\psi_i^{k,n}} \mathbf{V}_k^n \right)$, where minEig denotes the minimum eigenvalue of $\left(\mathbf{U}_k^{n\mathrm{H}} [\mathbf{H}_{kk}^n]_{\psi_i^{k,n}} \mathbf{V}_k^n \right)$ [101], [102]. Therefore, error-rate lower bound is optimized for the whole system when the antenna subset is selected through bulk selection as [87]

$$\gamma_{opt} = \arg\max_{\gamma_s \in \chi} \sum_{k=1}^{K} \sum_{n=1}^{N} \text{minEig} \left(\mathbf{U}_k^{n\mathrm{H}} [\mathbf{H}_{kk}^n]_{\psi_i^{k,n}} \mathbf{V}_k^n \right) . \tag{4.26}$$

While in per-subcarrier selection, the optimization problem is reformulated for the n^{th} subcarrier as follows

$$\gamma_{opt}^{n} = \arg\max_{\gamma_s \in \chi} \sum_{k=1}^{K} \text{minEig} \left(\mathbf{U}_k^{n\mathrm{H}} [\mathbf{H}_{kk}^n]_{\psi_i^{k,n}} \mathbf{V}_k^n \right) . \tag{4.27}$$

Min-EG bulk selection and per-subcarrier selection are described generally in Algorithms 4.1 and 4.2, respectively.

4.4 Transmit Antenna Selection with Power Balancing

While per-subcarrier selection strategy achieves more diversity gain than bulk selection does in high frequency selective channels, per-subcarrier selection may cause power imbalance across transmit antennas. This occurs if one antenna is loaded with a large number of subcarriers, which leads the power amplifier to work in the saturation region causing performance degradation [98,99]. Therefore, constrained transmit antenna selection is proposed to achieve the power balancing using the same methodology as in [103]. The constraint is to equally distribute the power between transmit antennas by assigning the same number of subcarriers to each antenna. This constraint can be reformulated as

$$\sum_{n=1}^{N}\{I_m^{k,n}\} \leq \left\lceil \frac{N \times M_s}{M_T} \right\rceil \qquad \forall m \quad \text{and} \quad \forall k, \tag{4.28}$$

where $\lceil B \rceil$ denotes the smallest integer larger than or equal to B. Since I_m is the indicator to the m^{th} transmit antenna and it equals 1 when the m^{th} transmit antenna is active and 0 otherwise. The summation in $\sum_{n=1}^{N}\{I_m^{k,n}\}$ counts the number of subcarriers that are allocated to the m^{th} antenna at the k^{th} transmitter.

A sequential reallocation method is used to achieve the constrained transmit antenna selection according to the following three steps:

1. In the first step, the unconstrained transmit antenna selection according to one of the selection criteria is performed as in Algorithm 4.2.

2. Then, a repeatable reallocation process is executed for the antennas with overloaded subcarriers to antennas with underloaded subcarriers subjected to the constraint that no loss is allowed in the selection rate.

3. If power balancing is achieved, per-subcarrier selection algorithm achieves power balancing without loss compared to the unconstrained selection. Otherwise, Step 2 is repeated in a way that loss in the rate is allowed to complete the reallocation process for the remaining overloaded antennas.

This approach is described in Algorithm 4.3.

Algorithm 4.3 The constrained transmit antenna selection

1: Perform transmit antenna selection using a specific selection criterion without constrains to obtain $\{\psi_o^{k,n}\}$ $\forall n$ and $\forall k$.
2: **for** $k = 1$ to K **do**
3: Find overloaded antenna subset Ω_+ and underloaded antenna subset Ω_-.
4: **for** $n = 1$ to N **do**
5: **while** $\Omega_+ \neq \phi$ **do**
6: Reallocate the subcarriers from the antennas in Ω_+ to the antennas in Ω_- without loss in the rate.
7: Modify Ω_+ and Ω_-
8: **end while**
9: **end for**
10: **if** $\Omega_+ \neq \phi$ **then**
11: **for** $n = 1$ to N **do**
12: **while** $\Omega_+ \neq \phi$ **do**
13: Reallocate the subcarriers from the antennas in Ω_+ to the antennas in Ω_- with loss in the rate.
14: Modify Ω_+ and Ω_-
15: **end while**
16: **end for**
17: **end if**
18: **end for**

4.5 Sub-Optimal Antenna Selection Algorithm

The proposed antenna selection technique for MIMO-OFDM IA interference channels in the previous sections is performed through exhaustive search over all possible combinations at the transmitter sides in order to select the optimal antenna subsets for the transmitters. This optimal solution requires a high computational complexity that grows with $\mathcal{O}\left(N\binom{M_T}{M_s}^K\right)$. In order to reduce this computational complexity, we propose a sub-optimal method to perform the selection process with less complexity. The proposed sub-optimal algorithm is based on a greedy strategy, in which we do the selection process for each user independently after initializing one antenna set for each user. The initial antenna set for a given user is the set that gives the maximum Frobenius norm of the direct channel matrix. We further describe the sub-optimal

method for bulk selection, which can be easily applied to per-subcarrier selection following Algorithm 4.2. The description of the sub-optimal method can be commenced by initializing the set $\mathcal{A} = \{\psi_{ini}^k\}_{k=1}^K$ that contains all the initial sets, where selection of the initial sets can be formulated in bulk selection for the k^{th} user as follows

$$\psi_{ini}^k = \arg\max_{\psi_i^k} \left\{ \sum_{n=1}^{N} \left\| [\mathbf{H}_{kk}^n]_{\psi_i^k} \right\|_F, \ i = 1, 2, .., A \right\}; \qquad \forall k. \tag{4.29}$$

Afterwards, the initial sets are modified sequentially for the users until all the initial sets in $\mathcal{A}$ are modified. The sequential modification is performed for each user independently, e.g. the k^{th} user, by selecting the subset of antennas at each user ψ_o^k that achieves the selection criterion while the other antenna subsets of the other $K-1$ users are fixed. Then, we modify the initial subset of this user ψ_{ini}^k to be ψ_o^k in the set $\mathcal{A}$. This process is repeated for all users in order to modify the initial antenna subsets. Hence, the computational complexity is reduced to be grown with $\mathcal{O}\left(NK\binom{M_T}{M_s}\right)$. Therefore, we c conclude that the vital role of the sub-optimal scheme is to reduce the exponential growth of the complexity to linear growth.

Furthermore, the correlation between subcarriers can be utilized in order to reduce the number of subcarriers that is considered in the selection process. The adjacent subcarriers may face correlated fading, which means that if one subcarrier is considered for the selection process, the chosen antenna set is also suitable for these correlated subcarriers. Therefore, the selection process can be employed for one subcarrier that represents a specific number of subcarriers. Assuming that one subcarrier presents a group of N_s subcarriers, the computational complexity becomes $\mathcal{O}\left(\frac{NK}{N_s}\binom{M_T}{M_s}\right)$. This sub-optimal approach is summarized in Algorithm 4.4 for bulk selection, which can be easily extended to per-subcarrier selection according to Algorithm 4.2.

4.6 System Implementation and Simulation Setups

We evaluate the sum-rate and error-rate performance of the antenna selection techniques in MIMO-OFDM IA system using measured channels, deterministic channels and analytical channels. In our evaluation, measured and deterministic channels are obtained for an indoor environment. In order to obtain measured channels, a basic MIMO-OFDM system testbed is implemented considering channel estimation and carrier recovery. Whereas deterministic channels are synthesized using 3-D ray-tracing, which can characterize the propagation channel with high accuracy. It was verified that the static measurement environment can ensure the validity of the

Algorithm 4.4 Sub-optimal bulk transmit antenna selection

Find $\psi_i^k;\ \forall i$ and $\forall k$;
Initialize the set $\mathcal{A}$ by finding ψ_{ini}^k, $\forall k$ according to (4.29);
Compute $\mathbf{V}_k^n$ and $\mathbf{U}_k^n$, $\forall k$ according to the set $\mathcal{A}$;
for $k = 1$ to K **do**
    for $i = 1$ to A **do**
        Modify the k^{th} element in the set $\mathcal{A}$ to be ψ_i^k;
        for $n = 1{:}N_s{:}N$ **do**
            Compute $\mathbf{V}_k^n$ and $\mathbf{U}_k^n$ according to the set $\mathcal{A}$;
        end for
        Compute the cost function of the selection criterion for the set $\mathcal{A}$ as in (4.20), (4.24), or (4.26);
    end for
    Find the set ψ_o^k satisfies the selection criterion and fix the k^{th} element in $\mathcal{A}$ to be ψ_o^k as in (4.3).
end for

results as claimed in [26]. Therefore, the measurements and 3D ray-tracing are performed for a static environment. It is worth mentioning that the deterministic channels are effective in offering an averaged performance for the environment by moving the nodes and extracting different channel realizations, which is hardly to be accomplished by measured channels. The analytical channels have been drawn from independent and identically distributed Gaussian distribution with zero mean and unit variance, which represents a high selective and scattered environment. Evaluating the proposed algorithms under different channel conditions provides a robust conclusion about the efficiency of antenna selection under the different circumstances.

A communication system at 2.4 GHz operating in the first floor of the electrical engineering building of Duisburg-Essen University is considered. According to the hardware limitation, we consider a three-users $(K = 3)$ MIMO-OFDM IA system with 64 subcarriers $(N = 64)$, where the channel bandwidth is 1 MHz. 3 antennas at each transmitting node $(M_T = 3,\ M_s = 2)$ and two antennas at each receiving node $(M_R = 2)$ are assumed, where each user transmits $d = 1$ stream. The antennas within each node are placed at a distance of $\lambda/2$ from each other as seen in Fig. 4.3. The values of transmit power, subcarrier spacing, guard interval, and symbol duration are set to 15 dBm, 15.625 kHz, 16 samples and 80 μs, respectively. The closed-form solution of IA is applied.

Next, we present our hardware setup that is used to collect the measured channels. Then, 3D ray-tracing channel model is exhibited.

Figure 4.3: IA testbed setup: Demonstration of the antennas within one transmitting node.

4.6.1 Software Implementation and Hardware Setup

In this section, we present the MIMO-OFDM IA wireless network testbed that is used in this work. The objective of the testbed is to assess antenna selection techniques in MIMO-OFDM IA systems in a realistic scenario. In this scenario, transmitter-receiver pairs were placed at distances ranging from 2 to 8 m apart, where we avoid the line-of-sight scenario between transmitter-receiver pairs during the measurements. It is worth mentioning that directional antennas or multibeam antennas offer better diversity than omnidirectional ones in the line-of-sight scenarios, where beam selection can be performed as discussed in [104–106]. During the measurements, clean channel at 2.4 GHz is used. Moreover, we ensure that there are no moving objects in the surroundings in order to collect static channels. The measured channel realizations are collected without moving the transmit nodes nor the receive nodes, where 100 channel realization are collected over different time slots.

Software Implementation

To realistically predict the performance of IA with antenna selection as stated in the objective of the testbed implementation, we put emphasis on channel estimation implementation. Users sequentially send OFDM preamble symbol as frequency-domain pilots that are known to all receivers to satisfy time orthogonality of training among all users as seen in Fig. 4.4 [107]. Each OFDM symbol in our experiment consists of 40 data subcarriers, 24 zeros, and 16 samples

as cyclic prefix for the guard interval. The preamble symbol contains similar arrangement as the usual OFDM symbols, except that all of 40 data subcarriers in the preamble are the known pseudo noise (PN) sequence used for training symbol-based channel estimation. In the training symbol-based channel estimation, all subcarriers of an OFDM symbol are dedicated for training. The PN sequence only contains +/-1 in even subcarriers and 0 in odd subcarriers. One OFDM frame has one preamble symbol. For slowly varying channels, the channels for the same subcarriers in one OFDM frame are assumed unchanged. From the preamble received at the output of FFT block in the receiver, we can obtain the least-square estimate of the channel frequency as was described in [108, 109].

In this experiment, synchronization is required to compensate time and carrier frequency offset between transmitters and receivers, which leads to the reduction of each OFDM symbol amplitude in time domain, shifting of the phase and inter-carrier interference that ruins subcarriers orthogonality. PN synchronization method is implemented to carry out time synchronization and fine frequency offset synchronization between each transmit-receive pair using the same methodology in [26, 110, 111].

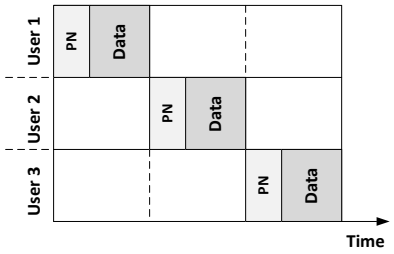

Figure 4.4: Illustration example for preamble and data example used in measurement.

Hardware Setup

In our hardware setup, universal software radio peripheral (USRP) units, GNU software, and personal computers (PC) are mainly used. The setup consists of 9 USRP N210 as transmitters connected to one PC and 3 USRP B210 as receivers connected to another PC, where each transmitting node requires 3 units of USRP N210 and each receiving node needs one USRP B210. USRP unit is the most common hardware used with GNU Radio to build a Software Defined Radio (SDR) system. Each USRP N210 consists of two main sub-devices, a motherboard and different daughterboards which can transmit and/or receive different frequency ranges. We used SBX USRP daughterboards that provides up to 100 mW output, 40 MHz of bandwidth and has 400 MHz-4400 MHz frequency range with Gigabit Ethernet interface. USRP B210 is fully in-

tegrated single board USRP platform with frequency coverage from 70 MHz-6 GHz and has universal serial bus (USB) 3.0 connectivity. The core component of each node is the PC which allocates USRPs as the baseband hardware, configures and controls the baseband hardware as well as RF front-end using the GNU Radio software. The hardware block diagram is illustrated in Fig. 4.5.

For the aim of synchronization, an external function generator is used to generate a 10 MHz clock and PPS signal to Ettus OctoClock, where this OctoClock can distribute the reference signal for the USRPs. Moreover, the MIMO cable can also share clock and PPS signals between USRP N210 within the node.

Through measurements, we only record the channels that achieve successful date transmission by all receivers. Moreover, the received signals have high SNR values of an average 18 dB. This methodology of tight synchronization and high power transmission guarantees that our measurements enclose only channel impairments and avoid the timing effects.

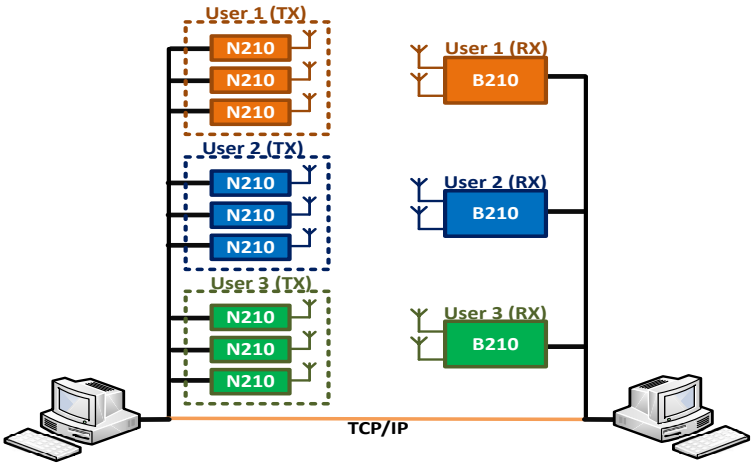

Figure 4.5: Hardware block diagram.

4.6.2 3D Ray-Tracing Channel Modelling

It was verified that characterization of the propagation channel and extraction of the channel parameters can be provided using 3D ray-tracing with high accuracy [112, 113]. Moreover, an excellent agreement with measurements for narrowband and wideband wireless channels was presented in the literature [113, 114]. This model considers the spatial channel and the environmental effects as path-loss, frequency dependence, reflections, transmissions and diffractions. It considers as well the characteristics of the antennas as part of the effective channel such as

directional gain, matching and polarization.

In our simulation, Wireless InSite is used as a 3D ray-tracing tool [115]. Unlike the measured channels, 1000 deterministic channel realizations are obtained by moving all nodes in this lab randomly using Wireless InSite in order to obtain an averaged performance for the system. The channel impulse response between the j^{th} transmit antenna and the k^{th} receive antenna at the n^{th} subcarrier is modeled as [116]

$$g_{kj}^{n}(t) = \sum_{c=1}^{P_T} \sqrt{P_c}.e^{j\theta_c}.\delta_c(t-\tau_c), \tag{4.30}$$

where P_c, θ_c and τ_c are the received power, phase angle, and time delay of the c^{th} path respectively. P_T is the total number of pathes and $\delta_c(t)$ is the delta impulse function. The frequency response between the j^{th} transmit antenna and the k^{th} receive antenna at the n^{th} subcarrier can be calculated as

$$h_{kj}^{n} = \sum_{c=1}^{PT} \sqrt{P_c}.e^{j\theta_c}.e^{j2\pi f_n \tau_c}, \tag{4.31}$$

where f_n is the carrier frequency of the n^{th} subcarrier.

4.6.3 Channel Normalization

Before evaluating the sum-rate and error-rate performance of MIMO-OFDM IA over the collected channels, the channel matrices should be normalized [24, 26, 101, 117].

The measured channels are normalized over the full data set. In order to obtain fair comparison with the simulated Rayleigh channels, we normalize our measurements to have elements of unit variance as follows [26, 117]

$$\bar{\mathbf{H}}_{kj}^{n}(\omega) = \sqrt{M_s M_R}\frac{\mathbf{H}_{kj}^{n}(\omega)}{\sqrt{\frac{1}{\Omega}\sum_{i=1}^{\Omega}\|\mathbf{H}_{kj}^{n}(i)\|_F^2}}, \tag{4.32}$$

where $\bar{\mathbf{H}}_{kj}(\omega)$ is the normalized channel matrix, and $\Omega = 100$ is the set of all measurements collected.

In the deterministic channels, the received power changes according to transmitter and receiver location. Therefore, the same normalization methodology is used in order to have

elements of unit variance as follows [24, 101]

$$\bar{\mathbf{H}}_{kj}^{n} = \sqrt{M_s M_R}\frac{\mathbf{H}_{kj}^{n}}{\sqrt{\|\mathbf{H}_{kj}^{n}\|_F^2}}. \tag{4.33}$$

4.7 Results and Discussions

In this section, we present the sum-rate and error-rate performance of the antenna selection techniques for the MIMO-OFDM IA system. The results are presented corresponding to the following three scenarios: Analytical channels, deterministic channels and measured channels. Max-SR, Min-ER and Min-EG antenna selection criteria are considered in the simulation including bulk selection and per-subcarrier selection. Moreover, constrained per-subcarrier and sub-optimal antenna selection are investigated. For the purpose of comparison, the following algorithms are considered in the simulation:

1. **Bulk:** This scenario denotes bulk antenna selection. The used selection criterion is added between parenthesis. In deterministic and measured channels, the separation between the antennas within the node is $\lambda/2$.

2. **Per-Subcarrier:** This scenario refers to use per-subcarrier antenna selection. The used selection criterion is added between a parenthesis. In deterministic and measured channels, the separation between the antennas within the node is $\lambda/2$.

3. **Constrained Per-Subcarrier:** This scenario refers to use constrained per-subcarrier antenna selection that is illustrated in Algorithm 4.3. The used selection criterion is added between a parenthesis. In deterministic and measured channels, the separation between the antennas within the node is $\lambda/2$.

4. **No Selection ($\lambda/2$):** This scenario shows the performance corresponding to the case where no selection strategy is used. In this case, 2 transmit antennas are always chosen at random. In deterministic and measured channels, the separation between the antennas within the node is $\lambda/2$.

5. **No Selection (2λ):** This scenario shows the performance corresponding to the case where only 2 transmit antennas exist at each transmit node and the separation between the antennas within the node is 2λ.

6. **TDMA:** We use TDMA as an orthogonal transmission scheme, where no selection strategy is used. In this case, 3 transmit antennas are always used with eigen beamforming. Furthermore, two data streams $d = 2$ are sent by each user in this case. In deterministic and measured channels, the separation between the antennas within the node is $\lambda/2$.

7. **TDMA with antenna selection:** This scenario shows the performance corresponding to the case where per-subcarrier antenna selection with eigen beamforming is used to maximize the capacity of TDMA system. Furthermore, two data streams are sent by each user in this case. In deterministic and measured channels, the separation between the antennas within the node is $\lambda/2$.

8. **Max-SINR:** In this scenario, full transmission is simulated, in which 3 transmit antennas are used for transmission as in [19]. In deterministic and measured channels, the separation between the antennas within the node is $\lambda/2$.

9. **Suboptimal:** In this scenario, sup-optimal antenna selection is performed. The used selection criterion is added between a parenthesis.

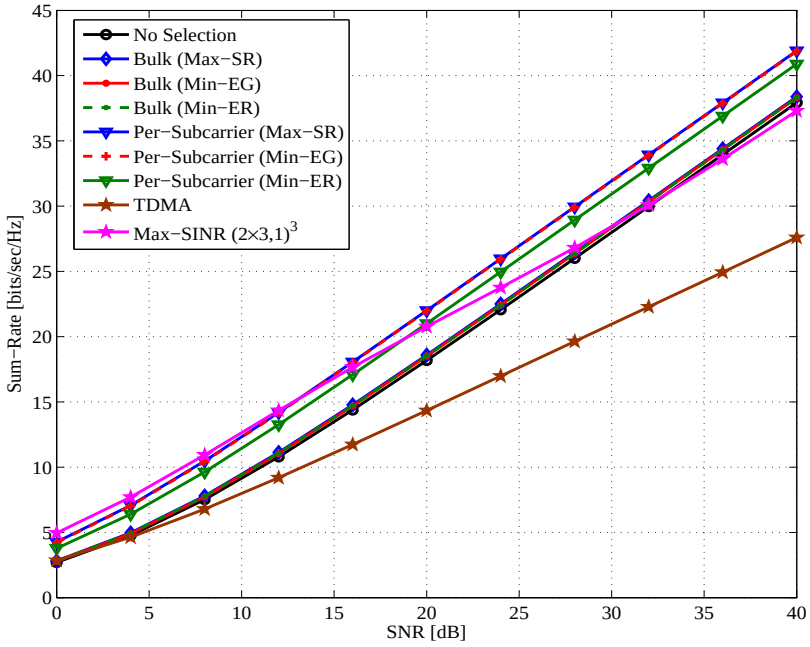

Figure 4.6: Sum-rate comparison between different antenna selection strategies using analytical channels.

4.7.1 Analytical Channels

The analytical channels have been drawn from independent and identically distributed Gaussian distribution with zero mean and unit variance, which represent high selective and scattered environments. Fig. 4.6 and Fig. 4.7 show the sum-rate and error-rate performance for the different antenna selection techniques using analytical channels, respectively. In general, per-subcarrier selection achieves high performance gain compared to bulk selection in terms of sum-rate and error-rate since the subcarriers are uncorrelated and have independent fading. It can be seen from Fig. 4.6 that Max-SR and Min-EG through per-subcarrier selection achieve the maximum sum-rate performance and result in approximately 1 bps/Hz gain compared to Min-ER. However, all bulk selection criteria have a very close sum-rate to IA without antenna selection because the subcarriers are uncorrelated and, hence, selecting one antenna subset suitable for all subcarriers is impossible. It is notable that the multiplexing gain of IA systems with and without antenna selection are identical, where the gain in per-subcarrier selection sum-rate curves is mainly due to diversity gain. This is justifiable since the MIMO channels are independent, and hence all antenna subset can achieve the maximum spatial multiplexing.

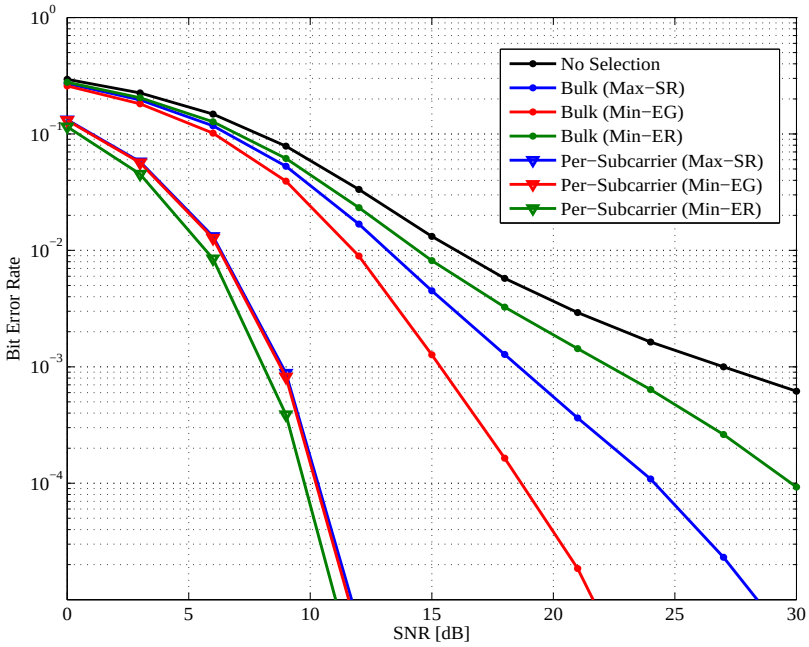

Figure 4.7: Bit error-rate comparison between different antenna selection strategies using analytical channels.

As anticipated in the theory for independent channels, Fig. 4.6 proves that IA sum-rate achieves better DoF compared to orthogonal transmission techniques such as TDMA. Fig. 4.6

exhibits that sum-rate of per-subcarrier selection surpasses Max-SINR sum-rate, while both approaches use the same hardware complexity (3 RF chains). It can be clearly observed from Fig. 4.8 that the constrained antenna selection, that is presented in algorithm 4.3, achieves mostly the same sum-rate performance as the unconstrained one in this type of channels. Turning to error-rate performance, Fig. 4.7 shows that Min-ER criterion through per-subcarrier selection offers the minimum error-rate compared to the other criteria in this system, while Max-SR and Min-EG have smaller performance loss compared to Min-ER. However, the behavior of selection criteria in bulk selection is different because selection is decided depending on all the independent subcarriers.

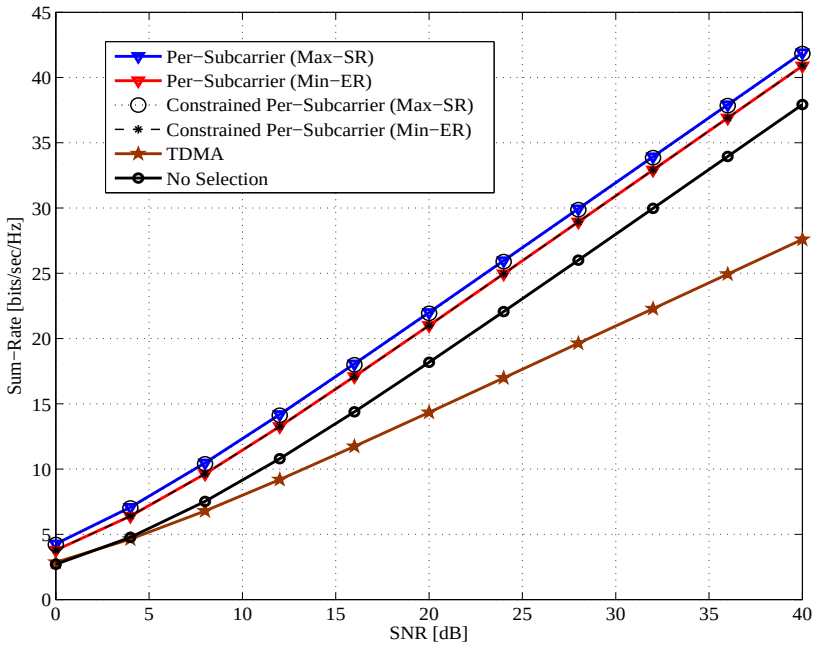

Figure 4.8: Sum-rate performance of constrained per-subcarrier selection using analytical channels.

For high frequency selective scenarios, it can be concluded that per-subcarrier selection efficiently improves the sum-rate and error-rate of MIMO-OFDM IA systems compared to the other IA approaches with power balancing among the different antennas. This evaluation is suited to multiband ultra wide band (MB-UWB) systems because their bands are highly selective.

4.7.2 Measured and Deterministic Channels

We consider in this part a realistic scenario in an indoor environment. We present the sum-rate and error-rate performance of the measured and deterministic channels. We mention again here that the measured channel realizations are collected for only one setup of transmitting and receiving nodes, while the deterministic channel realizations are collected for random positions of the transmitters and receivers in the considered environment. Therefore, the deterministic channels can provide an averaged performance for the considered environment.

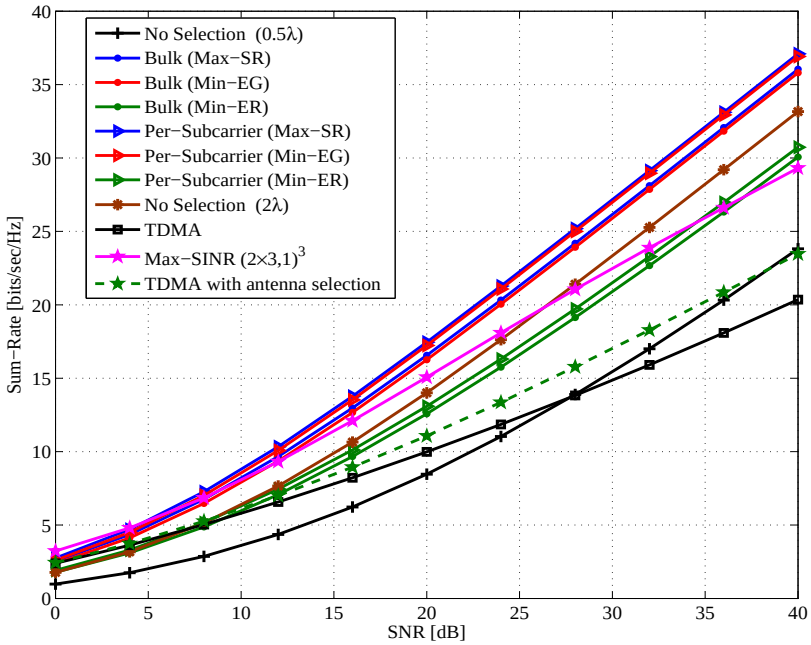

Figure 4.9: Sum-rate comparison between different antenna selection strategies using deterministic channels.

Fig. 4.9 exhibits the sum-rate performance for the different antenna selection techniques using deterministic channels. In this scenario, Fig. 4.9 shows that TDMA sum-rate outperforms IA sum-rate without antenna selection in the regime below 28 dB, which means that IA without antenna selection fails to achieve the promised theoretical result. The closely $\lambda/2$ spaced antennas exhibit significant spatial correlation across antennas, which causes high SNR loss after alignment. However, an appreciable sum-rate improvement can be observed by using Max-SR and Min-EG antenna selection techniques compared to TDMA and IA without antenna selection. Fig. 4.9 shows that Max-SR and Min-EG approaches based on per-subcarrier selection achieve the best sum-rate performance. Furthermore, bulk selection successes to offer better sum-rate than IA without antenna selection with small gain difference compared to per-

subcarrier selection. The convergence performance between bulk and per-subcarrier selection comes as a consequence of the correlation between the subcarriers that resulted from the used bandwidth in generating the deterministic and measured channels. It is clear that antenna selection technique increases the DoF of IA systems in such channels since this technique improves the multiplexing gain of MIMO channels, which is translated into the increase of the slope of antenna selection curves. As claimed in [26], Fig. 4.9 shows that increasing the separation between the antennas to 2λ within each node can improve the performance of IA. However, with Max-SR antenna selection technique, we achieve higher sum-rate performance with only $\lambda/2$ antenna separation. Moreover, Max-SR and Min-EG through bulk selection with 2 RF chains exhibit better sum-rate performance and less hardware complexity than Max-SINR, which requires more hardware complexity (3 RF chains). For more illustration, Fig. 4.10 introduces the cumulative distribution function (CDF) of the sum-rate for all antenna selection approaches at practical SNR value equals 12 dB. This figure states that antenna selection technique improves the sum-rate distribution.

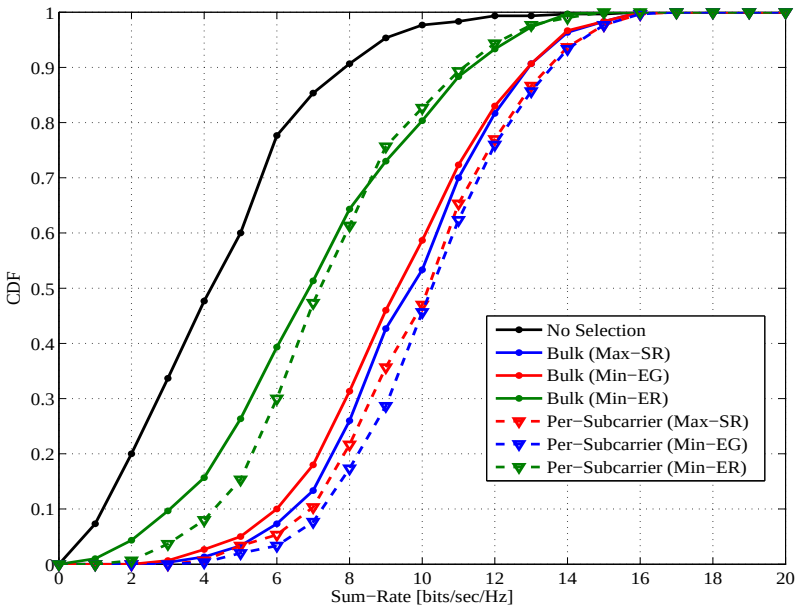

Figure 4.10: Comparison of sum-rate distribution between different antenna selection strategies using deterministic channels.

Fig. 4.11 presents the effect of applying the constrained per-subcarrier antenna selection algorithm on sum-rate performance. The performance is degraded according to the limited number of subcarriers on each antenna and the high correlation between subcarriers. For more clarification, the average percentage of SNR loss per subcarrier after performing Algorithm 4.3

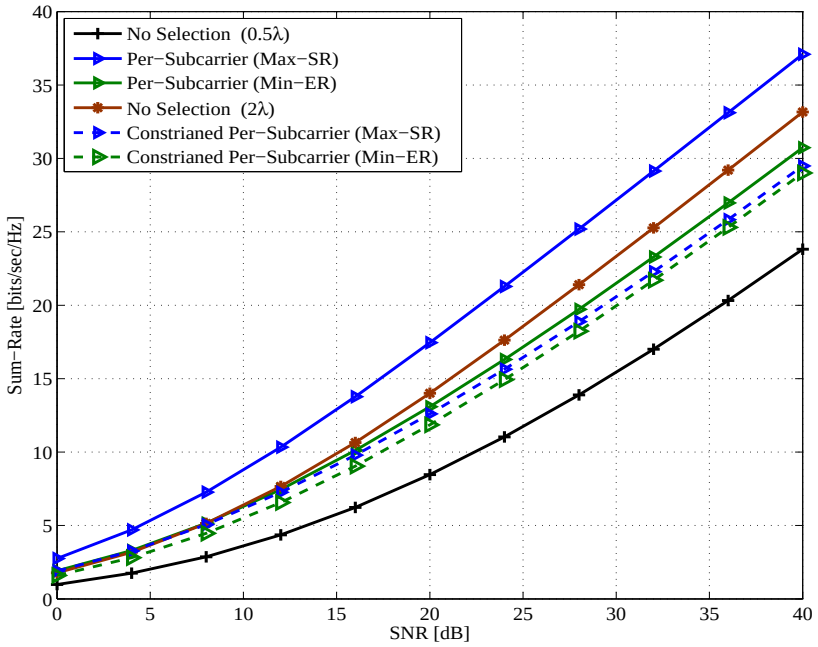

Figure 4.11: Sum-rate performance of constrained per-subcarrier selection using deterministic channels.

is presented in Fig. 4.12. We observe from this figure that the average SNR loss per-subcarrier due to the reallocation process is 12%. Hence, the reallocation process cannot guarantee the small rate loss. Therefore, antenna selection through per-subcarrier selection is not effective when the subcarriers are highly correlated channels, since it causes either overloaded antennas in the non-constrained case or performance degradation in the constrained case.

Fig. 4.13 shows the bit error-rate performance for the different antenna selection techniques, where Min-ER based on per-subcarrier selection introduces the minimum error-rate performance. By comparing antenna selection criteria that are based on bulk selection, we observe that bulk selection improves the error-rate compared to the no selection case. Therefore, Min-ER and Min-EG criteria are able to improve the error-rate performance of MIMO-OFDM IA systems.

Fig. 4.14 presents the sum-rate performance of measured channels using the Max-SR antenna selection criterion through bulk selection. It can be observed that TDMA sum-rate outperforms IA sum-rate without antenna selection. However, IA with Max-SR bulk antenna selection technique achieves a significant sum-rate improvement compared to TDMA and IA without antenna selection. The identical behaviour for deterministic channels was presented in Fig. 4.9. Therefore, we can conclude that 3D ray-tracing channels can characterize the performance of measured channels. Further, we use the deterministic channels to evaluate the

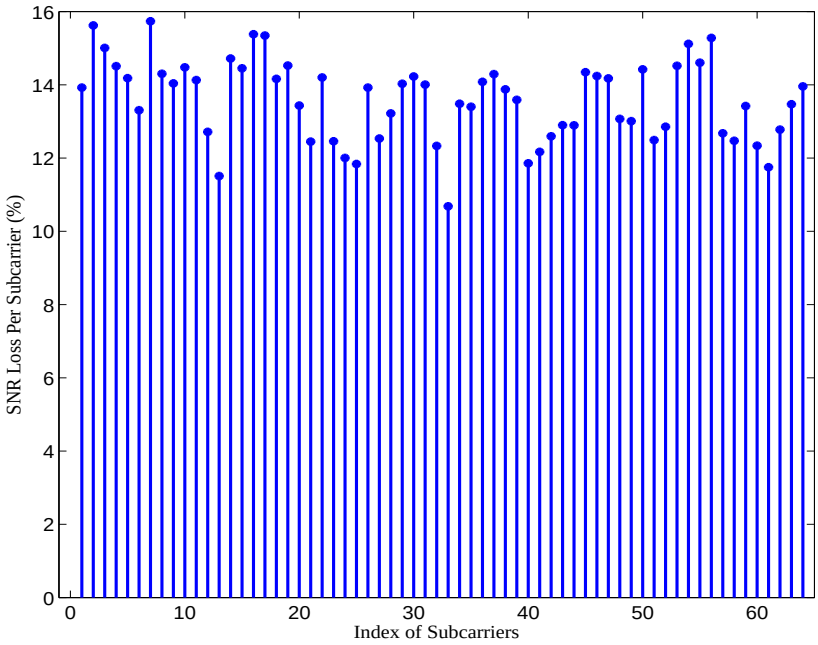

Figure 4.12: Averaged SNR loss per-subcarrier after applying constrained antenna selection of Algorithm 4.3 using deterministic channels in MIMO-OFDM IA system.

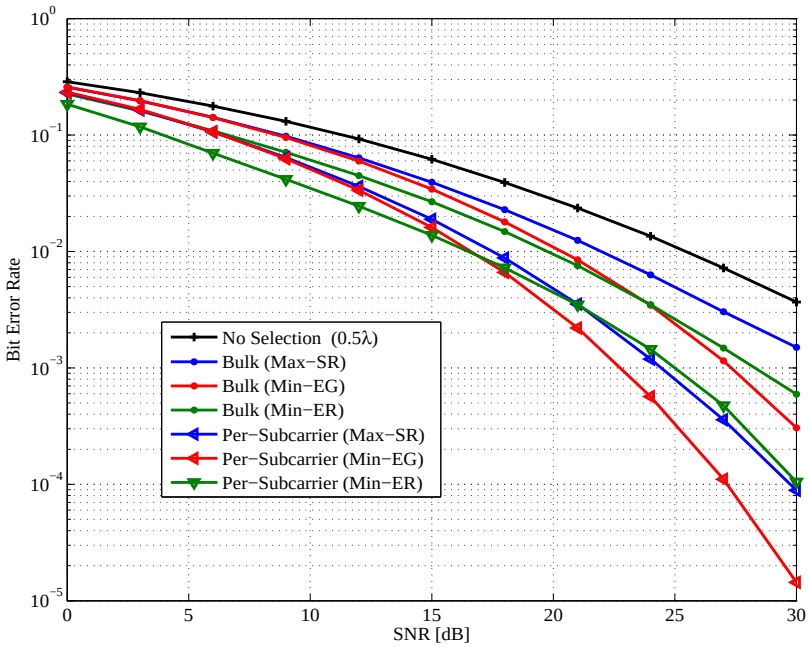

Figure 4.13: Bit error-rate comparison between different antenna selection strategies using deterministic channels.

performance of antenna selection since we can obtain averaged performances.

It is concluded that bulk selection can significantly improve sum-rate and error-rate with less complexity and without the need for power-balancing consideration when the subcarriers are correlated.

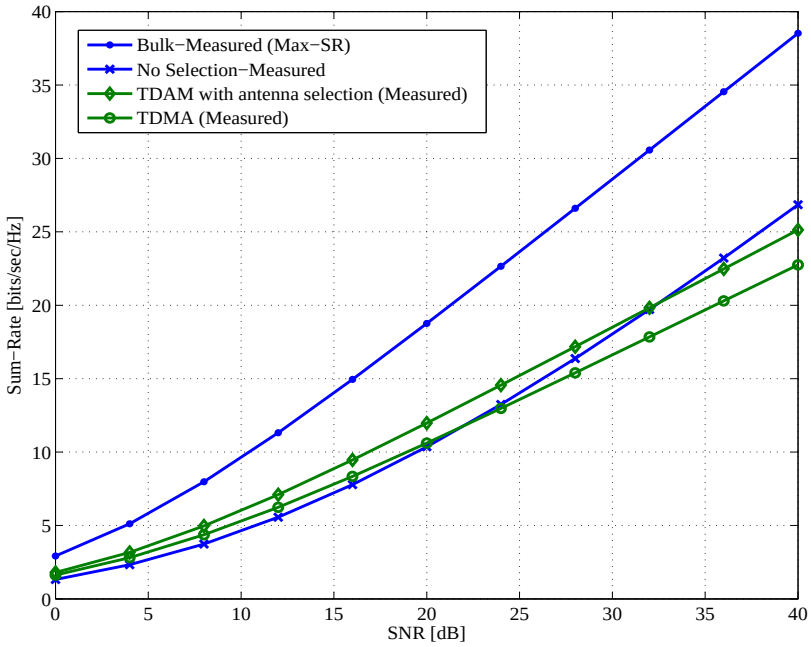

Figure 4.14: Sum-rate performance of measured channels using Max-SR bulk selection criterion.

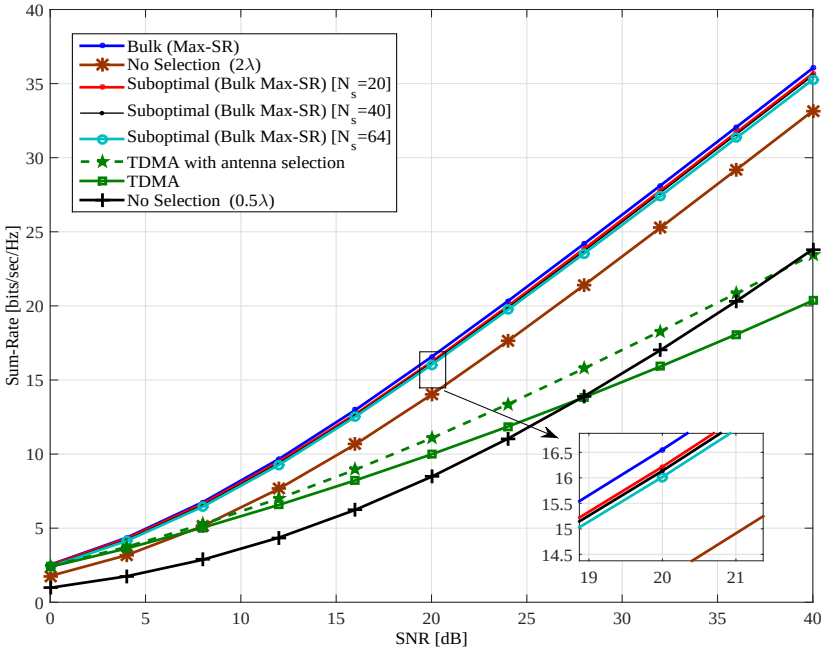

Figure 4.15: Sum-rate for sub-optimal Max-SR bulk selection using deterministic channels.

4.7.3 Performance of The Sub-Optimal Antenna Selection

Fig. 4.15 shows the performance of the sub-optimal bulk antenna selection technique using Max-SR selection criterion for different N_s values using deterministic channels. Generally,

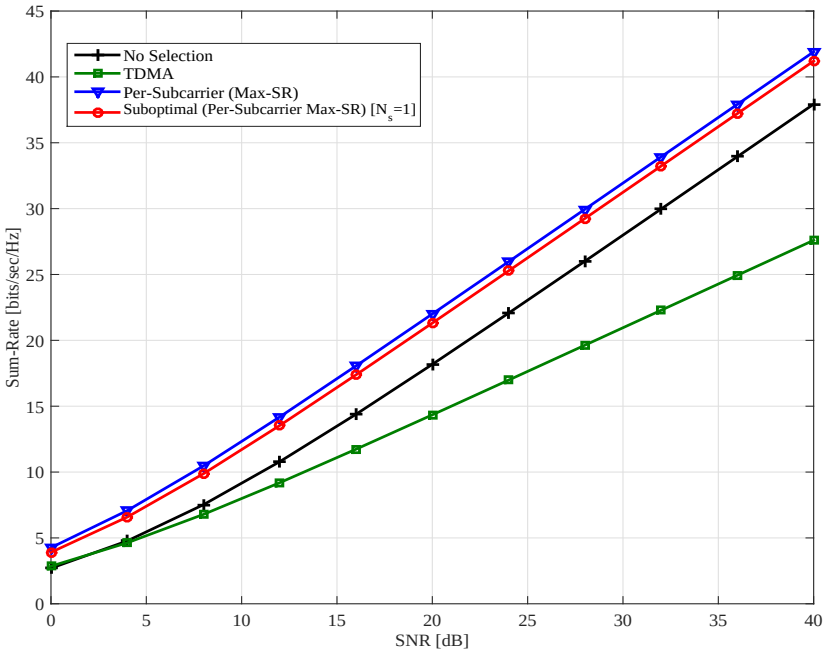

Figure 4.16: Sum-rate for sub-optimal Max-SR per-subcarrier selection using analytical channels.

the sub-optimal algorithm achieves a very close performance to the exhaustive search method with less computational complexity. Moreover, performing antenna selection for one subcarrier every 20 subcarriers ($N_s = 20$) only causes a loss of 0.2 bps/Hz compared to the optimal Max-SR bulk selection. As a worst case, if the antenna selection is executed only for one subcarrier among all subcarriers ($N_s = 64$), approximately 0.6 bps/Hz is lost. However, the sub-optimal algorithm with $N_s = 64$ offers better sum-rate performance for MIMO-OFDM IA system compared to IA system with no selection and 2λ spaced antennas. Therefore, the sub-optimal algorithm is considered efficient to perform antenna selection algorithm with minimal computational complexity.

Fig. 4.16 presents the sub-optimal per-subcarrier selection using Max-SR selection criterion for analytical channels when $N_s = 1$. It is noted that the sup-optimal algorithm achieves a very close sum-rate to the optimal one, which proves the efficiency of the algorithm for all kinds of channels. Therefore, we conclude that the sub-optimal algorithm is efficient under all channel circumstances, and it opens the door for a hybrid combination between bulk and per-subcarriers algorithm depending on the channel circumstances and subcarriers correlation.

Our evaluation concludes that antenna selection can play an important role in enhancing the practical feasibility of MIMO-OFDM IA systems under real-world channels.

5 Interference Alignment Based Resource Management in Cognitive Radio Networks

In this chapter, we investigate the resource management problem in multicarrier MIMO cognitive radio systems. We perform IA based resource allocation in order to improve the spectral efficiency of cognitive radio systems without disturbing the primary system transmission. Moreover, we consider in problem formulation the power budget of the cognitive users as well as the throughput fairness among the cognitive users. This problem is formulated as a mixed-integer problem which has a high computational complexity. Therefore, an efficient sub-optimal algorithm is proposed to reduce the computational complexity of the optimal problem through two phases. The performance of the proposed technique is evaluated and compared to cognitive radio systems with orthogonal multiple access transmission techniques. The contents of this chapter have been partially published in references [118–122].

5.1 Introduction

The governmental agencies are currently using a static spectrum licensing model to regulate the frequency allocation. By this model, the spectrum is divided into several bands that are generally allocated exclusively to specific users or services. As conducted by practical measurements, this model leads to inefficient utilization of the spectrum since it was shown by Federal Communications Commission (FCC) that the actual spectrum usage varies between 15% and 85% based on location and time variations [123, 124]. This is considered as a reason for spectrum scarcity, which bounds the increasing demand for the frequency spectrum and, hence, the rapid growth of communication services. Cognitive radio is proposed to overcome the spectrum underutilization problem by introducing a new licensing scheme that allows a group of users called non-licensed, secondary users (SUs), to access the vacant portion of the spectrum left by the licensed users, also called primary users (PUs), without affecting the performance of the

licensed system or inducing harmful interference to it [27, 28].

To support and guarantee efficient spectrum sharing between the primary and cognitive networks, the cognitive radio system must possess cognitive capabilities to monitor the surrounding environment and adopt its transmission aiming at restricting interference harming the primary system. Therefore, cognitive radio is required to perform three main functions: spectrum sensing, spectrum analysis and spectrum decision. In spectrum sensing, the cognitive radio monitors its radio environment to identify the unoccupied spectrum bands, captures their information and then detects the spectrum holes that can be used for the cognitive radio transmission in a particular time, frequency and location [123, 125]. Spectrum analysis function analyzes the characteristics of the detected spectrum holes, the probability of the PU appearance and the possible sensing errors in order to determine whether these holes are suitable for SUs operation [126]. Whereas in spectrum decision, the appropriate band is selected and, then, the cognitive radio has to optimize the available system resources in order to achieve the required objective [126]. Once the operating spectrum band is decided, the communication can be performed over this spectrum band. However, because the radio environment changes over time and space, the cognitive radio should keep track of the changes of the radio environment. If the current spectrum band in use becomes unavailable, searching for another available spectrum band is performed to provide a continuous transmission.

Multicarrier transmission schemes, like OFDM and filter bank multicarrier (FBMC), offer several advantages over the single carrier scheme in cognitive radio context. Multicarrier schemes provide high spectral efficiency and robustness in selective fading channels. Additionally, they offer more flexibility in distributing the system resources among the different users and subcarriers [127]. Furthermore, multicarrier systems have the ability to operate in discontinues portions of the spectrum and have the capability to control the transmission parameters to avoid inducing severe interference to the PUs, which make it very attractive for the cognitive radio applications. OFDM is the most common multicarrier technique that is considered by several communication standards including IEEE 802.22 TV based cognitive radio system [128]. However, OFDM has large frequency-domain sidelobes that cause high mutual interference to the adjacent primary bands [128]. Additionally, the overall spectrum efficiency of the OFDM system is reduced due to the use of the cyclic prefix that is added to combat the multipath propagation effect. From another side, FBMC can overcome the spectral leakage problem by minimizing the sidelobes of each subcarrier, which leads to high efficiency in terms of spectrum and interference. Furthermore, cyclic prefix is not required any more in FBMC

systems since the channels are designed in the frequency domain to have the required spectral containment [128–130]. In this regards, combining MIMO technology with multicarrier transmission can increase the diversity gain and accordingly the system data-rate. Thereby, MIMO multicarrier systems have been considered recently as a promising candidate for cognitive radio systems [29].

The resource allocation problem in the non-cognitive multicarrier MIMO systems was widely considered in the literature (e.g. [131–134] and references therein). Using of the previously proposed algorithms for the non-cognitive scenarios is not always effective in the cognitive radio scenarios because the limitation introduced by interference constraints to the cognitive radio system should be taken into consideration. Therefore, consideration of the cognitive radio regulations in resource allocation problem was considered in [29, 127, 135–137]. Optimum power allocation with beamforming is performed to maximize the capacity without violating the interference and power constraints in [29, 127]. A game theory based decentralized approach was proposed in [135] to design a cognitive MIMO transceivers, which compete with each other to maximize their date-rate. In [136], the DoF provided by the MIMO is utilized to construct a cooperative paradigm that can be applied by the SUs to simultaneously relay the PUs traffic and transmit their own traffic over the same accessed band. Nguyen and Krunz in [137] reformulated the non-convex resource allocation optimization problem into a distributed non-cooperative game, in which a set of precoding matrices is designed at each of the cognitive radio nodes to maximize the capacity without affecting the primary system transmission.

Recently, IA as a means of effective interference management has received much of interest in cognitive radio systems. In this context, IA was investigated in cognitive radio systems with MIMO employment on both PUs and SUs in order to allow SUs to utilize both free and non-free eigenmodes of PUs. This employment helps in removing the interference constraints from the optimization problem since it assumes that the PUs cooperate with the SUs and can suppress the received interference at the primary side [138–142]. In [138], the authors considered only one MIMO SU link to coexist with one MIMO PU link aiming at that the SU achieves the same transmission rate as of the PU. This work was extended in [139] by redesigning the decoding matrix of the SU receiver in order to combat PU interference in a more effective manner, where the SU is enabled to compute blindly the required CSI. Similarly, the work in [140] enables one SU to share the unused eigenmodes of the PU considering the power and interference constraints. In the same way, the work in [141] considered MIMO employment at SUs and a PU with frequency scheduling. In [142], the authors formulated the cooperative spectrum leasing

with IA into a Stackelberg game, where the PU is the leader, and SUs are followers. This work assumed feasible IA system, which is not always valid. The aforementioned works assumed the existence of a certain level of coordination and cooperation between cognitive and primary systems. Nevertheless, the cooperation between the primary and cognitive systems is not always guaranteed, and it requires a permission from the primary system to denote some of its DoF to the SUs. Furthermore, to the best of the authors' knowledge, overloaded cognitive radio networks -where IA problems are infeasible- have not been considered in the literature. Additionally, because of the challenges associated with joint power and spectrum optimization, most existing works on MIMO IA cognitive radio systems do not consider resource management over the multicarrier systems (frequency dimension) as it is not fairly trivial.

In this chapter, IA with frequency-clustering is proposed in overloaded cognitive radio systems in order to improve the spectral efficiency of MIMO cognitive radio systems while protecting the primary system performance. The tackled system model considers a practical scenario by assuming that there is no coordination between the cognitive and the primary network. IA based resource management problem in cognitive radio systems is formulated, where the using of IA increases the DoF per SU by enabling the SUs to effectively share the available spectrum. In the problem formulation, each subcarrier is assigned to a feasible number of SUs in order to meet the IA feasibility conditions, where the fair distribution of the resources among the different SUs is taken into account. Considering that there is no coordination between the primary and the cognitive systems, the primary system should be protected from receiving severe induced interference from the cognitive radio systems by ensuring that the received interference is below a prescribed limit. Accordingly, several interference constraints are added to the optimization problem. As the computational complexity of the optimal scheme is quite high, the paper further proposes an efficient sub-optimal resource allocation algorithm with two phases. In the first phase, frequency-clustering method is employed in order to assign each subcarrier to a feasible number of SUs with fairness consideration. Frequency-clustering operation considers the interference channel qualities of the subcarriers as well as the generated interference to PUs. In the second phase, the power is allocated among all subcarriers and SUs considering the power budget of the SUs and the interference limits at the PUs.

The rest of this chapter is organized as follows. The system model is described and the optimization problem is formulated in Section 5.2. Section 5.3 presents the phase of frequency-clustering with and without fairness consideration. The optimal and the sub-optimal power allocation algorithm are introduced in Section 5.4. The computational complexity illustration

is presented in Section 5.5. Finally, simulation setups and results are discussed in Section 5.6.

5.2 IA Based Resource Management Problem Formulation

5.2.1 System Model

In this work, a secondary communication system with K SUs is considered, where each SU has one transmitter with M_T antennas in order to communicate with one receiver with M_R antennas. The assumed secondary system is co-located with a primary system in the same geographical area. The PUs are assumed to be equipped with M_P antennas. The side-by-side frequency distribution of active and non-active bands is assumed as shown in Fig. 5.1. The active primary system bands represent the portions of the spectrum already occupied by the PUs while the non-active bands refer to the vacant bands that can be used by SUs. L active PU bands ($W_1, W_2, ..., W_L$) are assumed. Additionally, the non-active bands are divided into N equal subcarriers each with Δf bandwidth. The SUs are connected to a local gateway, which works as a centralized controller and is in charge of the resource management task of the network. Fig.5.2 shows an example of 6 SUs, in which the transmission of the different SUs causes interference to the PUs as well as to the other unintended SU receivers. The induced interference should not exceed the prescribed limit of the allowable interference that can be tolerated by each PU, i.e. I_{th}^{l}. The numbers above the arrows represent the frequency-clustering that will be described later.

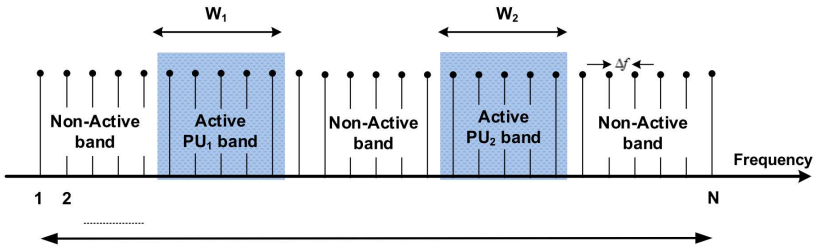

Figure 5.1: Frequency distribution of active and non-active bands.

In our model, the transmission on a given subcarrier is not restricted to one user at a given time. Rather, different SUs are allowed to share the different subcarriers by employing IA. Accordingly, the interference between SUs is managed by generating different precoding matrices based on MIMO IA technique [14, 16]. By considering a multicarrier technique, the frequency orthogonality can be achieved between subcarriers, which enables the independent application

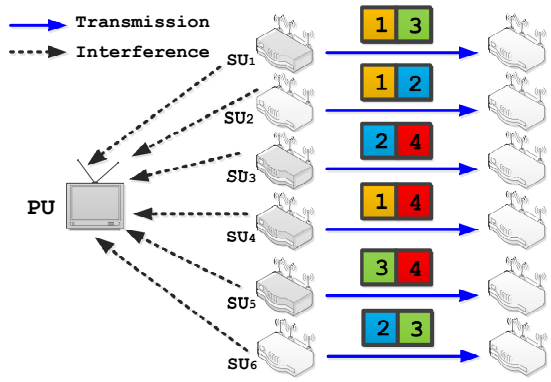

Figure 5.2: Example of a cognitive radio network with 6 SU pairs. Different numbers and colors denote different subcarriers.

of IA on each subcarrier. Each SU transmitter sends d data streams to its intended receiver. The transmitted data stream $\mathbf{x}_k^n \in \mathbb{C}^{d\times 1}$ over the n^{th} subcarrier is multiplied by the precoder matrix $\mathbf{V}_k^n \in \mathbb{C}^{M_T\times d}$. By assuming a perfect CSI of the SUs at each node, the discrete-time complex received signal at the k^{th} receiver over the n^{th} subcarrier is represented as

$$\mathbf{y}_k^n = \mathbf{U}_k^{n\mathrm{H}}\left[\mathbf{H}_k^n\mathbf{V}_k^n\mathbf{x}_k^n + \sum_{j=1,j\neq k}^{K}\mathbf{H}_{kj}^n\mathbf{V}_j^n\mathbf{x}_j^n + \mathbf{z}_k^n + \sum_{l=1}^{L}\mathbf{w}_{l,k}^n\right], \tag{5.1}$$

where $\mathbf{U}_k^n \in \mathbb{C}^{M_R\times d}$ is an orthonormal linear interference suppression matrix applied at the k^{th} SU receiver, $\mathbf{H}_{kj}^n \in \mathbb{C}^{M_R\times M_T}$ denotes the channel frequency response between the j^{th} SU transmitter and the k^{th} SU receiver. $\mathbf{S}_k^n = \mathbb{E}\left[\mathbf{x}_k^n\mathbf{x}_k^{n\mathrm{H}}\right] \in \mathbb{R}^{d\times d}$ is the input covariance matrix of the k^{th} SU at the n^{th} subcarrier and can be expressed as $\mathbf{S}_k^n = \mathrm{diag}\left(P_{k,n}(1),..,P_{k,n}(d)\right)$, where $P_{k,n}(i)$ is the allocated power to the i^{th} data stream at the k^{th} user over the n^{th} subcarrier. Therefore, the transmitted power by the k^{th} SU user over the n^{th} subcarrier is $P_{k,n} = \mathrm{Tr}\left(\mathbf{S}_k^n\right)$. $\mathbf{z}_k^n \in \mathbb{C}^{M_R\times 1}$ is the AWGN at the k^{th} SU receiver with zero mean and variance of σ_{AWGN}^2. $\mathbf{w}_{l,k}^n \in \mathbb{R}^{M_T\times 1}$ is the interference signal introduced from the l^{th} PU band over the n^{th} subcarrier to the k^{th} SU with power $J_{l,k}^n$, that can be expressed as [143]

$$J_{kl}^n\left(Dn\right) = \sum_{m=1}^{M_R}\sum_{i=1}^{M_P}\left(\int_{Dn-\Delta f/2}^{Dn+\Delta f/2}\left|g_{kl}^{n,m,i}\right|^2\psi_l\left(e^{j\omega}\right)\,d\omega\right), \tag{5.2}$$

where Dn represents the spectral distance between the n^{th} cognitive radio subcarrier and l^{th} PU band. $\psi_l\left(e^{j\omega}\right)$ is the power spectral density (PSD) of the l^{th} PU signal, and $g_{kl}^{n,m,i}$ is the channel gain between the m^{th} SU antenna at the k^{th} SU receiver and the i^{th} antenna at the l^{th} PU over

the n^{th} subcarrier.

Similarly, the interference introduced by the k^{th} SU transmitter over the n^{th} cognitive radio subcarrier transmission to the l^{th} PU receiver can be expressed as [143]

$$I_{lk}^{n}\left(Dn, P_{k,n}\right) = \sum_{m=1}^{M_T}\sum_{i=1}^{M_P}\left(\int_{Dn-W_l/2}^{Dn+W_l/2}\left|g_{lk}^{n,i,m}\right|^2 P_{k,m,n}\Phi^{n}\left(f\right)\,df\right), \tag{5.3}$$

where $P_{k,m,n}$ denotes the power transmitted from the m^{th} transmit antenna of the k^{th} SU over subcarrier n, and Φ^n is the PSD of the n^{th} subcarrier. Eq. (5.3) can be reformulated into

$$I_{lk}^{n}\left(Dn, P_{k,n}\right) = \mathrm{Tr}\left(\Omega_l^n \mathbf{G}_{lk}^{n}\mathbf{V}_k^n\mathbf{S}_k^n\mathbf{V}_k^{n\mathrm{H}}\mathbf{G}_{lk}^{n\,\mathrm{H}}\right), \tag{5.4}$$

where $\mathbf{G}_{lk}^{n} \in \mathbb{C}^{M_p\times M_T}$ denotes the channel gain between the k^{th} SU transmitter and the l^{th} PU over the n^{th} subcarrier, and Ω_l^n is the interference factor of the n^{th} subcarrier to the l^{th} PU, which is represented as

$$\Omega_l^n = \int_{Dn-W_l/2}^{Dn+W_l/2}\Phi^{n}\left(f\right)\,df\,. \tag{5.5}$$

It is also assumed that all the cognitive radio system has the perfect information of interference channel gains $\mathbf{G}_{lk}^{n}$. Practically, the cognitive radio system is able to obtain the information through periodic sensing of pilot signal from the primary system by assuming the channel reciprocity [144, 145].

Assuming perfect IA is achieved, the received signal in (5.1) becomes

$$\mathbf{y}_k^n = \mathbf{U}_k^{n\mathrm{H}}\mathbf{H}_{kk}^{n}\mathbf{V}_k^n\mathbf{x}_k^n + \mathbf{U}_k^{n\mathrm{H}}\left[\mathbf{z}_k^n + \sum_{l=1}^{L}\mathbf{w}_{l,k}^n\right]. \tag{5.6}$$

The term $\mathbf{U}_k^{n\mathrm{H}}\mathbf{z}_k^n$ follows the distribution of AWGN with zero mean and variance of σ_{AWGN}^2. Moreover, using the central limit theorem, $\sum_{l=1}^{L}\mathbf{w}_{l,k}^n$ can be modeled as AWGN which is a general assumption in this research area (e.g. [146] and references therein). Therefore, we can describe $\sigma_k^{n2} = \sigma_{AWGN}^2 + \sum_{l=1}^{L} J_{kl}^n$. Accordingly, the total sum-rate of the SUs over the n^{th} subcarrier is

$$R_T^n = \sum_{k=1}^{K} R_k^n\left(\mathbf{H}_{kk}^n, S_k^n\right), \tag{5.7}$$

where R_k^n is the capacity of the k^{th} SU user over the n^{th} subcarrier and can be expressed as

$$R_k^n\left(\mathbf{H}_{kk}^n, \mathbf{S}_k^n\right) = \log_2 \left| \mathbf{I}_d + \frac{1}{\sigma_k^{n2}} \mathbf{U}_k^{n\mathrm{H}} \mathbf{H}_{kk}^n \mathbf{V}_k^n \mathbf{S}_k^n \mathbf{V}_k^{n\mathrm{H}} \mathbf{H}_{kk}^{n\ \mathrm{H}} \mathbf{U}_k^n \right|. \tag{5.8}$$

5.2.2 Problem Formulation

In resource management problem formulation, our objective is to maximize the total throughput of the multicarrier MIMO cognitive radio system subject to the interference introduced to the PUs and transmit power budget constraints. Moreover, the problem formulation guarantees the fairness among the SUs by considering per-SU minimum throughput constraints. IA allows the SUs to share the spectrum resources simultaneously, which increases the DoF of the cognitive radio system. However, this advantage of using IA is restricted by IA feasibility conditions in (2.40) and (2.41) since perfect IA can be attained up to a certain number of SUs $\bar{K}$, where $\bar{K} = \frac{M_T + M_R}{d} - 1$. Therefore, the formulation of IA based resource allocation problem should consider this limitation by scheduling only $\bar{K}$ SUs to share a given subcarrier. Furthermore, the interference from SUs to PUs should be considered in the formulation since no coordination is assumed between the cognitive radio and the primary system. The problem can be formulated as

$$P1: \max_{\mathbf{S}_k^n, w_k^n} \sum_{n=1}^{N} \sum_{k=1}^{K} w_k^n R_k^n\left(\mathbf{H}_{kk}^n, \mathbf{S}_k^n\right) \tag{5.9a}$$

$$\text{s.t.}: \sum_{n=1}^{N} w_k^n \mathrm{Tr}\left(\mathbf{S}_k^n\right) \leq P_k \quad \forall k \tag{5.9b}$$

$$\mathbf{S}_k^n \geq 0, \qquad \forall n \text{ and } \forall k \tag{5.9c}$$

$$\sum_{n=1}^{N} \sum_{k=1}^{K} w_k^n \Omega_l^n \mathrm{Tr}\left(\mathbf{G}_{lk}^n \mathbf{V}_k^n \mathbf{S}_k^n \mathbf{V}_k^{n\mathrm{H}} \mathbf{G}_{lk}^{n\ \mathrm{H}}\right) \leq I_{th}^l, \ \forall l \tag{5.9d}$$

$$w_k^n \in \{0,1\} \ \forall k, n \tag{5.9e}$$

$$\sum_{k=1}^{K} w_k^n = \bar{K} \ \forall n \tag{5.9f}$$

$$\sum_{n=1}^{N} w_k^n R_k^n\left(\mathbf{H}_{kk}^n, \mathbf{S}_k^n\right) \geq R_{\min}\ , \forall k, \tag{5.9g}$$

where w_k^n is a binary variable that indicates whether the n^{th} subcarrier is allocated to the k^{th} SU. $w_k^n = 1$ if and only if the n^{th} subcarrier is allocated to the k^{th} SU and zero implies

otherwise. The constraint (5.9b) represents the k^{th} SU total power constraint (P_k), while a positive transmission power at each antenna is guaranteed by (5.9c). The constraint (5.9d) ensures that the total interference induced by the SUs to the l^{th} PU is below the prescribed interference threshold I_{th}^{l}. The equality condition $\sum_{k=1}^{K} w_k^n = \bar{K}$ in (5.9f) ensures that any given subcarrier can be shared by only $\bar{K}$ SU links. This constraint of (5.9f) accomplishes the IA feasibility conditions and, consequentially, perfect IA can be achieved. The last constraint in (5.9g) ensures that the fairness among the SUs is guaranteed by assuming that every SU has a minimum instantaneous rate of $R_{\min}$.

The optimization problem in $P1$ is a mixed-integer optimization problem, where the mixed-integer nature comes from the integer constraint in (5.9e) that is used for SUs scheduling. Moreover, the minimum throughput constraints in (5.9g) increase the complexity of the problem since the cognitive radio system may not be able to satisfy this minimum rate due to the limitation introduced by the interference and power budget constraints as well as the channel qualities. Therefore, the complexity of the optimal scheme is generally prohibitive as detailed in Section 5.5. To solve the resource allocation Problem $P1$ efficiently with low computational complexity, a two-phase sub-optimal algorithm is proposed. In the first phase, for overloaded secondary systems where the number of SUs doesn't satisfy IA feasibility conditions, IA frequency-clustering is performed in order to schedule $\bar{K}$ SUs per subcarrier with fairness consideration. This phase can guarantee feasible and perfect IA on each subcarrier [147, 148]. Afterwards, the available power is distributed among users and subcarriers without violating the interference constraints in the second phase. Moreover, the minimum throughput constraints in (5.9g) are relaxed by minimizing the number SUs whose rates are below the minimum, i.e. reducing the outage probability of having SUs whose rates are below the minimum. In the sequel, detailed description of the two phases is provided.

5.3 Phase I: Frequency-Clustering

This phase is required to be performed in the case of having an overloaded cognitive radio system, where the number of SUs K doesn't satisfy the IA feasibility conditions. As perfect IA cannot be obtained in this case, frequency-clustering algorithm is executed to cluster the SUs into feasible groups from IA point of view. As an example for frequency-clustering, consider that 6 SUs are operated with $M_R = M_T = 2$ and $d = 1$ over $N = 4$ subcarriers as seen in Fig. 5.2. This network is considered overloaded since it does not satisfy the feasibility condition of

$M_T + M_R - (K+1)d \geq 0$. Therefore, IA frequency-clustering is performed, and the users are scheduled according to the numbers above the arrows in Fig.5.2. This means that SU_1, SU_2 and SU_4 are scheduled to use the first subcarrier while the second subcarrier is shared between SU_2, SU_3 and SU_6.

In this section, we propose an algorithm for frequency-clustering operation by considering not only their channel quality and per-user power budget constraints but considering also the induced interference to the PU band. Moreover, fairness among the SUs is guaranteed by assuming that every SU has a minimum instantaneous rate of R_{min}.

5.3.1 Frequency-Clustering without Fairness Consideration

In this part, we consider frequency-clustering without fairness consideration. Two power distributions are assumed in order to consider the power-limited regime as well as the interference-limited regime. These power distributions only benefit the clustering operation, where the actual power allocation is executed in the second phase. In the power-limited regime, the power allocation among the subcarriers is mainly restricted by the SUs power budgets. In this case and assuming that all the SUs are allocated to equal number of subcarriers, the power budget of each SU is equally distributed among the subcarriers, where the allocated power for the k^{th} user at the n^{th} subcarrier is expressed as

$$P_{k,n}^{\text{UF}} = \frac{KP_k}{\bar{K}N}. \tag{5.10}$$

In the interference-limited regime, the power allocation is mainly restricted by the interference threshold of the primary system. Hence, we assume that the generated interference to the primary system, i.e. I_{th}^l, is equally distributed among the different subcarriers [146]. Consequently, by using (5.4) and (5.5), the maximum power, $P_{k,n}^{\text{D}}$, that can be allocated to the n^{th} subcarrier at the k^{th} SU is

$$P_{k,n}^{\text{D}} = \frac{dI_{th}^l}{N\bar{K}\Omega_l^n \text{Tr}\left(\mathbf{V}_k^{n\text{H}}\mathbf{G}_{lk}^{n\ \text{H}}\mathbf{G}_{lk}^n\mathbf{V}_k^n\right)}. \tag{5.11}$$

The description of the clustering phase can be commenced by defining $\mathcal{A}$ and $\mathcal{N}$ to be the sets that contain all the non-assigned subcarriers and assigned subcarriers, respectively. Furthermore, $\mathcal{B}$ denotes the set of all SUs and $\mathcal{C} = \{c(1), .., c(A_\mathcal{C})\}$ to be the sets of all possible clustering combinations where $A_\mathcal{C}$ refers to the number of clusters while $c(i) \in \mathcal{C}$ refers to the group of SUs inside the i^{th} cluster. Each cluster has $\bar{K}$ SUs and, hence, $\mathcal{C}$ can be formed by generating all the possible combinations of $\bar{K}$ users from SUs in the set $\mathcal{B}$. Each cluster must

Algorithm 5.1 IA Frequency-Clustering without Fairness Consideration

Initialize $\mathcal{A} = \{1, 2, \cdots, N\}$, $\mathcal{B} = \{1, 2, \cdots, K\}$ and $\mathcal{N} = \emptyset$.
Find $\mathcal{C}$ from $\mathcal{B}$.
$n = \mathcal{A}(1)$; (the first element in $\mathcal{A}$).
while $\mathcal{A}$ is not empty **do**
    for all $c(i) \in \mathcal{C}$ **do**
        for all $k \in c(i)$ **do**
            Find $\mathbf{V}_k^n$ and $\mathbf{U}_k^n$.
            Evaluate $P_{k,n}^{UF}$ and $P_{k,n}^{D}$ using (5.10) and (5.11), respectively.
            Let $P_{k,n}^{F} = \min\left(P_{k,n}^{D}, P_{k,n}^{UF}\right)$.
        end for
        Evaluate $R_T^n = \sum_{k \in c(i)} R_k^n \left(\mathbf{H}_{kk}^n, P_{k,n}^F\right)$.
    end for
    Find the set $c_n^* = \max_{c(i)} \sum_{k \in c(i)} R_k^n \left(\mathbf{H}_{kk}^n, P_{k,n}^F\right)$, set $w_k^n = 1 \; \forall k \in c(i)$.
    Move n from $\mathcal{A}$ to $\mathcal{N}$ and Set $n = n + 1$.
end while

satisfy that $c(i) \neq c(j) \; \forall (i \neq j)$.

For each subcarrier, the cluster that has the maximum sum-rate after performing IA is selected considering the power-limited and interference-limited regimes. For a specific subcarrier, we determine to which regime a given SU is restricted. If $P_{k,n}^{D}$ exceeds $P_{k,n}^{UF}$, i.e. $P_{k,n}^{D} \geq P_{k,n}^{UF}$, then the power allocation for the SU is power-limited and, hence, the allocated power $P_{k,n}^{F}$ is fixed to $P_{k,n}^{UF}$. Otherwise, the power allocation is interference-limited, and the allocated power $P_{k,n}^{F}$ is fixed to $P_{k,n}^{D}$. Hence, the considered allocated power in clustering operation can be expressed as

$$P_{k,n}^{F} = \min\left(P_{k,n}^{D}, P_{k,n}^{UF}\right). \tag{5.12}$$

Accordingly, for the n^{th} subcarrier, the cluster selection process can be formulated mathematically to select c_n^* as

$$c_n^* = \max_{c(i)} \sum_{k \in c(i)} R_k^n \left(\mathbf{H}_{kk}^n, P_{k,n}^F\right). \tag{5.13}$$

The users inside this cluster are the only allowed SUs in the system to transmit over that subcarrier.

The criterion of clustering is now illustrated in (5.12) and (5.13). Follows, the selection

mechanism is described. The subcarriers are sequentially assigned to clusters. Initially, all the possible cluster combinations $\mathcal{C}$ are generated using the SUs in the set $\mathcal{B}$. To allocate a given subcarrier, the algorithm evaluates the allocated power $P_{k,n}^{F}$ using (5.12). Afterwards, the subcarrier is allocated to the cluster c_n^* that achieves the maximum sum-rate according to (5.13), and then this subcarrier is moved to the set $\mathcal{N}$. The scheme is repeated until the allocation of all subcarriers in order to find the selected clusters for all subcarriers, $\mathcal{X} = \{c_1^*, .., c_N^*\}$. The clustering procedures are summarized in Algorithm 5.1.

5.3.2 Frequency-Clustering with Fairness Consideration

With fairness consideration, the mechanism of Algorithm 5.1 is modified in order to consider the fairness among SUs. Update the definition of $\mathcal{B}$ to be the set that contains all SUs whose rates are below R_{min}, and define $\mathcal{U}$ to be the set of SUs whose rates are greater than R_{min}. Moreover, we define $\Delta = \{\Delta_1, .., \Delta_K\}$ to be the instantaneous rates for all SUs. In this method, (5.12) and (5.13) are used for frequency-clustering. The algorithm starts by sequentially allocating the subcarriers that are located next to the PU band and moving towards the distant ones since the subcarriers close to the PU bands will potentially use low transmit power even that they have good channel conditions. Keeping those subcarriers to the end of the assignment in the frequency clustering algorithm will make them suffer not only from the transmission power limitation but also from the low diversity in choosing the users from the set of users whose instantaneous rate below the minimum. The subcarriers are assigned sequentially to clusters. Initially, the possible cluster combinations are generated using the SUs in the set $\mathcal{B}$, where $\mathcal{B}$ is assumed to contain all SUs at the beginning. Throughout the allocation of the different subcarriers, if the rate of the k^{th} SU becomes more than the minimum required rate R_{min}, the user will be moved form the set $\mathcal{B}$ to the set $\mathcal{U}$. If the minimum rate constraints are satisfied for all the users, i.e. $\mathcal{B}$ is empty, the subcarrier can be allocated to one of the clusters that are generated from SUs in the set $\mathcal{U}$, which will contain all SUs at this moment. To allocate a given subcarrier, the algorithm initially forms all cluster combinations of the SUs in the set $\mathcal{B}$ and evaluates the allocated power $P_{k,n}^{F}$ using (5.12). Afterwards, the subcarrier is allocated to the cluster c_n^*, that achieves the maximum sum-rate according to (5.13), and this subcarrier is moved to $\mathcal{N}$. Then, the instantaneous rates Δ of the SUs in c_n^* is updated, and the SUs whose rates are greater that the minimum required rate R_{min} are moved form the set $\mathcal{B}$ to the set $\mathcal{U}$. The scheme is repeated until the allocation of all subcarriers among the clusters, $\mathcal{X} = \{c_1^*, .., c_N^*\}$. The clustering procedures are summarized in Algorithm 5.2.

Algorithm 5.2 IA Frequency-Clustering with Fairness Consideration

Initialize $\mathcal{A} = \{1, 2, \cdots, N\}$, $\mathcal{B} = \{1, 2, \cdots, K\}$, $\mathcal{N} = \emptyset$, $\mathcal{U} = \emptyset$ and $\Delta = \{0, 0, .., 0\}$.
while $\mathcal{A}$ is not empty **do**
    Find $\mathcal{C}$ from $\mathcal{B}$.
    $n = \mathcal{A}(1)$; (the first element in $\mathcal{A}$).
    for all $c(i) \in \mathcal{C}$ **do**
        for all $k \in c(i)$ **do**
            Find $\mathbf{V}_k^n$ and $\mathbf{U}_k^n$.
            Evaluate $P_{k,n}^{UF}$ and $P_{k,n}^{D}$ using (5.10) and (5.11), respectively.
            Let $P_{k,n}^{F} = \min\left(P_{k,n}^{D}, P_{k,n}^{UF}\right)$.
        end for
        Evaluate $R_T^n = \sum_{k \in c(i)} R_k^n \left(\mathbf{H}_{kk}^n, P_{k,n}^F\right)$.
    end for
    Find the set $c_n^* = \max_{c(i)} \sum_{k \in c(i)} R_k^n \left(\mathbf{H}_{kk}^n, P_{k,n}^F\right)$, set $w_k^n = 1 \; \forall k \in c(i)$.
    Update the instantaneous rates Δ for the SUs $\forall k \in c_n^*$.
    If $\Delta_k \geq R_{min}$, move SU k from $\mathcal{B}$ to $\mathcal{U}$. **If** $\mathcal{B}$ is empty, set $\mathcal{B} = \{1, 2, \cdots, K\}$.
    Move n from $\mathcal{A}$ to $\mathcal{N}$ and Set $n = n + 1$
end while

5.4 Phase II: Power Allocation Algorithm

By performing the frequency-clustering phase, the subcarriers are allocated to the different clusters. Therefore, the subcarrier indicators w_k^n are already determined from the previous phase. Therefore, the power allocation problem can be formulated as follows

$$P2: \max_{\mathbf{S}_k^n} \sum_{n=1}^{N} \sum_{k \in c_n^*} R_k^n \left(\mathbf{H}_{kk}^n, \mathbf{S}_k^n\right) \tag{5.14a}$$

$$\text{s.t.}: \sum_{n=1}^{N} \text{Tr}\left(\mathbf{S}_k^n\right) \leq P_k \quad \forall k \tag{5.14b}$$

$$\mathbf{S}_k^n \geq 0, \qquad \forall n \text{ and } \forall k \tag{5.14c}$$

$$\sum_{n=1}^{N} \sum_{k \in c_n^*} \Omega_l^n \text{Tr}\left(\mathbf{G}_{lk}^n \mathbf{V}_k^n \mathbf{S}_k^n \mathbf{V}_k^{n\text{H}} \mathbf{G}_{lk}^{n\,\text{H}}\right) \leq I_{th}^l, \;\; \forall l \tag{5.14d}$$

Since $\mathbf{U}_k^{n\mathrm{H}}\mathbf{H}_{kk}^n\mathbf{V}_k^n$ is considered as the effective channel and has a rank of d, the sum rate in (5.8) can be formulated using spectral decomposition into

$$R_k^n\left(\mathbf{H}_{kk}^n, P_{k,n}(i)\right) = \sum_{i=1}^{d} \log_2\left(1 + \frac{P_{k,n}(i)\nu_i^2\left(\mathbf{U}_k^{n\mathrm{H}}\mathbf{H}_{kk}^n\mathbf{V}_k^n\right)}{\sigma_k^{n2}}\right), \tag{5.15}$$

where $\nu_i\left(\mathbf{U}_k^{n\mathrm{H}}\mathbf{H}_{kk}^n\mathbf{V}_k^n\right)$ is the i^{th} eigenvalue of $\mathbf{U}_k^{n\mathrm{H}}\mathbf{H}_{kk}^n\mathbf{V}_k^n$. Further, we denote $\nu_i\left(\mathbf{U}_k^{n\mathrm{H}}\mathbf{H}_{kk}^n\mathbf{V}_k^n\right)$ as $\nu_{k,i}^n$. Therefore, the power allocation problem can be formulated as follows

$$P3: \max_{P_{k,n}(i)} \sum_{n=1}^{N}\sum_{k\in c_n^*}\sum_{i=1}^{d} \log_2\left(1 + \frac{P_{k,n}(i)\nu_{k,i}^n}{\sigma_k^{n2}}\right) \tag{5.16a}$$

$$\text{s.t.}: \sum_{n=1}^{N}\sum_{i=1}^{d} P_{k,n}(i) \le P_k \quad \forall k \tag{5.16b}$$

$$P_{k,n}(i) \ge 0, \qquad \forall n \text{ and } \forall k \tag{5.16c}$$

$$\sum_{n=1}^{N}\sum_{k\in c_n^*}\sum_{i=1}^{d} \Omega_l^n P_{k,n}(i)\bar{g}_k^n(i) \le I_{th}^l, \ \forall l, \tag{5.16d}$$

where $\bar{g}_k^n(i)$ is the i^{th} element in the diagonal of matrix $\bar{\mathbf{G}}_k^n = \mathbf{V}_k^{n\mathrm{H}}\mathbf{G}_{lk}^{n\,\mathrm{H}}\mathbf{G}_{lk}^n\mathbf{V}_k^n$.

In this context, the optimal power allocation is presented in the next part. Then, an efficient sub-optimal power allocation algorithm is proposed to reduce the computational complexity of the optimal one.

5.4.1 Optimal Power Allocation

In this part, the optimal power allocation is found. Since Problem $P3$ is convex, the Lagrangian can be written as

$$\begin{aligned}\mathcal{L} = &-\sum_{n=1}^{N}\sum_{k\in c_n^*}\sum_{i=1}^{d} \log_2\left(1 + \frac{1}{\sigma_k^{n2}}P_{k,n}(i)\nu_{k,i}^n\right) + \sum_{k=1}^{K}\beta_k\left(\sum_{n=1}^{N}\sum_{i=1}^{d} P_{k,n}(i) - P_k\right) \\ &+ \sum_{l=1}^{L}\eta^l\left(\sum_{n=1}^{N}\sum_{k\in c_n^*}\sum_{i=1}^{d}\Omega_l^n P_{k,n}(i)\bar{g}_k^n(i) - I_{th}^l\right) - \sum_{n=1}^{N}\sum_{k=1}^{K}\sum_{i=1}^{d} P_{k,n}(i)\vartheta_k^n,\end{aligned} \tag{5.17}$$

where β_k, η^l and ϑ_k^n are the non-negative Lagrange multipliers. The Karush-Kuhn-Tucker (KKT) conditions can be described as follows

$$P_k^n \geq 0;\ \beta_k \geq 0;\ \eta^l \geq 0;\ \vartheta_k^n \geq 0 \tag{5.18a}$$

$$\beta_k \left(\sum_{n=1}^{N} \sum_{i=1}^{d} P_{k,n}(i) - P_k \right) = 0,\ \forall k \tag{5.18b}$$

$$\eta^l \left(\sum_{n=1}^{N} \sum_{k \in c_n^*} \sum_{i=1}^{d} \Omega_l^n P_{k,n}(i) \bar{g}_k^n(i) - I_{th}^l \right) = 0,\ \forall l \tag{5.18c}$$

$$\frac{\partial \mathcal{L}}{\partial P_{k,n}(i)} = \frac{-1}{\frac{\sigma_k^{n\,2}}{\nu_{k,i}^n} + P_{k,n}(i)} + \sum_{k=1}^{K} \beta_k + \sum_{l=1}^{L} \eta^l \Omega_l^n \bar{g}_k^n(i) - \vartheta_k^n = 0. \tag{5.18d}$$

After rearranging (5.18d), we get

$$P_{k,n}(i) = \left[\frac{1}{\sum_{l=1}^{L} \eta^l \Omega_l^n \bar{g}_k^n(i) + \sum_{k=1}^{K} \beta_k} - \frac{\sigma_k^{n\,2}}{\nu_{k,i}^n} \right]^+, \tag{5.19}$$

The optimal solution of Problem $P3$ requires high computational complexity that grows exponentially with the number of subcarriers. Therefore, the sub-optimal power allocation is proposed in the next part.

5.4.2 Sub-Optimal Power Allocation Algorithm

In this part, the sub-optimal power allocation is described through four steps, where this method allocates the power in a novel way by dividing Problem $P3$ into two sub-problems: power allocation problem considering only interference constraint and, then, a cap-limited waterfilling problem considering only the power budget of SUs. In order to make the analysis more clear and without loss of generality, we assume that each SU sends one data stream to its intended receiver. Accordingly, $\bar{g}_k^n = \mathbf{V}_k^{n\mathrm{H}} \mathbf{G}_{lk}^{n\,\mathrm{H}} \mathbf{G}_{lk}^n \mathbf{V}_k^n$. Moreover, the sum rate in (5.8) can be written as

$$R_k^n = \log_2 \left(1 + \frac{1}{\sigma_k^{n\,2}} P_{k,n} \bar{h}_k^n \right), \tag{5.20}$$

where $\bar{h}_k^n \triangleq \mathbf{U}_k^{n\mathrm{H}} \mathbf{H}_{kk}^n \mathbf{V}_k^n \mathbf{V}_k^{n\mathrm{H}} \mathbf{H}_{kk}^{n\,\mathrm{H}} \mathbf{U}_k^n$. Accordingly, the power can be allocated to SUs and subcarriers as stated in the following stages.

Step 1: In the first step, the maximum power $P_{k,n}^{\max}$ that can be allocated to the k^{th} user over the n^{th} subcarrier is determined by ignoring the per-SU power constraints and considering only the interference constraints. Therefore, by considering only the l^{th} PU interference constraint, the problem is reduced to

$$P4: \max_{\widehat{P}_{k,n}} \sum_{n=1}^{N} \sum_{k \in c_n^*} \log_2 \left(1 + \frac{1}{\sigma_k^{n2}} \widehat{P}_{k,n} \bar{h}_k^n\right) \tag{5.21a}$$

$$\text{s.t.}: \sum_{n=1}^{N} \sum_{k \in c_n^*} \Omega_l^n \, \widehat{P}_{k,n} \bar{g}_k^n \leq I_{th}^l \tag{5.21b}$$

$$\widehat{P}_{k,n} \geq 0, \qquad \forall n \text{ and } \forall k, \tag{5.21c}$$

where $(\widehat{\cdot})$ represents the variables that are optimized under the interference constraint only. By solving $P4\,; \forall l \in \{1, 2, \cdots, L\}$, we obtain

$$\widehat{P}_{k,n}^l = \left[\frac{1}{\widehat{\alpha}^l \Omega_l^n \, \bar{g}_k^n} - \frac{\sigma_k^{n2}}{\bar{h}_k^n}\right]^+, \tag{5.22}$$

where the Lagrange multiplier $\widehat{\alpha}^l$ is evaluated using (5.22) and (5.21b) as

$$\widehat{\alpha}^l = \frac{\left|N \bar{K}\right|}{I_{th}^l + \sum\limits_{n=1}^{N} \sum\limits_{k \in c_n^*} \frac{\Omega_l^n \sigma_k^{n\,2} \bar{g}_k^n}{\bar{h}_k^n}}. \tag{5.23}$$

By solving $P4$ for every interference constraint, $P_{k,n}^{\max}$ is evaluated as

$$P_{k,n}^{\max} = \min \left\{\widehat{P}_{k,n}^l\right\}_{l=1}^{L}. \tag{5.24}$$

By applying this formula, one can guarantee that the interference introduced to the PU bands is below the maximum limit. This step is expressed graphically in Fig. 5.3.a.

Step 2: Second step tests the per-SU power constraints using the maximum power $P_{k,n}^{\max}$. If the relation $\sum_{n=1}^{N} P_{k,n}^{\max} \leqslant P_k$ is satisfied for all SUs, the optimal solution of the optimization problem $P3$ is determined to be $\overline{P}_{k,n} = P_{k,n}^{\max}$ which is equal to the maximum power that can be allocated to each subcarrier. Otherwise, proceed to the next steps.

Step 3: In the third step, the power budget P_k for each SU is distributed among its allocated subcarriers subject to be lower that or equal to the power upper-bound of each user at

each subcarrier $P_{k,n}^{\max}$. The problem is formulated as a cap-limited waterfilling problem as follows [149]

$$P5: \max_{\widetilde{P}_{k,n}} \sum_{n=1}^{N} \sum_{k \in c_n^*} \log_2 \left(1 + \frac{1}{\sigma_k^{n2}} \widetilde{P}_{k,n} \bar{h}_k^n\right) \tag{5.25a}$$

$$\text{s.t.}: \sum_{n=1}^{N} \widetilde{P}_{k,n} \leq P_k \tag{5.25b}$$

$$0 \leq \widetilde{P}_{k,n} \leq P_{k,n}^{\max}, \tag{5.25c}$$

where $\widetilde{P}_{k,n}$ is the allocated power by solving problem $P5$. This problem can be solved efficiently using a successive application of the conventional waterfilling concept. As a starting point, the waterfilling solution is found as [150]

$$\widetilde{P}_{k,n}^{\text{WF}} = \left[\zeta - \frac{\sigma_k^{n2}}{\bar{h}_k^n}\right]^+, \tag{5.26}$$

where $\widetilde{P}_{k,n}^{\text{WF}}$ is the allocated power by waterfilling solution for the k^{th} user at the n^{th} subcarrier, and ζ is the waterfilling level. Thereafter, if the power allocated by waterfilling solution $\widetilde{P}_{k,n}^{\text{WF}}$ is greater than $P_{k,n}^{\max}$, the power is readjusted to $P_{k,n}^{\max}$ and the already allocated power is subtracted from the total power budget. Then, successive waterfilling is performed over the users and subcarriers that did not exceed the maximum power $P_{k,n}^{\max}$ in the last step until reaching the iteration in which $\widetilde{P}_{k,n}$ doesn't exceed $P_{k,n}^{\max}$ for any user and subcarrier. This step is described graphically in Fig. 5.3.b.

Step 4: In the last step, the allocated power per subcarrier $\widetilde{P}_{k,n}$ found by solving $P5$ is less than or equal $P_{k,n}^{\max}$. Therefore, some of the allocated power $\widetilde{P}_{k,n}$ doesn't not reach the maximum allowed power. Consequently, the system loses some of the allowed power resources as the interference constraint is not satisfied with equality which decreases the capacity of cognitive radio system. Therefore, some power can be moved from one subcarrier to another in order to enhance system throughput. This can be achieved by updating the maximum power that can be allocated to each subcarrier $P_{k,n}^{\max}$ depending on the residual interference I_R^l, which can be calculated as follows

$$I_R^l = I_{th}^l - \sum_{n=1}^{N} \sum_{k \in c_n^*} \widetilde{P}_{k,n} \Omega_l^n \bar{g}_k^n. \tag{5.27}$$

Assuming that B_l is the set of subcarriers that reach the maximum allowed power, i.e. $\widetilde{P}_{k,n} = P_{k,n}^{\max}; \forall n \in B_l$, then, $P_{k,n}^{\max}; \forall n \in B_l$ can be updated by applying the equations (5.22)-(5.24) on the subcarriers in the set B_l with the updated interference constraints, which can be evaluated as

$$I_{th}^{\prime l} = I_R^l + \sum_{n \in B_l} \sum_{k \in c_n^*} \widetilde{P}_{k,n} \Omega_l^n \bar{g}_k^n. \tag{5.28}$$

Finally, the procedures of the cap-limited waterfilling that were used to solve problem $P4$ is re-performed to find the final solution $\overline{P}_{k,n} = \widetilde{P}_{k,n}$. At this point, the solution $\overline{P}_k^n$ is approaching the optimal solution and satisfying the interference constraints with equality as well as guaranteeing that the total power budget constraints are satisfied. Fig. 5.3.c summarizes the procedures of this step graphically.

The flowcharts of the proposed power allocation algorithm is given in Fig. 5.4 and described in Algorithm 5.3.

Algorithm 5.3 Sub-Optimal Power Allocation Algorithm

1: $\forall l \in \{1, \cdots, L\}$, Find $\widehat{P}_{k,n}(l)$ using (5.22) and (5.23).
2: $\forall n$ and $\forall k$, Evaluate $P_{k,n}^{\max} = \min \left\{ \widehat{P}_{k,n}(l) \right\}_{l=1}^{L}$.
3: **if** $\sum_{n=1}^{N} P_{k,n}^{\max} \leqslant P_k; \forall k$ **then**
4: Let $\overline{P}_{k,n} = P_{k,n}^{\max}$ and stop the algorithm.
5: **end if**
6: $\forall n$ and $\forall k$, Execute the cap-limited waterfilling under the per-user constraint P_k and the maximum power that can be allocated to each subcarrier $P_{k,n}^{\max}$ and find the set B_l where $\widetilde{P}_{k,n} = P_{k,n}^{\max}$.
7: Evaluate the residual interference I_R^l using (5.27) and the updated interference constraints $I_{th}^{\prime l}$ using (5.28).
8: Perform Steps (1-2) to update $P_{k,n}^{\max}$.
9: $\forall n$ and $\forall k$, Execute the cap-limited waterfilling under the per-user constraint P_k and the updated maximum power that can be allocated to each subcarrier $P_{k,n}^{\max}$ and set $\overline{P}_{k,n} = \widetilde{P}_{k,n}$.

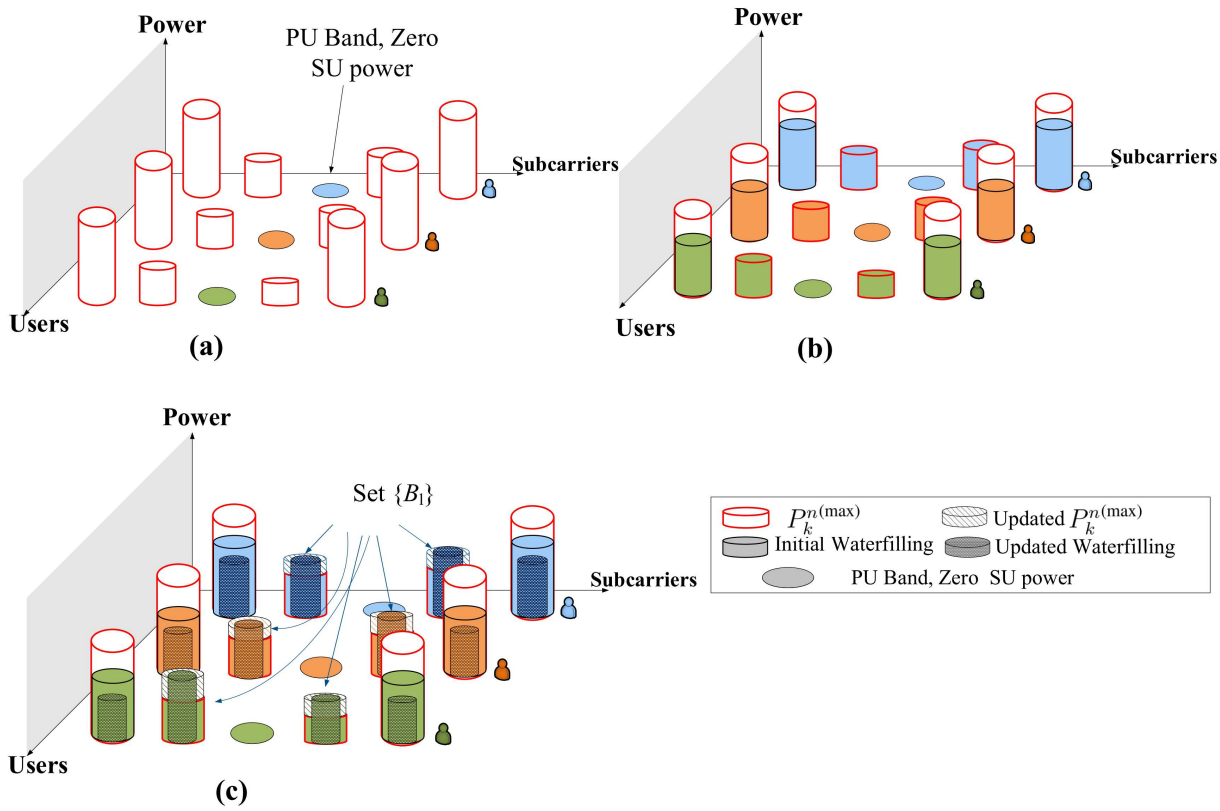

Figure 5.3: Graphical representation of the proposed power allocation algorithm.

5.5 Computational Complexity Analysis

In this section, we present the computational analysis of the optimal solution and the proposed algorithm. In terms of complexity, the optimal solution that is formulated in Problem $P1$ needs to iterate $\binom{K}{\bar{K}}^N$ times to exhaust all the cluster combinations of SUs, where the power allocation of Problem $P3$ is performed and IA solution is computed for each combination. The complexity of IA solution is dependent on the algorithm that is used to find IA solution. As an example, minimum leakage interference (MLI) method requires a complexity of $\bar{K}.T.\left[\mathcal{O}\left(M_T^3\right)+\mathcal{O}\left(M_R^3\right)\right]+\bar{K}.T.\left[2\left(\bar{K}-1\right)\left(\mathcal{O}\left(M_R M_T^2\right)+\mathcal{O}\left(M_T M_R^2\right)\right)\right]$, where T is the number of iterations in the reciprocity channel [151]. Many research work in the literature tackled the problem of designing low complexity solutions for IA as in [20, 152, 153] and references therein. The design of such solutions is out of the scope of this paper. Therefore, we denote the complexity of finding IA solution by Υ. Accordingly, the computational complexity of the

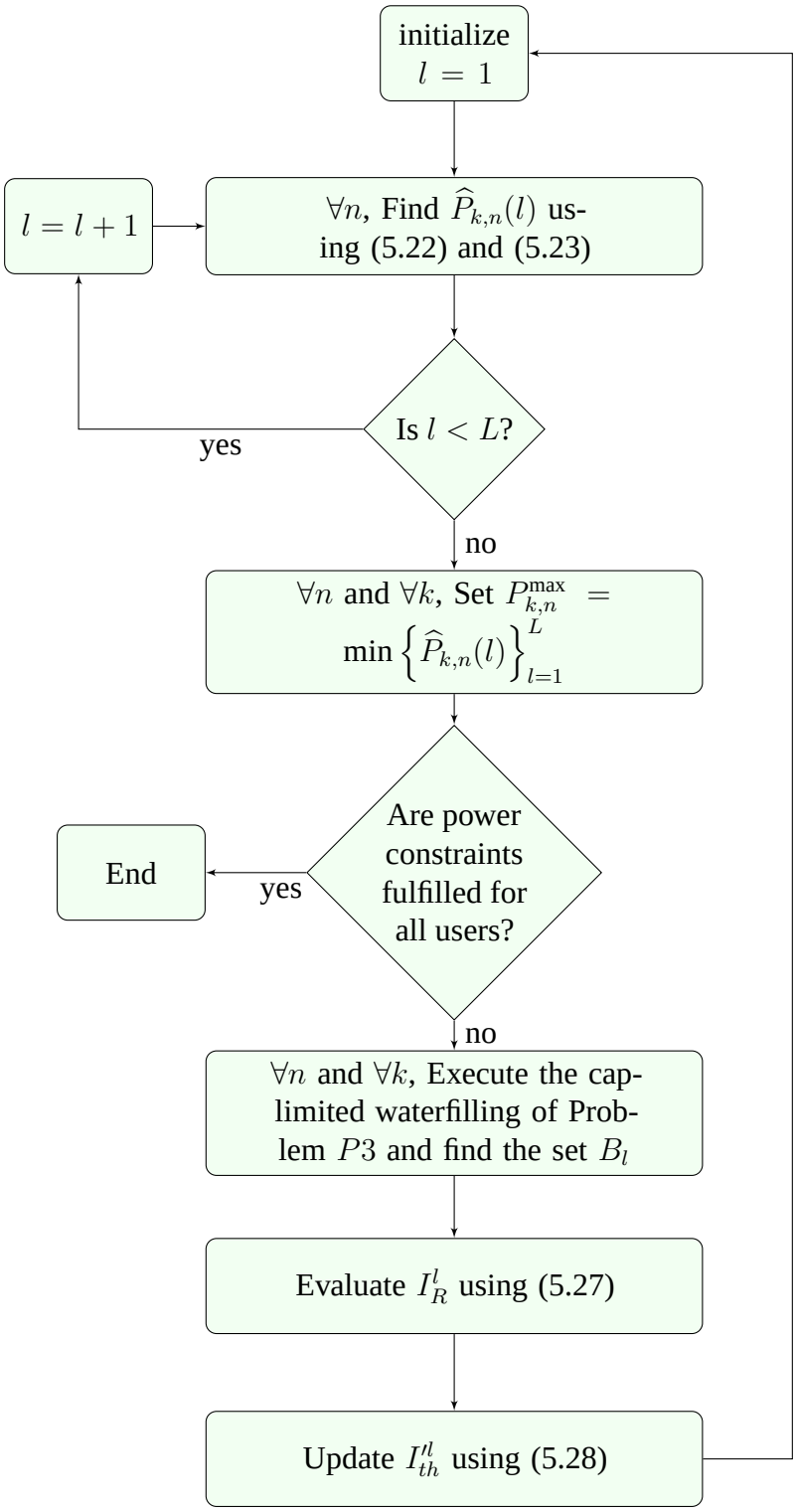

Figure 5.4: Flowchart of the sub-optimal power loading algorithm

optimal scheme is

$$\mathcal{O}\left(\binom{K}{\bar{K}}^{N} \cdot \left(\Upsilon + \left(\bar{K}dN\right)^{3}\right)\right),$$

where $\bar{K}dN$ is the number of the variables that needed to be optimized using the interior point optimization technique.

Since the complexity of the optimal scheme is very hard to afford, the sub-optimal approach is proposed through two phases as discussed before. In the frequency-clustering algorithm, a maximum of $\binom{K}{\bar{K}}$ IA solutions are found for every subcarrier. Accordingly, the complexity of frequency-clustering phase is

$$\mathcal{O}\left(\binom{K}{\bar{K}} \cdot N \cdot \Upsilon\right).$$

Referring to the sub-optimal power allocation in Algorithm 5.3, step 1 has a waterfilling like computational complexity of $\mathcal{O}\left(\bar{K}dN \log\left(\bar{K}dN\right)\right)$ [154,155]. Step 1 should be performed for L interference constraints, hence the complexity of step 1 is $\mathcal{O}\left(L\bar{K}dN \log\left(\bar{K}dN\right)\right) \leq \mathcal{O}\left(KL\bar{K}dN \log\left(\bar{K}dN\right)\right)$. Steps 6 and 9 in the algorithm execute the cap-limited waterfilling for all SUs with a complexity of $\mathcal{O}\left(\bar{K}dN \log\left(\bar{K}dN\right)\right)$. Accordingly, the complexity of steps 6 and 9 is $\mathcal{O}\left(K\bar{K}dN \log\left(\bar{K}dN\right)\right) \leq \mathcal{O}\left(KL\bar{K}dN \log\left(\bar{K}dN\right)\right)$. Step 8 has a complexity of $\mathcal{O}\left(|B_l| \log |B_l|\right) \leq \mathcal{O}\left(KL\bar{K}dN \log\left(\bar{K}dN\right)\right)$ considering all SUs. As a result of that and considering the previous steps, the computational complexity of the sub-optimal power allocation algorithm is lower than $\mathcal{O}\left(KL\bar{K}dN \log\left(\bar{K}dN\right)\right)$.

Correspondently, the complexity of the proposed sub-optimal resource allocation algorithm through the two phases is lower than $\mathcal{O}\left(\binom{K}{\bar{K}} \cdot N \cdot \Upsilon + KL\bar{K}dN \log\left(\bar{K}dN\right)\right)$, which is much lower than the computational complexity of the optimal solution.

5.6 Simulation Setup and Results

In our simulation, we investigate the performance of IA based resource management algorithms in MIMO cognitive radio systems. Two active PU bands are assumed with $W_1 = W_2 = 10$ MHz, where $I_{th}^1 = I_{th}^2$. Moreover, the non active band is located between the active bands and has 10 MHz of bandwidth. It is assumed that the cognitive radio system has K SUs with $M_T = M_R = 2$ antennas at each SU node and a single antenna at each PU node. The closed-form solution of IA is applied. The value of noise variance σ_k^{n2} is assumed to be 10^{-6}. Channel realizations have been drawn from independent and identically distributed Gaussian distribution

with zero mean and unit variance. All the results have been averaged over 1000 iterations. CVX toolbox is used to obtain the optimal solution of the optimization problems [73]. Obtaining the optimal solution of Problem $P1$, which is NP-hard problem, is very hard even for small number of subcarriers and users. For the purpose of performance comparison, the following algorithms are considered in the simulation:

1. **IA Optimal**: This scheme is used when the cognitive radio system is feasible, where $K = 3$. Therefore, frequency-clustering is not required. In this case, optimal power distribution is performed as in (5.19).

2. **IA Suboptimal**: This scheme is used when the cognitive radio system is feasible, where $K = 3$. Hence, frequency-clustering is not required. In this case, sub-optimal power distribution using Algorithm 5.3 is performed.

3. **IA FC+Optimal**: This scheme is used when the cognitive radio system is overloaded, where $K > 3$. In this case, frequency-clustering using Algorithm 5.1 and the optimal power distribution as in (5.19) are performed. The word Fairness is added between a parenthesis when frequency-clustering with fairness consideration is considered using Algorithm 5.2.

4. **IA FC+Suboptimal**: This scheme is used when the cognitive radio system is overloaded, where $K > 3$. In this case, frequency-clustering using Algorithm 5.1 and the power allocation based on Algorithm 5.3 are performed. The word Fairness is added between a parenthesis when frequency-clustering with fairness consideration is considered using Algorithm 5.2.

5. **IA RandFC+Optimal**: This scheme is used when the cognitive radio system is overloaded, where $K > 3$. In this case, random frequency-clustering and the optimal power distribution are performed.

6. **CR-FDMA**: In this scheme, the different radio resources are distributed optimally using FDMA multiple access technique as in [29].

In our simulation, OFDM and FBMC physical layers are considered. Next, a short description of them is given.

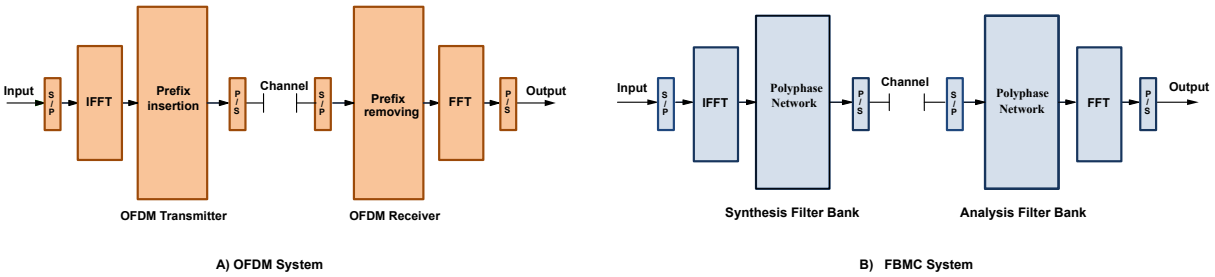

Figure 5.5: Block diagrams of OFDM and FBMC systems.

5.6.1 OFDM Physical Layer

A general block diagram of an OFDM system can be found in Fig. 5.5. Firstly, the bits are mapped into complex symbols. Then, the time domain samples of an OFDM symbol are generated using the inverse discrete Fourier transform (IDFT). After that, the cyclic prefix is added to form the transmitted signal. Assume that Φ^n is the PSD of the n^{th} subcarrier. In OFDM system with rectangular pulse of length $T_s = N + C$, where C is the length of the cyclic prefix, $\Phi^n(f)$ can be written as follows

$$\Phi^n(f) = P^n \left(T_s + 2 \sum_{r=1}^{T_s-1} (T_s - r)\, cos\,(2\pi f r) \right). \tag{5.29}$$

where P^n is the total transmit power emitted by the n^{th} subcarrier.

5.6.2 FBMC Physical Layer

In FBMC, the transmultiplexer configuration is adopted using the synthesis filter bank at the transmitter side and the analysis filter banks at the receiver side as described in Fig. 5.5 [128,129]. In FBMC systems, the use of critically sampled filter banks is problematic, since the aliasing effects would make it difficult to compensate imperfections of the channel by processing the sub-channel signals while the FBMC with the offset quadrature amplitude modulation (OQAM) OQAM/FBMC symbols can be formed by modulating each subcarrier with a staggered QAM. The basic idea of FBMC is to transmit real-valued symbols instead of transmitting complex valued ones. Due to this time staggering of the in-phase and quadrature components of the symbols, orthogonality is achieved between adjacent subcarriers.

The synthesized signal burst is therefore a composite of multiple subchannel signals. Each signal consists of a linear combination of time-shifted (by multiples of $T_s/2$) and overlapping

impulse responses of the prototype filter, weighted by the respective symbol values [129]. Note that each sub-carrier is modulated with an OQAM. OQAM inserts a shift of half the symbol period between the real and the imaginary part of the complex data symbol [129].

In FBMC systems, if the prototype filter with coefficients $b[i]$ with $i = 0, \cdots, Y-1$ is used, where $Y = Q_f N$ and Q_f is overlapping factor which represents the length of each polyphase components and under the assumption of the even symmetry of prototype coefficients around the $\left(\frac{Q_f N}{2}\right)^{th}$ coefficient with zero coefficient in the beginning, the FBMC PSD can be expressed as $\Phi^n(f) = |B_n(f)|^2$, where $|B_n(f)|$ is the frequency response of the prototype filter and can be written as [129]

$$|B_n(f)| = b[Y/2] + 2\sum_{r=1}^{\frac{Y}{2}-1} b[(Y/2) - r]\cos(2\pi f r). \tag{5.30}$$

5.6.3 Results and Discussions

The simulation results are divided into three cases: In the first case, a feasible MIMO-OFDM cognitive radio system with $K = 3$ SUs is assumed while an overloaded system is assumed in the second case with $K = 12$ SUs. The third case compares the performance of the OFDM and FBMC physical layers systems.

Case I: Feasible MIMO-OFDM cognitive radio system

In this case, a MIMO-OFDM based cognitive radio system with $K = 3$ SUs and $N = 64$ is assumed. In this case, frequency-clustering is not required since the cognitive radio system achieves IA feasibility conditions.

Fig. 5.6 presents the average sum-rate against the interference thresholds when the per-SU power budget is set to be $P_k = 15$ dBm. In general, for all scenarios, the average sum-rate increases as the interference threshold levels increase since each SU has more flexibility to allocate more power on its subcarriers. It can be observed that *IA Optimal* algorithm achieves higher sum-rate gain compared to *CR-FDMA* algorithm since IA benefits from the available DoF better than FDMA. It is further shown that *IA Suboptimal* algorithm presents very close sum-rate performance to the *IA optimal* with less complexity, which reveals the efficiency of the suboptimal power allocation algorithm. Furthermore, the sum-rate gap between IA based resource allocation algorithms and *CR-FDMA* increases with the increase of interference threshold until

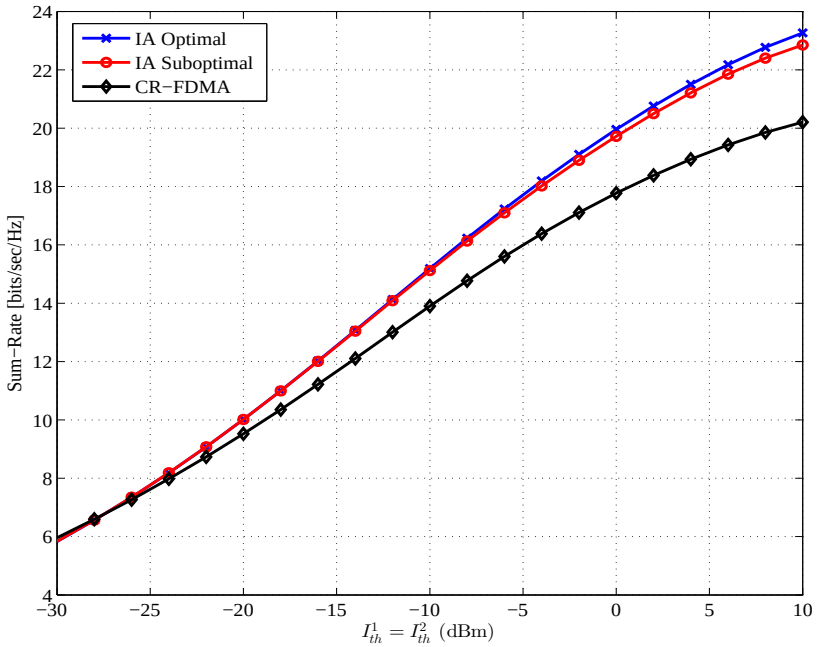

Figure 5.6: Achieved sum-rate vs. allowed interference threshold when $K = 3$, $P_k = 15$ dBm and $N = 64$.

a certain interference threshold value. After this value, the gap remains constant as the cognitive radio system behaves like a non-cognitive radio system where the interference constraint has no effect on the optimization problem.

Fig. 5.7 plots the instantaneous data rate for a given user over time for *IA Optimal* and *IA Suboptimal* algorithms compared to *CR-FDMA* when $I_{th}^1 = I_{th}^2 = -30$ dBm and $P_k = 15$ dBm. It is noted from the figure that the instantaneous rates fluctuate along the time. In *CR-FDMA*, the high values mean that this user is assigned a larger number of subcarriers compared to others, while low values mean that other users have greater number of subcarriers causing the deep rate. However, IA based resource allocation allows the 3 SUs to share all the available subcarriers, which leads to better instantaneous rate compared to *CR-FDMA*. The fluctuations in IA curves are due to the channel quality. Assuming that our rate target per SU is R_{min} = 200 bits per OFDM symbol, It is noted that *IA Optimal* and *IA Suboptimal* algorithms keep the instantaneous rate mostly above our target.

Fig. 5.8 presents the outage sum-rate probability of the different algorithms when P_k = 10 dBm, where the minimum rate for each SU is set to be R_{min} = 160 bits per OFDM symbol. Generally, outage probability decreases as the interference constraint increases since the ability of the algorithms to give the minimum instantaneous rate for the different users increases. Furthermore, the outage probability of *IA optimal* scheme is very close to *IA Optimal* one, and

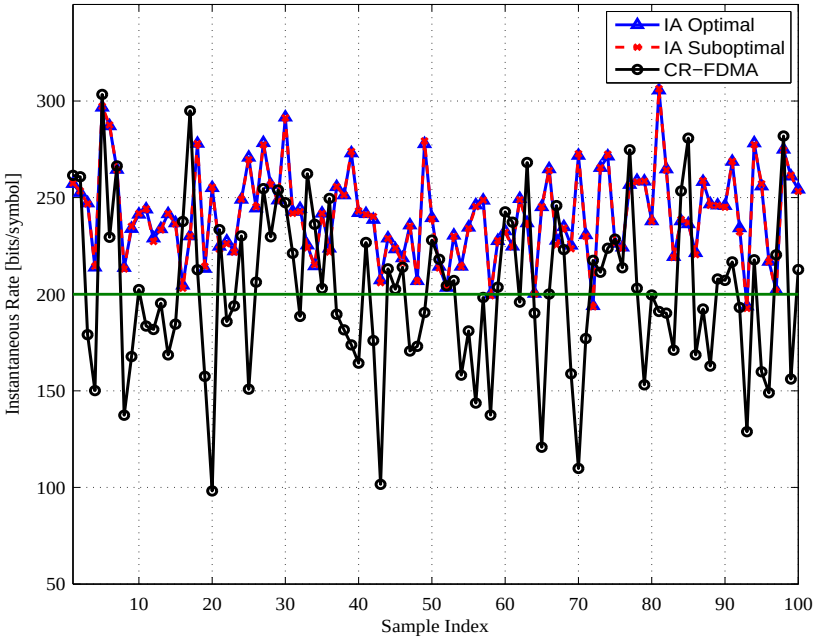

Figure 5.7: Achieved instantaneous rate when $K = 3$, $P_k = 15$ dBm, $I_{th}^1 = I_{th}^2 = -30$ dBm and $N = 64$.

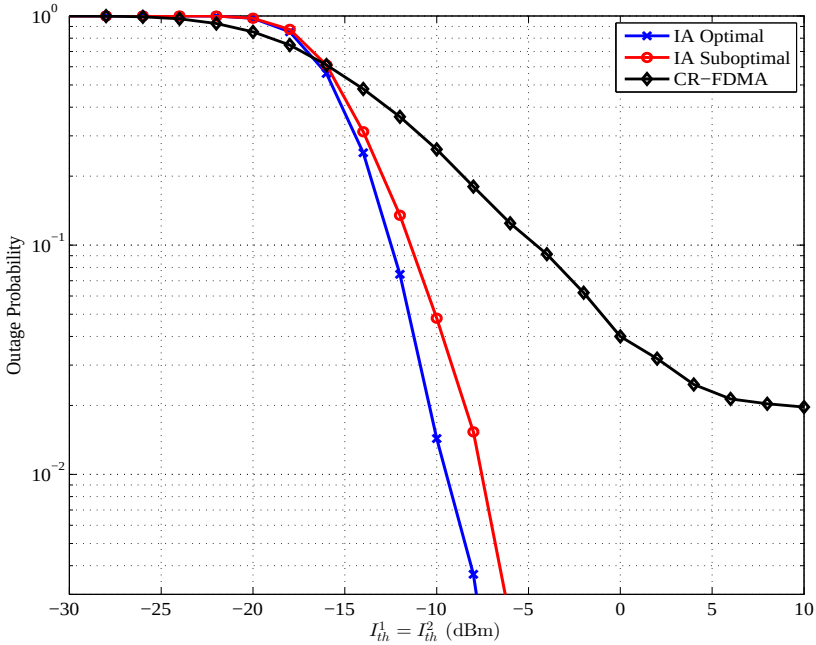

Figure 5.8: Outage probability versus interference thresholds, $K = 3$, $P_k = 10$ dBm, $N = 64$ and $R_{min} = 160$ bits/symbol.

both are much lower than that of *CR-FDMA* algorithm. It is clearly observed from Fig. 5.7 and Fig. 5.8 that IA based algorithms are able to achieve a high-level of fairness among the different

users since all the SUs share the available subcarriers.

Case II: Overloaded MIMO-OFDM cognitive radio system

In this case, a MIMO-OFDM based cognitive radio system is considered with $K = 12$ SUs and $N = 128$. Since this system is overloaded, frequency-clustering phase should be performed before power allocation phase. For fairness consideration, the minimum rate for each SU is set to be R_{min} = 150 bits per OFDM symbol.

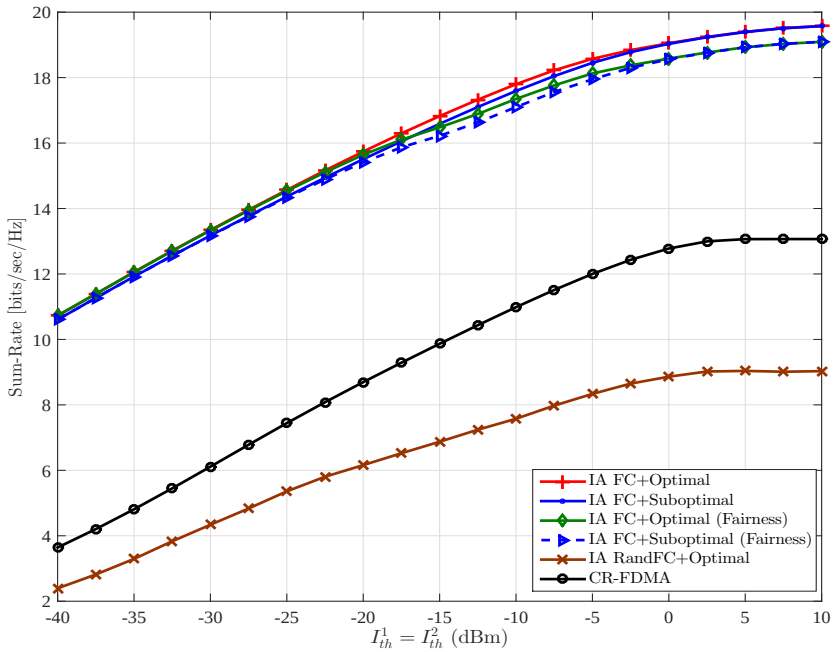

Figure 5.9: Achieved sum-rate versus allowed interference threshold when $K = 12$, $P_k = 0$ dBm and $N = 128$.

We first show the impact of the interference threshold on the average sum-rate when the per-SU power budget is set to be $P_k = 0$ dBm, as shown in Fig. 5.9. In general, for all resource allocation methods, the average sum rate increases as the interference threshold levels increase since each SU has more flexibility to allocate more power on its subcarriers. It can be observed also that *IA FC+Suboptimal* algorithm strictly matches the corresponding curves of *IA FC+Optimal*, which reveals the efficiency of the sub-optimal algorithm. It can be observed that *IA FC+Optimal* and *IA FC+Suboptimal* algorithms achieves higher sum rate in compared with *CR-FDMA* algorithm. Furthermore, the sum rate increases with the increase of interference threshold until a certain interference threshold value. After this value, the sum rate remains constant as the cognitive radio behaves like a non-cognitive radio system where the interference

constraint has no effect on the optimization problem. In low interference threshold values, the algorithms with fairness perform very close to those without fairness consideration as the fairness constraint can not be achieved with this low interference threshold value. Accordingly, the algorithm acts as there is no fairness constraint. After a certain interference constraint value (-20 dBm in the figure), the fairness constraint can be satisfied for the users. The loss in the sum rate is because of the activation of the fairness constraint. It is noted in this figure that frequency-clustering is very important for performing IA in overloaded networks since *IA RandFC+Optimal* presents very bad performance compared to all the other considered curves.

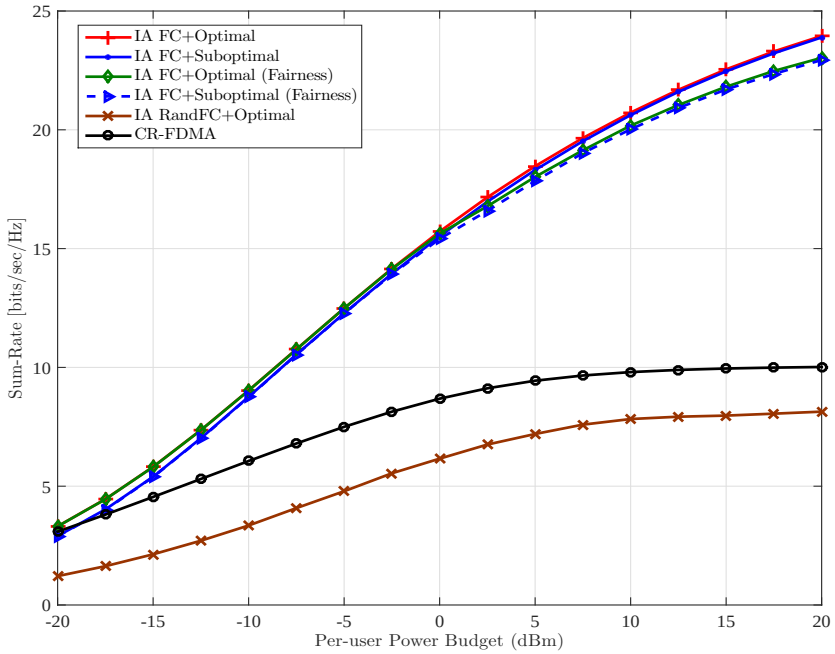

Figure 5.10: Achieved sum-rate versus per-SU power budget when $K = 12$, $I_{th}^1 = I_{th}^2 = -20$ dBm and $N = 128$.

The average sum-rate versus per-SU power constraint is presented in Fig. 5.10 where $I_{th}^1 = I_{th}^2 = -20$ dBm. The sum-rate of the cognitive radio systems increases as the per-SU power budget increases up to certain power value, afterwards the sum-rate remains constant because the cognitive radio system reaches to the maximum power that can be allocated under the interference threshold. The sum-rate of IA based resource allocation algorithms presents better performance than *CR-FDMA* curve, and the gap between them increases with the increase of the power constraints, which shows the efficiency of IA in utilizing the available resources. The behavior of the algorithms in this figure can be described according to three regions

1. When $P_k < -18$ dBm: *IA FC+Optimal* with and without fairness present the best sum-

rate performance among the algorithms. It is noted that the sub-optimal power allocation curves, *IA FC+Suboptimal* with and without fairness, cause small sum-rate loss compared to the optimal ones. This regime is considered very confined.

2. When $-18 < P_k < 0$ dBm: *IA FC+Optimal* and *IA FC+Suboptimal* curves are very close. In this regime, the algorithms with fairness perform very close to those without fairness consideration as the fairness constraint can not be achieved with this low power budget value. Accordingly, the algorithm acts as there is no fairness constraint.

3. When $P_k > 0$ dBm: In this regime, *IA FC+Optimal* and *IA FC+Suboptimal* curves are very close. It is noted in this regime that the curves of fairness consideration present small sum-rate loss compared to the non-fairness curves since the fairness constraint can be satisfied for the users.

In all the three cases, the behavior of *IA RandFC+Optimal* algorithm is very poor since frequency-clustering is performed randomly. This reveals the importance of using frequency-clustering algorithms.

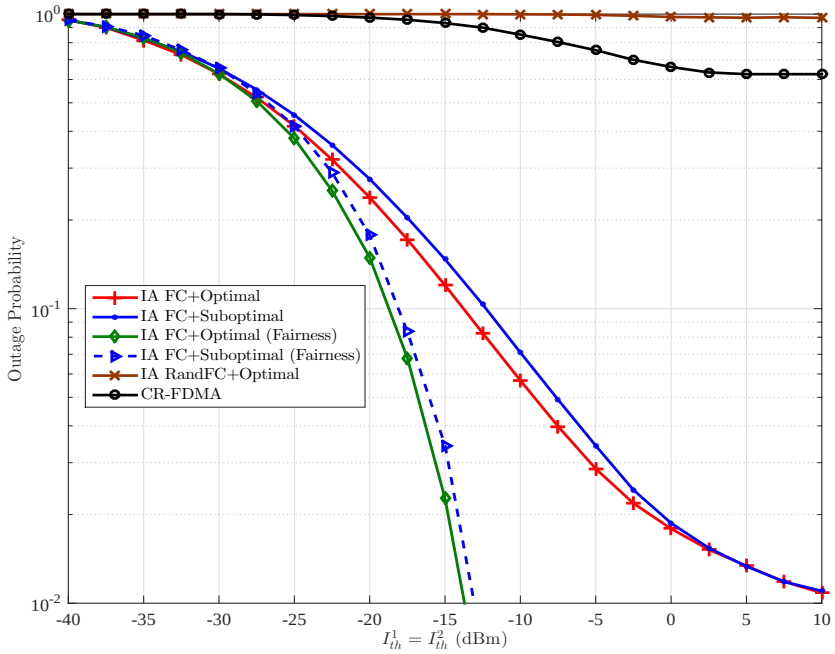

Figure 5.11: Outage probability versus interference thresholds, when $K = 12$, $P_k = 0$ dBm, $N = 128$ and $R_{min} = 150$ bits/symbol.

Fig. 5.11 presents the outage probability of the different algorithms against the interference threshold when the per-SU power budget is set to be $P_k = 0$ dBm and $R_{min} = 150$ bits/symbol.

Generally, the outage probability decreases with the increase of interference constraint as the algorithms become more able to support the instantaneous rate for the different users. Furthermore, the outage probability of *IA FC+Suboptimal* scheme is very close to *IA FC+Optimal* one, and both are much lower than that of *CR-FDMA* scheme. It is clearly observed from this figure that IA based resource allocation algorithms are able to achieve a high-level of fairness among the different users. The best outage probability is achieved, as expected, by the algorithms of fairness consideration. Again, *IA RandFC+Optimal* exhibits the worst performance compared to all simulated curves.

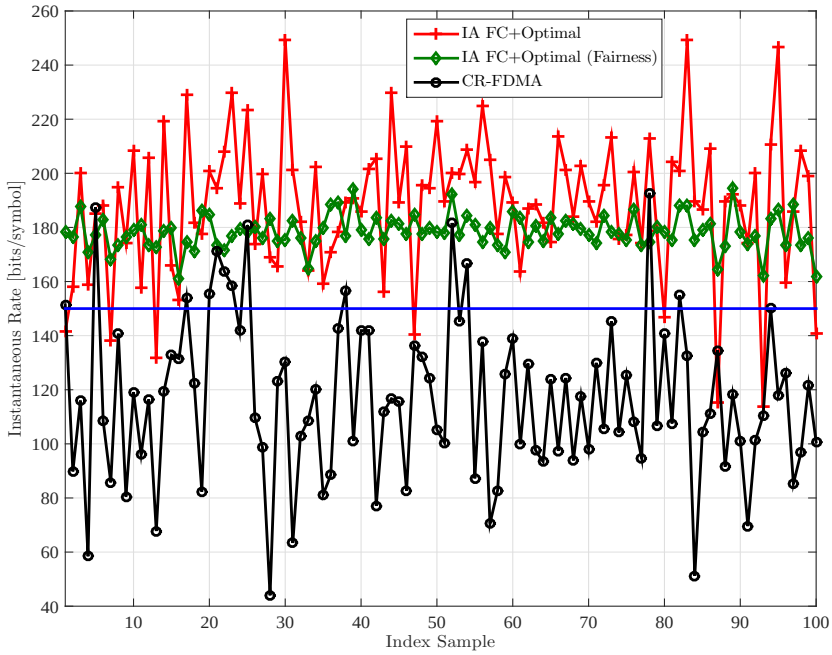

Figure 5.12: Achieved instantaneous rate when $K = 12$, $P_k = 0$ dBm, $I_{th}^1 = I_{th}^2 = -10$ dBm, $N = 128$ and $R_{min} = 150$ bits/symbol.

Fig. 5.12 plots the instantaneous rate for a given user over time when $I_{th}^1 = I_{th}^2 = -10$ dBm, $P_k = 0$ dBm and R_{min} = 150 bits per OFDM symbol. It is noted from the figure that the instantaneous rate fluctuates along the time. The high values mean that this user is assigned a larger number of subcarriers compared to others, while low values mean that other users have greater number of subcarriers causing the deep rate. Therefore, IA based resource allocation exhibits better instantaneous rate compared to *CR-FDMA* algorithm since the fluctuations of *CR-FDMA* algorithm is stronger and changes dramatically, which causes deep rate degradation at some time samples. Moreover, *IA FC+Optimal* scheme with fairness consideration presents smooth instantaneous rate compared to others, which means that the users get fair allocation of

the subcarriers. Clearly, *IA FC+Optimal* method with fairness always achieves better rate than the minimum unlike the other compared methods.

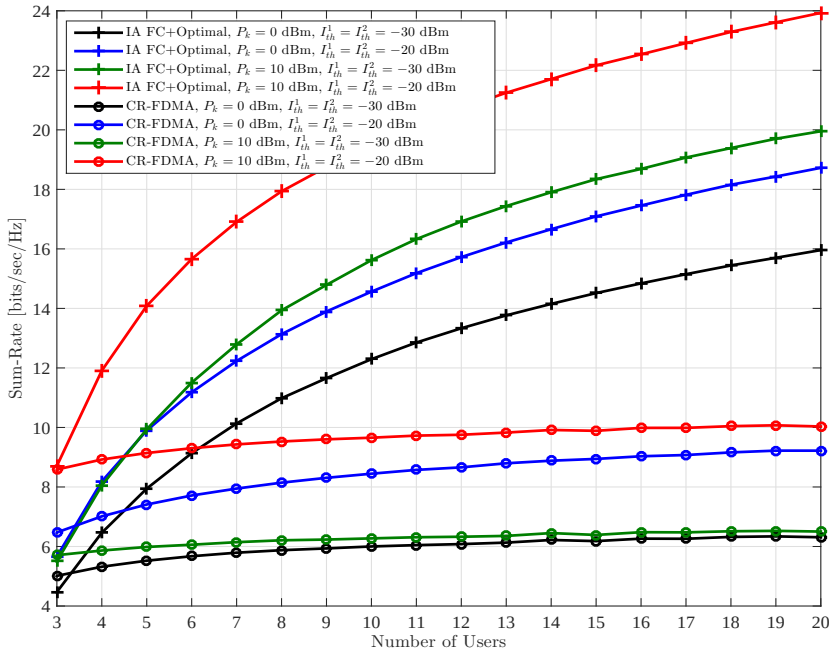

Figure 5.13: Achieved sum-rate versus number of SUs when $N = 128$ for different interference threshold and per-SU power values.

Fig. 5.13 presents the average sum-rate versus the number of SUs for different interference threshold and per-SU power values. Generally, the sum-rate increases with the number of SUs due to the increase of the multiuser diversity. Moreover, IA based resource allocation algorithms exploit much more gain from the increase of the multiuser diversity than *CR-FDMA* scheme since IA based resource allocation algorithms allow the users to share the available resources. It is noted from this figure that *CR-FDMA* scheme is more restricted to the interference limit, where increasing the per-SU power from 0 dBm to 10 dBm at $I_{th}^1 = I_{th}^2 = -30$ dBm slightly improves the sum-rate while increasing the interference limit from -30 dBm to -20 dBm at $P_k = 0$ dBm improves the sum-rate much more than modifying the power budget. However, the situation in IA curves is different, where the system benefits more from increasing the per-SU power budget.

Case III: Comparison between OFDM and FBMC physical Layers

In this part, we compare between OFDM and FBMC physical layers in MIMO cognitive radio systems. Note that in all the figures, the **FBMC** simulated results are denoted by **dash** curves,

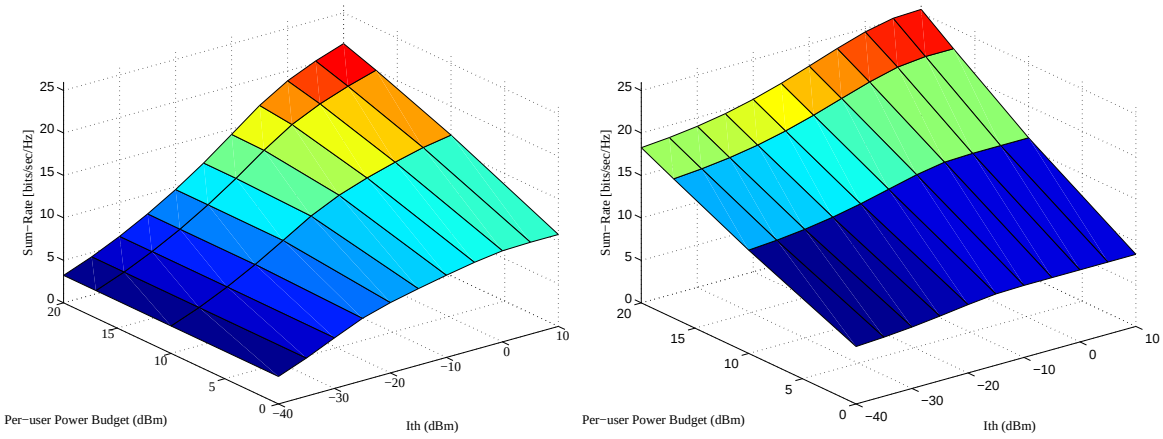

(a) OFDM physical layer. **(b)** FBMC physical layer.

Figure 5.14: Achieved sum-rate of *IA Optimal* versus power budget and interference threshold for OFDM and FBMC based physical layers when $K = 3$, $I_{th}^1 = I_{th}^2$ and $N = 64$.

while the **OFDM** simulated results are denoted by **solid** curves.

Fig. 5.14a and Fig. 5.14b present the average sum-rate of *IA Optimal* against the interference thresholds and power budget constrains for OFDM and FBMC physical layers, respectively, when $K = 3$ and $N = 64$. It is noted for the two physical layers cases that by fixing one of the constraints, the achieved capacity increases with the other up. This can be verified by the increase of the cognitive radio system ability to allocate more transmission powers for all users on the subcarriers. However, FBMC based cognitive radio achieves higher sum-rate compared to OFDM based cognitive radio at fixed interference and power values. This results from the small sidelobes of FBMC systems and the spectrum efficiency loss in OFDM due to the use of the cyclic prefix.

Fig. 5.15 presents the impact of interference threshold on the sum-rate when OFDM and FBMC physical layers are used in feasible cognitive radio systems with $K = 3$, $P_k = 15$ dBm and $N = 64$. In general, as the interference threshold levels increase, the restrictions on power allocation decrease and, consequentially, the sum-rate of cognitive radio systems increases. It can be observed that the interference constraint has more effect on the performance of OFDM systems rather than FBMC systems due to the sidelobes of each case. Therefore, FBMC based IA algorithms achieve higher sum-rate gain compared to OFDM based IA algorithms. When the interference constraint is flexible as in non cognitive-like environment, both physical layers have identical performance. The same conclusion can be extracted from Fig. 5.16 for an overloaded system with $K = 9$, $P_k = 0$ dBm and $N = 128$.

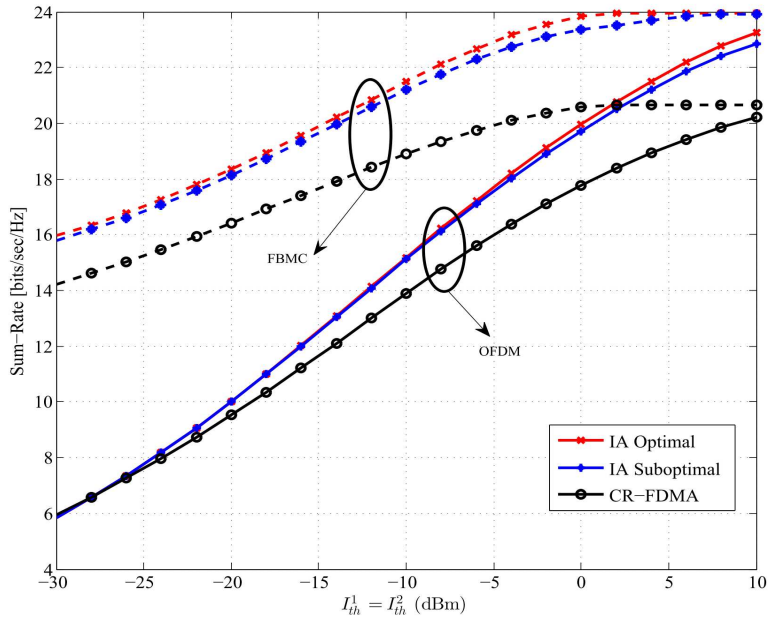

Figure 5.15: Achieved sum-rate versus allowed interference threshold for OFDM and FBMC based physical layers when $K = 3$, $P_k = 15$ dBm and $N = 64$.

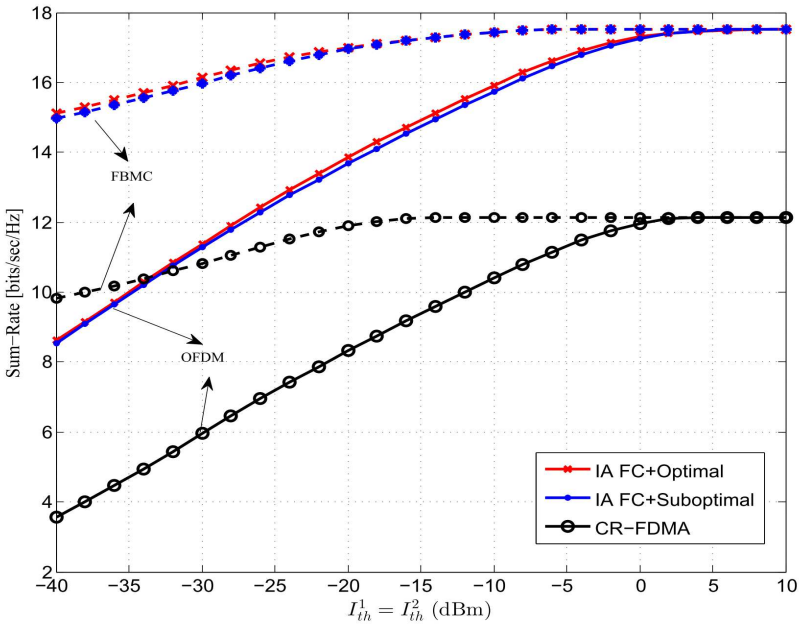

Figure 5.16: Achieved sum-rate versus allowed interference threshold for OFDM and FBMC based physical when $K = 9$, $P_k = 0$ dBm and $N = 128$.

The presented performance evaluation proves that IA based resource management has an essential responsibility in increasing the spectral efficiency of multicarrier MIMO cognitive radio systems.

6 CONCLUSIONS AND FUTURE WORK

In this chapter, we summarize the conclusions that we have achieved throughout the thesis in addition to future work tracks.

6.1 Conclusions

In this dissertation, we deal with three important aspects that are related to IA in K-user MIMO interference channels in order to improve the spectral efficiency of wireless communications. In the first aspect, we design the precoders and decoders of IA using Min-Maxing strategy in order to improve the spectral efficiency of K-user MIMO interference channels. Increasing the practical feasibility of MIMO IA systems under real-world environments is the target of the second aspect. The third aspect exploits IA as a base of resource allocation in MIMO cognitive radio systems aiming at increasing their spectral efficiency.

In Chapter 3, we focus on designing IA matrices that improve the sum-rate performance of general K-user MIMO interference channels by proposing a new distributed algorithm using Min-Maxing strategy. The proposed algorithm is formulated as a novel optimization problem that aims at maximizing the power of the desired signal while keeping the minimum leakage interference obtained from MLI method. Min-Maxing method is handled by convex optimization after reformulating and relaxing the optimization problem into a standard semidefinite programming approximation. Furthermore, the convergence of this method is established, and a simplified version of the optimal Min-Maxing method is proposed for rank-deficient interference channels. The proposed algorithm is extended to K-user multicarrier interference channels. We evaluate the proposed scheme by numerical simulation under three types of K-user MIMO interference channels: proper, marginal proper, and improper interference channels. Unlike the other algorithms, simulation results show that Min-Maxing technique achieves the best sum-rate performance compared to the other approaches at high SNR values in various interference channels, and it has a very close performance to the best sum-rate performance at low SNR

regime. The simplified technique presents identical sum-rate performance to the optimal one when the interference channel is rank-deficient with less complexity.

In Chapter 4, we consider improving the practical feasibility of IA under realistic channels. We propose to apply transmit antenna selection in MIMO-OFDM IA interference channels through bulk selection and per-subcarrier selection. Three selection criteria are considered: Max-SR, Min-ER, and Min-EG. Max-SR criterion is used to improve the sum-rate performance while Min-ER and Min-EG are used to enhance the error-rate performance. To overcome the power unbalancing that occurs in per-subcarrier selection, a constrained per-subcarrier selection is developed to attain power balancing among the antennas of each node. Furthermore, a sub-optimal antenna selection algorithm is proposed to reduce the computational complexity of the optimal selection. The sub-optimal algorithm reduces the complexity from $\mathcal{O}\left(N\binom{M_T}{M_s}^K\right)$ required in the exhaustive search to $\mathcal{O}\left(NK\binom{M_T}{M_s}\right)$. In order to examine the proposed technique under real circumstances, we implement IA testbed to collect measured channels. Moreover, deterministic channels, that are extracted from ray-tracing, are also used in performance evaluation. In deterministic and measured channels, antenna separation within each node is fixed to $\lambda/2$ in all cases. The following results are outlined:

- In analytical channels (independent channels and subcarriers), IA without antenna selection exhibits the promised results in the literature, where it surpasses the performance of TDMA multiple access technique and achieves the ideal DoFs. Moreover, our results state that unconstrained and constrained per-subcarrier selection matches each other, and both achieve high gain in sum-rate and error-rate performances compared to IA without antenna selection. However, bulk selection does not provide performance improvement when it is used for this type of channels since the subcarriers have independent fading and, therefore, it is impossible to select one antenna set suitable for all subcarriers.

- In measured and deterministic channels, IA fails to present the ideal results due to the spatial correlation between channels, where TDMA outperforms IA in this kind of channels. We show that the sum-rate of MIMO-OFDM IA with bulk antenna selection and $\lambda/2$ separation of antennas within each node outperforms sum-rate of the system without antenna selection and 2λ separated antennas. Furthermore, the sub-optimal algorithm achieves close performance to bulk selection with less complexity even the selection is performed only for one subcarrier. It is noted that constrained per-subcarrier selection causes a high rate loss compared to the unconstrained per-subcarrier selection due to the

high correlation between channels in indoor environments. Therefore, bulk selection is more suitable to be used in such channels.

We conclude that antenna selection can improve the performance of MIMO-OFDM IA systems, and, hence, increases the practical feasibility of IA systems.

In Chapter 5, we deal with IA in MIMO cognitive radio systems that are coexisted with primary systems. We perform efficient resource allocation in overloaded MIMO cognitive radio systems based on IA without affecting the QoS of the primary system. Moreover, we consider in problem formulation the power budget of the SUs as well as the throughput fairness among the SUs. This problem is formulated as a mixed-integer problem which has a high computational complexity. Therefore, an efficient sub-optimal algorithm is proposed to reduce the computational complexity of the optimal problem through two phases. In the first phase, frequency-clustering is performed to overcome IA feasibility conditions where one group of a feasible number of SUs is assigned to each subcarrier considering channel quality, per-user power budget, and the induced interference to the PU bands. Frequency-clustering phase considers achieving a high degree of fairness among the SUs. In the second phase, the power is distributed among subcarriers considering the induced interference limits. Sub-optimal power allocation algorithm is also proposed to reduce the complexity of the optimal power allocation. Performing resource allocation using frequency-clustering and the sub-optimal power allocation reduces the complexity from $\mathcal{O}\left(\binom{K}{\bar{K}}^{N} \cdot \left(\Psi + \left(\bar{K}dN\right)^{3}\right)\right)$ required in the optimal resource allocation scheme to $\mathcal{O}\left(\binom{K}{\bar{K}} \cdot N \cdot \Upsilon + KL\bar{K}dN \log\left(\bar{K}dN\right)\right)$. The following results are outlined:

- IA based resource management achieves a considerable increase in the spectral efficiency of MIMO cognitive radio systems compared to orthogonal multiple access techniques.
- The sup-optimal power allocation algorithm successes to present close performance to the optimal power allocation algorithm with fewer computational complexity.
- In feasible cognitive radio scenarios, outage probability and instantaneous rate curves reveal that IA can achieve a high degree of fairness among the SUs since IA allows the SUs to share the available resources in the system, where all SUs communicate simultaneously using the same resources.
- In overloaded cognitive radio scenarios, frequency-clustering is a necessity to achieve

IA feasibility conditions on subcarriers. By comparing the achieved sum-rate of the frequency-clustering with and without applying the fairness constraints, it is noted that the frequency-clustering with fairness can maintain the fairness between the SUs with small sum-rate loss compared to the scheme without fairness consideration. This result is also observed from the outage probability curves.

- FBMC physical layer achieves higher performance than OFDM since FBMC has small sidelobes and OFDM requires cyclic prefix insertion.

We conclude that IA based resource management is a novel technique that is able to achieve a considerable spectral efficiency improvement in MIMO cognitive radio systems.

6.2 Future Work

In this section, we present some important future research directions on IA in the following listed points.

- K-user interference channels are only considered through this dissertation. Recent works on IA in cellular systems have appeared as in [156, 157]. Therefore, extension to cellular systems is a promising future direction for this work, where considering the effect of cellular system complexities such as scheduling and interference is a challenge.

- Through this work, the global CSI is assumed to be perfectly known, where it is an unrealistic assumption. Recently, some research works were done in order to evaluate IA systems with imperfect CSI. In [158], the performance of IA with imperfect channel knowledge was studied. Moreover, blind IA schemes without both the CSI at the transmitters and the receivers were studied in [159]. In [160], the authors analyzed the performance of IA with CSI feedback using a limited number of bits. Thus, more investigation for the proposed schemes in this dissertation with imperfect/partial CSI will be an interesting topic for future investigation.

- In chapter 5, the resource management is performed in a centralized way. Distributed resource allocation algorithm is of great interest to be observed in the future. Moreover, considering energy-efficiency resource allocation is a possible extension to the proposed algorithm.

LIST OF PUBLICATIONS

Publications derived from this dissertation

The following list of publications are derived from the results presented in this dissertation.

Journal Papers

[1] **M. El-Absi**, M. Shaat, F. Bader, and T. Kaiser, ”Interference Alignment with Frequency Clustering for Efficient Resource Allocation in Cognitive Radio Networks,” *IEEE Transactions on Wireless Communications (Minor Revision round)*, May 2015.

[2] **M. El-Absi**, S. Galih, M. Hoffmann, M. El-Hadidy, and T. Kaiser, ”Antenna Selection for Reliable MIMO-OFDM Interference Alignment Systems: Measurement Based Evaluation,” *IEEE Transactions on Vehicular Technology*, 2015.

[3] **M. El-Absi**, M. El-Hadidy, T. Kaiser, ”A distributed Interference Alignment Algorithm using Min-Maxing Strategy,” *Transactions on Emerging Telecommunications Technologies*, doi: 10.1002/ett.2897, 2014.

Conference Papers

[1] **M. El-Absi**, M. Shaat, F. Bader, and T. Kaiser, ”Interference Alignment with Frequency Clustering for Efficient Resource Allocation in Cognitive Radio Networks,” *IEEE Global Communications Conf. (Globecom)*, 8-12 Dec. 2014, pp. 979-985.

[2] **M. El-Absi**, M. Shaat, F. Bader, and T. Kaiser, ”Power loading and spectral efficiency comparison of MIMO OFDM/FBMC for interference alignment based cognitive radio systems,” *11th Int. Symp. Wireless Communication Systems (ISWCS)*, Aug. 2014, pp. 480–485.

[3] **M. El-Absi**, T. Kaiser, ”Optimal Resource Allocation Based on Interference Alignment for OFDM and FBMC MIMO Cognitive Radio Systems,” *Proceedings of 23rd European Conference on Networks and Communications (EuCNC)*, 23-25 June 2014, pp. 1–5.

[4] **M. El-Absi**, M. Shaat, F. Bader, T. Kaiser, ”Interference Alignment Based Resource Management in MIMO Cognitive Radio Systems,” *IEEE Proceedings of the 20th European Wireless Conference*, 14-16 May 2014, pp. 1-6.

[5] **M. El-Absi**, M. El-Hadidy, T. Kaiser, ”Reliability of MIMO-OFDM Interference Alignment Systems with Antenna Selection under Real-World Environments,” *IEEE Proceedings of the 20th European Wireless Conference*, 14-16 May 2014, pp.1-6.

[6] **M. El-Absi**, M. El-Hadidy, T. Kaiser, ”Min-Maxing Interference Alignment Algorithm as a Semidefinite Programming Problem,” *IEEE 14th Workshop on Signal Processing Advances in Wireless Communications (SPAWC)*, June 2013, pp. 290–294.

[7] **M. El-Absi**, M. El-Hadidy, T. Kaiser, ”Antenna selection for interference alignment based on subspace canonical correlation,” *International Symposium on Communications and Information Technologies (ISCIT)*, 2012, pp. 423–427.

Related work by the author

[1] **M. El-Absi**, A. Ali, M. El-Hadidy, T. Kaiser, ”Energy-Efficient Resource Allocation Based on Interference Alignment in MIMO-OFDM Cognitive Radio Networks,” *Int. Conf. Cognitive Radio Oriented Wireless Networks (CROWNCOM)*, 21-23 April 2015.

[2] **M. El-Absi**, A. Güven, T. Kaiser, ”Interference Alignment for OFDM Cognitive Radio Networks in TV White Space Spectrum,” *18th International OFDM-Workshop 2014 (InOWo14)*, 29-30 Aug. 2014, pp. 1-6.

[3] M. El-Hadidy, **M. El-Absi**, T. Kaiser, ”Artificial diversity for UWB MB-OFDM interference alignment based on real-world channel models and antenna selection techniques,” *2012 IEEE International Conference on Ultra-Wideband (ICUWB)*, 17-20 Sep. 2012, pp. 338–342.

[4] M. El-Hadidy, **M. El-Absi**, L. Sit, M. Kock, T. Zwick, H. Blume, and T. Kaiser, ”Improved interference alignment performance for MIMO OFDM systems by multimode MIMO antennas,” *in 17th International OFDM Workshop*, Aug. 2012, pp. 1–5.

[5] M. El-Hadidy, **M. El-Absi**, Y. L. Sit, M. Kock, T. Zwick, H. Blume, and T. Kaiser, ”Interference Alignment for UWB-MIMO Communication Systems,” in *Ultra-Wideband Radio*

Technologies for Communications, Localization and Sensor Applications (ISBN 978-953-51-0936-5), R. Thomäs, R. H. Knöchel, J. Sachs, I. Willms, and T. Zwick (ed.), Chapter 6, INTECH, 2013.

BIBLIOGRAPHY

[1] D. Miorandi, S. Sicari, F. De Pellegrini, and I. Chlamtac, "Internet of things: Vision, applications and research challenges," *Ad Hoc Networks*, vol. 10, no. 7, pp. 1497 – 1516, 2012.

[2] J. A. Stankovic, "Research directions for the internet of things," *IEEE Internet of Things Journal*, vol. 1, no. 1, pp. 3–9, Feb 2014.

[3] D. Liu B. Hu H. Wang S. Chen, H. Xu, "A vision of IoT: Applications, challenges, and opportunities with China perspective," 2014.

[4] Huawei, "5G: A technology vision," 2013, Available at `http://www.huawei.com/5gwhitepaper/`.

[5] Cisco, "Cisco visual networking index (VNI)," 2014. Available at `http://www.cisco.com/c/en/us/solutions/service-provider/visual-networking-index-vni/index.html`.

[6] Ericsson, "Ericsson mobility report," 2014. Available at `http://www.ericsson.com/res/docs/2014/ericsson-mobility-report-june-2014.pdf`.

[7] A. S. Motahari and A. K. Khandani, "To decode the interference or to consider it as noise," *IEEE Transactions on Information Theory*, vol. 57, no. 3, pp. 1274–1283, March 2011.

[8] H. Sato, "The capacity of the gaussian interference channel under strong interference (corresp.)," *IEEE Transactions on Information Theory*, vol. 27, no. 6, pp. 786–788, Nov 1981.

[9] G. Bresler, D. Cartwright, and D. Tse, "Feasibility of interference alignment for the MIMO interference channel: The symmetric square case," in *IEEE Information Theory Workshop (ITW)*, 2011, pp. 447–451.

[10] V. R. Cadambe and S. Jafar, "Interference alignment and degrees of freedom of the K-user interference channel," *IEEE Transactions on Information Theory*, vol. 54, no. 8, pp. 3425–3441, 2008.

[11] M. A. Maddah-Ali, AS. Motahari, and AK. Khandani, "Communication over MIMO X channels: Interference alignment, decomposition, and performance analysis," *IEEE Transactions on Information Theory*, vol. 54, no. 8, pp. 3457–3470, Aug 2008.

[12] B. Nazer, M. Gastpar, S. Jafar, and S. Vishwanath, "Ergodic interference alignment," in *IEEE International Symposium on Information Theory (ISIT)*, June 2009, pp. 1769–1773.

[13] B. Da and R. Zhang, "Exploiting interference alignment in multi-cell cooperative OFDMA resource allocation," in *IEEE Global Telecommunications Conference (GLOBECOM)*, Dec 2011, pp. 1–5.

[14] S. Gollakota, S. Perli, and D. Katabi, "Interference alignment and cancellation," in *Proceedings of the ACM SIGCOMM Conference on Data Communication*, 2009, SIGCOMM '09, pp. 159–170.

[15] AS. Motahari, S. Oveis-Gharan, M.-A Maddah-Ali, and AK. Khandani, "Real interference alignment: Exploiting the potential of single antenna systems," *IEEE Transactions on Information Theory*, vol. 60, no. 8, pp. 4799–4810, Aug 2014.

[16] V. R. Cadambe and S. Jafar, "Reflections on interference alignment and the degrees of freedom of the K-user MIMO interference channel," in *IEEE Information Theory Society Newsletter*, 2009, pp. 5–8.

[17] S. Jafar and M. J. Fakhereddin, "Degrees of freedom for the MIMO interference channel," *IEEE Transactions on Information Theory*, vol. 53, no. 7, pp. 2637–2642, 2007.

[18] C. M. Yetis, T. Gou, S. Jafar, and A. H. Kayran, "On feasibility of interference alignment in MIMO interference networks," *IEEE Transactions on Signal Processing*, vol. 58, no. 9, pp. 4771–4782, 2010.

[19] K. Gomadam, V. R. Cadambe, and S. Jafar, "A distributed numerical approach to interference alignment and applications to wireless interference networks," *IEEE Transactions on Information Theory*, vol. 57, no. 6, pp. 3309–3322, 2011.

[20] S. W. Peters and R. W. Heath, "Interference alignment via alternating minimization," in *IEEE International Conference on Acoustics, Speech and Signal Processing (ICASSP)*, 2009, pp. 2445–2448.

[21] I. Santamaria, O. Gonzalez, R. W. Heath, and S. W. Peters, "Maximum sum-rate interference alignment algorithms for MIMO channels," in *IEEE Global Telecommunications Conference (GLOBECOM)*, 2010, pp. 1–6.

[22] D. S. Papailiopoulos and A. G. Dimakis, "Interference alignment as a rank constrained rank minimization," *IEEE Transactions on Signal Processing*, vol. 60, no. 8, pp. 4278–4288, 2012.

[23] M. Shen, C. Zhao, X. Liang, and Z. Ding, "Best-effort interference alignment in OFDM systems with finite SNR," in *IEEE International Conference on Communications (ICC)*, 2011, pp. 1–6.

[24] J. W. Wallace and M. A. Jensen, "Modeling the indoor MIMO wireless channel," *IEEE Transactions on Antennas and Propagation*, vol. 50, no. 5, pp. 591–599, 2002.

[25] D. Shiu, G. J. Foschini, M. J. Gans, and J. M. Kahn, "Fading correlation and its effect on the capacity of multielement antenna systems," *IEEE Transactions on Communications*, vol. 48, no. 3, pp. 502–513, Mar 2000.

[26] O. El Ayach, S. W. Peters, and R. W. Heath, "The feasibility of interference alignment over measured MIMO-OFDM channels," *IEEE Transactions on Vehicular Technology*, vol. 59, no. 9, pp. 4309–4321, 2010.

[27] S. Haykin, "Cognitive radio: brain-empowered wireless communications," *IEEE Journal on Selected Areas in Communications*, vol. 23, no. 2, pp. 201–220, Feb 2005.

[28] J. Mitola and Jr. Maguire, G.Q., "Cognitive radio: making software radios more personal," *IEEE Personal Communications*, vol. 6, no. 4, pp. 13–18, Aug 1999.

[29] R. Zhang and Y. Liang, "Exploiting multi-antennas for opportunistic spectrum sharing in cognitive radio networks," *IEEE Journal of Selected Topics in Signal Processing*, vol. 2, no. 1, pp. 88–102, 2008.

[30] D. Tse and P. Viswanath, *Fundamentals of Wireless Communication*, Wiley series in telecommunications. Cambridge University Press, 2005.

[31] A. Molisch, *Wireless Communications*, Wiley-IEEE Press, 2005.

[32] A. Goldsmith, *Wireless Communications*, Cambridge University Press, New York, NY, USA, 2005.

[33] B. Hassibi and M. Sharif, "Fundamental limits in MIMO broadcast channels," *IEEE Journal on Selected Areas in Communications*, vol. 25, no. 7, pp. 1333–1344, September 2007.

[34] C. Chan-Byoung, D. Mazzarese, N. Jindal, and R. W. Heath, "Coordinated beamforming with limited feedback in the MIMO broadcast channel," *IEEE Journal on Selected Areas in Communications*, vol. 26, no. 8, pp. 1505–1515, October 2008.

[35] L. H. Ozarow, "The capacity of the white gaussian multiple access channel with feedback," *IEEE Transactions on Information Theory*, vol. 30, no. 4, pp. 623–629, Jul 1984.

[36] H. Permuter, T. Weissman, and J. Chen, "Capacity region of the finite-state multiple-access channel with and without feedback," *IEEE Transactions on Information Theory*, vol. 55, no. 6, pp. 2455–2477, June 2009.

[37] A. Carleial, "Interference channels," *IEEE Transactions on Information Theory*, vol. 24, no. 1, pp. 60–70, Jan 1978.

[38] M. H. Costa, "On the gaussian interference channel," *IEEE Transactions on Information Theory*, vol. 31, no. 5, pp. 607–615, Sep 1985.

[39] R. Benzel, "The capacity region of a class of discrete additive degraded interference channels (corresp.)," *IEEE Transactions on Information Theory*, vol. 25, no. 2, pp. 228–231, Mar 1979.

[40] S. Karmakar and M. K. Varanasi, "The capacity region of the MIMO interference channel and its reciprocity to within a constant gap," *IEEE Transactions on Information Theory*, vol. 59, no. 8, pp. 4781–4797, Aug 2013.

[41] R. Ahlswede, "The capacity region of a channel with two senders and two receivers," *The Annals of Probability*, vol. 2, no. 5, pp. pp. 805–814, 1974.

[42] M. H. Costa and AE. Gamal, "The capacity region of the discrete memoryless interference channel with strong interference (corresp.)," *IEEE Transactions on Information Theory*, vol. 33, no. 5, pp. 710–711, Sep 1987.

[43] T. Han and K. Kobayashi, "A new achievable rate region for the interference channel," *IEEE Transactions on Information Theory*, vol. 27, no. 1, pp. 49–60, Jan 1981.

[44] H. Chong, M. Motani, H. Garg, and H. El Gamal, "On the Han-Kobayashi region for the interference channel," *IEEE Transactions on Information Theory*, vol. 54, no. 7, pp. 3188–3195, July 2008.

[45] X. Shang, G. Kramer, and B. Chen, "A new outer bound and the noisy interference sum rate capacity for gaussian interference channels," *IEEE Transactions on Information Theory*, vol. 55, no. 2, pp. 689–699, Feb 2009.

[46] G. Foschini and M. Gans, "On limits of wireless communications in a fading environment when using multiple antennas," *Wireless Personal Communications*, vol. 6, pp. 311–335, 1998.

[47] A. Poon, R. Brodersen, and D. Tse, "Degrees of freedom in multiple-antenna channels: A signal space approach," *IEEE Transactions on Information Theory*, vol. 51, pp. 523–536, 2005.

[48] L. Zheng and D. Tse, "Diversity and multiplexing: a fundamental tradeoff in multiple-antenna channels," *IEEE Transactions on Information Theory*, vol. 49, no. 5, pp. 1073–1096, May 2003.

[49] R. Somaraju and J. Trumpf, "Degrees of freedom of a communication channel: Using DOF singular values," *IEEE Transactions on Information Theory*, vol. 56, no. 4, pp. 1560–1573, April 2010.

[50] C. Geng, N. Naderializadeh, A. Avestimehr, and S. Jafar, "On the optimality of treating interference as noise," *arXiv preprint arXiv:1305.4610*, 2013.

[51] B. Sklar, *Digital Communications: Fundamentals and Applications*, Prentice-Hall, Inc., Upper Saddle River, NJ, USA, 1988.

[52] Y. Xu and S. Mao, "On interference alignment in multi-user OFDM systems," in *IEEE Global Communications Conference (GLOBECOM)*, 2012, pp. 5339–5344.

[53] Q. Shi, M. Razaviyayn, Z. Luo, and C. He, "An iteratively weighted MMSE approach to distributed sum-utility maximization for a MIMO interfering broadcast channel," *IEEE Transactions on Signal Processing*, vol. 59, no. 9, pp. 4331–4340, 2011.

[54] O. Gonzalez, I. Santamaria, and C. Beltran, "A general test to check the feasibility of linear interference alignment," in *IEEE International Symposium on Information Theory Proceedings (ISIT)*, 2012, pp. 2481–2485.

[55] R. Tresch, M. Guillaud, and E. Riegler, "On the achievability of interference alignment in the K-user constant MIMO interference channel," in *15th IEEE/SP Workshop on Statistical Signal Processing*, Aug 2009, pp. 277–280.

[56] C. Rose, S. Ulukus, and R. D. Yates, "Wireless systems and interference avoidance," *IEEE Transactions on Wireless Communications*, vol. 1, no. 3, pp. 415–428, Jul 2002.

[57] W. Yu, W. Rhee, S. Boyd, and J. M. Cioffi, "Iterative water-filling for gaussian vector multiple-access channels," *IEEE Transactions on Information Theory*, vol. 50, no. 1, pp. 145–152, Jan 2004.

[58] C. Withers and S. Nadarajah, "Reciprocity for MIMO systems," *European Transactions on Telecommunications*, vol. 22, no. 6, pp. 276–281, 2011.

[59] S. Sodagari and T. C. Clancy, "On singularity attacks in MIMO channels," *Transactions on Emerging Telecommunications Technologies*, 2013.

[60] M. El-Absi, M. El-Hadidy, and T. Kaiser, "Min-maxing interference alignment algorithm as a semidefinite programming problem," in *14th IEEE Workshop on Signal Processing Advances in Wireless Communications (SPAWC)*, June 2013, pp. 290–294.

[61] M. El-Absi, M. El-Hadidy, and T. Kaiser, "A distributed interference alignment algorithm using min-maxing strategy," *Transactions on Emerging Telecommunications Technologies*, 2014.

[62] S. W. Peters and R. W. Heath, "Cooperative algorithms for MIMO interference channels," *IEEE Transactions on Vehicular Technology*, vol. 60, no. 1, pp. 206–218, 2011.

[63] H. Yu and Y. Sung, "Least squares approach to joint beam design for interference alignment in multiuser multi-input multi-output interference channels," *IEEE Transactions on Signal Processing*, vol. 58, no. 9, pp. 4960–4966, 2010.

[64] C. Wilson and V. Veeravalli, "A convergent version of the Max SINR algorithm for the MIMO interference channel," *IEEE Transactions on Wireless Communications,*, vol. 12, no. 6, pp. 2952–2961, 2013.

[65] C. Yetis, Y. Zeng, K. Anand, Y. Guan, and E. Gunawan, "Sub-stream fairness and numerical correctness in MIMO interference channels," in *IEEE Symposium on Wireless Technology and Applications*, 2013.

[66] D. A. Schmidt, C. Shi, R. A. Berry, M. L. Honig, and W. Utschick, "Minimum mean squared error interference alignment," in *Conference Record of the Forty-Third Asilomar Conference on Signals, Systems and Computers*, 2009, pp. 1106–1110.

[67] H. Shen and B. Li, "A novel iterative interference alignment scheme via convex optimization for the MIMO interference channel," in *IEEE 72nd Vehicular Technology Conference Fall*, 2010, pp. 1–5.

[68] M. Razaviyayn, M. Sanjabi, and Z. Luo, "Linear transceiver design for interference alignment: Complexity and computation," *IEEE Transactions on Information Theory*, vol. 58, no. 5, pp. 2896–2910, 2012.

[69] F. Negro, S. P. Shenoy, I. Ghauri, and D. T. Slock, "On the MIMO interference channel," in *Information Theory and Applications Workshop (ITA)*, 2010, pp. 1–9.

[70] M. Overton and R. Womersley, "On the sum of the largest eigenvalues of a symmetric matrix," *SIAM Journal on Matrix Analysis and Applications*, vol. 13, pp. 41–45, 1992.

[71] M. Overton and R. Womersley, "Optimality conditions and duality theory for minimizing sums of the largest eigenvalues of symmetric matrices," in *Mathematical Programming: Series A and B*, 1993, vol. 62, pp. 321–375.

[72] J. Berge, "Least squares optimization in multivariate analysis," in *Least Squares Optimization in Multivariate Analysis*, 1993.

[73] M. Grant and S. Boyd, ," in `http://cvxr.com/cvx`.

[74] G. Bresler and D. Tse, "3 user interference channel: Degrees of freedom as a function of channel diversity," in *47th Annual Allerton Conference on Communication, Control, and Computing*, 2009, pp. 265–271.

[75] M. El-Absi, M. El-Hadidy, and T. Kaiser, "Antenna selection for interference alignment based on subspace canonical correlation," in *International Symposium on Communications and Information Technologies (ISCIT)*, 2012, pp. 423–427.

[76] M. El-Absi, M. El-Hadidy, and T. Kaiser, "Reliability of MIMO-OFDM interference alignment systems with antenna selection under real-world environments," in *Proceedings of 20th European Wireless Conference*, May 2014, pp. 1–6.

[77] M. Hoffmann M. El-Absi, S. Galih, M. El-Hadidy, and T. Kaiser, "Antenna selection for reliable MIMO-OFDM interference alignment systems: Measurement based evaluation," *IEEE Transactions on Vehicular Technology*, 2015.

[78] O. Gonzalez, D. Ramirez, I. Santamaria, J. A. Garcia-Naya, and L. Castedo, "Experimental validation of interference alignment techniques using a multiuser MIMO testbed," in *International ITG Workshop on Smart Antennas (WSA)*, 2011, pp. 1–8.

[79] JA. Garcia-Naya, L. Castedo, O. Gonzalez, D. Ramirez, and I. Santamaria, "Experimental evaluation of interference alignment under imperfect channel state information," *19th European Signal Processing Conference (EUSIPCO 2011). Barcelona, Spain*, 2011.

[80] J. W. Massey, J. Starr, S. Lee, D. Lee, A Gerstlauer, and R. W. Heath, "Implementation of a real-time wireless interference alignment network," in *Conference Record of the Forty Sixth Asilomar Conference on Signals, Systems and Computers (ASILOMAR)*, Nov 2012, pp. 104–108.

[81] P. Zetterberg and N. N. Moghadam, "An experimental investigation of SIMO, MIMO, interference-alignment (IA) and coordinated multi-point (CoMP)," in *19th International Conference on Systems, Signals and Image Processing (IWSSIP)*, April 2012, pp. 211–216.

[82] P. Zetterberg, "Interference alignment (IA) and coordinated multi-point (CoMP) with IEEE802.11AC feedback compression: Testbed results," in *IEEE International Conference on Acoustics, Speech and Signal Processing (ICASSP)*, May 2014, pp. 6176–6180.

[83] A. Molisch, "MIMO systems with antenna selection - an overview," in *Proceedings Radio and Wireless Conference*, Aug 2003, pp. 167–170.

[84] D. A. Gore, R. W. Heath, and A. Paulraj, "Transmit selection in spatial multiplexing systems," *IEEE Communications Letters*, vol. 6, no. 11, pp. 491–493, Nov 2002.

[85] R. W. Heath and A. Paulraj, "Antenna selection for spatial multiplexing systems based on minimum error rate," in *IEEE International Conference on Communications (ICC)*, 2001, vol. 7, pp. 2276–2280.

[86] A. Gorokhov, D. A. Gore, and A. Paulraj, "Receive antenna selection for MIMO spatial multiplexing: theory and algorithms," *IEEE Transactions on Signal Processing*, vol. 51, no. 11, pp. 2796–2807, Nov 2003.

[87] J. G. Klotz and A. Sezgin, "Antenna selection criteria for interference alignment," in *IEEE 21st International Symposium on Personal Indoor and Mobile Radio Communications (PIMRC)*, 2010, pp. 527–531.

[88] J. Lee and D. Park, "Antenna selection and unitary precoding for interference alignment with ML receiver," *IEEE Communications Letters*, vol. 16, no. 8, pp. 1216–1219, 2012.

[89] M. El-Hadidy, M. El-Absi, and T. Kaiser, "Artificial diversity for UWB MB-OFDM interference alignment based on real-world channel models and antenna selection techniques," in *IEEE International Conference on Ultra-Wideband (ICUWB)*, 2012, pp. 338–342.

[90] M. El-Hadidy, M. El-Absi, L. Sit, M. Kock, T. Zwick, H. Blume, and T. Kaiser, "Improved interference alignment performance for MIMO OFDM systems by multimode MIMO antennas," in *17th International OFDM Workshop*, Aug 2012, pp. 1–5.

[91] N. Zhao, F. R. Yu, H. Sun, A. Nallanathan, and H. Yin, "A novel interference alignment scheme based on sequential antenna switching in wireless networks," *IEEE Transactions on Wireless Communications*, vol. 12, no. 10, pp. 5008–5021, October 2013.

[92] J. H. Winters, "On the capacity of radio communication systems with diversity in a rayleigh fading environment," *IEEE Journal on Selected Areas in Communications*, vol. 5, no. 5, pp. 871–878, Jun 1987.

[93] A. Molisch, M. Z. Win, and J. H. Winters, "Reduced-complexity transmit/receive-diversity systems," in *IEEE 53rd Vehicular Technology Conference (VTC)*, 2001, vol. 3, pp. 1996–2000.

[94] A. Molisch, M. Z. Win, and J. H. Winters, "Capacity of MIMO systems with antenna selection," in *IEEE International Conference on Communications (ICC)*, 2001, vol. 2, pp. 570–574.

[95] M. Z. Win and J. H. Winters, "Analysis of hybrid selection/maximal-ratio combining in rayleigh fading," *IEEE Transactions on Communications*, vol. 47, no. 12, pp. 1773–1776, Dec 1999.

[96] J. B. Andersen, "Antenna arrays in mobile communications: gain, diversity, and channel capacity," *IEEE Antennas and Propagation Magazine*, vol. 42, no. 2, pp. 12–16, Apr 2000.

[97] H. Zhang, A. Molisch, and J Zhang, "Applying antenna selection in WLANs for achieving broadband multimedia communications," *IEEE Transactions on Broadcasting*, vol. 52, no. 4, pp. 475–482, 2006.

[98] H. Shi, M. Katayama, T. Yamazato, H. Okada, and A. Ogawa, "An adaptive antenna selection scheme for transmit diversity in OFDM systems," in *IEEE 54th Vehicular Technology Conference (VTC)*, 2001, vol. 4, pp. 2168–2172.

[99] H. Zhang and R. U. Nabar, "Transmit antenna selection in MIMO-OFDM systems: Bulk versus per-tone selection," in *IEEE International Conference on Communications (ICC)*, 2008, pp. 4371–4375.

[100] A. Bjoerck and G. H. Golub, "Numerical methods for computing angles between linear subspaces," Tech. Rep., Stanford, CA, USA, 1971.

[101] R. W. Heath, S. Sandhu, and A. Paulraj, "Antenna selection for spatial multiplexing systems with linear receivers," *IEEE Communications Letters*, vol. 5, no. 4, pp. 142–144, April 2001.

[102] R. Chen, R. W. Heath, and J. G. Andrews, "Transmit selection diversity for unitary precoded multiuser spatial multiplexing systems with linear receivers," *IEEE Transactions on Signal Processing*, vol. 55, no. 3, pp. 1159–1171, March 2007.

[103] K. Park, Y. Ko, and M.-S. Alouini, "Low complexity transmit antenna selection with power balancing in OFDM systems," *IEEE Transactions on Wireless Communications*, vol. 9, no. 10, pp. 1–6, 2010.

[104] P. Almers, T. Santos, F. Tufvesson, A. Molisch, J. Karedal, and A. Johansson, "Antenna subset selection in measured indoor channels," *IET Microwaves, Antennas Propagation*, vol. 1, no. 5, pp. 1092–1100, October 2007.

[105] Y. Choi and S. Alamouti, "Performance analysis and comparisons of antenna and beam selection diversity," in *60th IEEE Vehicular Technology Conference (VTC-Fall).*, Sept 2004, vol. 1, pp. 165–170 Vol. 1.

[106] J. Jiang and M.-A. Ingram, "Comparison of beam selection and antenna selection techniques in indoor MIMO systems at 5.8 GHz," in *Proceedings of Radio and Wireless Conference (RAWCON)*, Aug 2003, pp. 179–182.

[107] G. Stuber, J. Barry, S. McLaughlin, Y. Li, M.-A. Ingram, and T. Pratt, "Broadband MIMO-OFDM wireless communications," *Proceedings of the IEEE*, vol. 92, no. 2, pp. 271–294, Feb 2004.

[108] J.-J. van de Beek, O. Edfors, M. Sandell, S. K. Wilson, and P. Ola Borjesson, "On channel estimation in OFDM systems," in *IEEE 45th Vehicular Technology Conference*, Jul 1995, vol. 2, pp. 815–819.

[109] E. Karami, "Tracking performance of least squares MIMO channel estimation algorithm," *IEEE Transactions on Communications*, vol. 55, no. 11, pp. 2201–2209, Nov 2007.

[110] T. M. Schmidl and D. C. Cox, "Robust frequency and timing synchronization for OFDM," *IEEE Transactions on Communications*, vol. 45, no. 12, pp. 1613–1621, Dec 1997.

[111] X. He, X. Peng, Y. Xiao, and S. Li, "A novel time and frequency synchronization technique for MIMO-OFDM system," in *Fourth Advanced International Conference on Telecommunications*, June 2008, pp. 360–363.

[112] G. German, Q. Spencer, L. Swindlehurst, and R. Valenzuela, "Wireless indoor channel modeling: statistical agreement of ray tracing simulations and channel sounding measurements," in *IEEE International Conference on Acoustics, Speech, and Signal Processing (ICASSP)*, 2001, vol. 4, pp. 2501–2504.

[113] T. Fugen, J. Maurer, T. Kayser, and W. Wiesbeck, "Capability of 3-D ray tracing for defining parameter sets for the specification of future mobile communications systems," *IEEE Transactions on Antennas and Propagation*, vol. 54, no. 11, pp. 3125–3137, 2006.

[114] M. El-Hadidy and T. Kaiser, "An UWB channel model considering angular antenna impulse response and polarization," in *The Second European Conference on Antennas and Propagation (EuCAP)*, 2007, pp. 1–5.

[115] Wireless InSite User Manual, "version 1.5.1," in *http://www.remcom.com/WirelessInSite/*, 2003.

[116] C. Valenzuela, C. Chuah, G. Foschini, R. A. Valenzuela, D. Chizhik, J. Ling, and J. M. Kahn, "Capacity growth of multi-element arrays in indoor and outdoor wireless channels," 2000, vol. 3, pp. 1340–1344.

[117] J. W. Wallace, M. A. Jensen, A. L. Swindlehurst, and B. D. Jeffs, "Experimental characterization of the MIMO wireless channel: data acquisition and analysis," *IEEE Transactions on Wireless Communications*, vol. 2, no. 2, pp. 335–343, 2003.

[118] M. El-Absi, M. Shaat, F. Bader, and T. Kaiser, "Interference alignment based resource management in MIMO cognitive radio systems," in *Proceedings of 20th European Wireless Conference*, May 2014, pp. 1–6.

[119] M. El-Absi and T. Kaiser, "Optimal resource allocation based on interference alignment for OFDM and FBMC MIMO cognitive radio systems," in *European Conference on Networks and Communications (EuCNC)*, June 2014, pp. 1–5.

[120] M. El-Absi, M. Shaat, F. Bader, and T. Kaiser, "Power loading and spectral efficiency comparison of MIMO OFDM/FBMC for interference alignment based cognitive radio systems," in *11th International Symposium on Wireless Communications Systems (ISWCS)*, Aug 2014, pp. 480–485.

[121] M. El-Absi, M. Shaat, F. Bader, and T. Kaiser, "Interference alignment with frequency-clustering for efficient resource allocation in cognitive radio networks," in *IEEE Global Communications Conference (GLOBECOM)*, Dec 2014, pp. 979–985.

[122] M. El-Absi, M. Shaat, F. Bader, and T. Kaiser, "Interference alignment with frequency clustering for efficient resource allocation in cognitive radio networks," *IEEE Transactions on Wireless Communications (Minor Revision round)*, 2015.

[123] I. Akyildiz, L. Won-Yeol, M. C. Vuran, and S. Mohanty, "NeXt generation/dynamic spectrum access/cognitive radio wireless networks: A survey," *Computer Networks*, vol. 50, no. 13, pp. 2127 – 2159, 2006.

[124] I. F. Akyildiz, W. Lee, M. Vuran, and S. Mohanty, "Next generation/dynamic spectrum access/cognitive radio wireless networks: A survey," *Computer Networks*, vol. 50, no. 13, pp. 2127 – 2159, 2006.

[125] T. Yucek and H. Arslan, "A survey of spectrum sensing algorithms for cognitive radio applications," *IEEE Communications Surveys Tutorials*, vol. 11, no. 1, pp. 116–130, First 2009.

[126] V. K. Bhargava and E. Hossain, *Cognitive Wireless Communication Networks*, Springer-Verlag New York, Inc., Secaucus, NJ, USA, 2007.

[127] T. Weiss, J. Hillenbrand, A. Krohn, and F. K. Jondral, "Mutual interference in OFDM-based spectrum pooling systems," in *IEEE 59th Vehicular Technology Conference*, 2004, vol. 4, pp. 1873–1877.

[128] B. Farhang-Boroujeny, "OFDM versus filter bank multicarrier," *IEEE Signal Processing Magazine*, vol. 28, no. 3, pp. 92–112, May 2011.

[129] M. G. Bellanger, "Specification and design of a prototype filter for filter bank based multicarrier transmission," in *2001 IEEE International Conference on Acoustics, Speech, and Signal Processing.*, 2001, vol. 4, pp. 2417–2420 vol.4.

[130] R. Zakaria and D. Le Ruyet, "A novel FBMC scheme for spatial multiplexing with maximum likelihood detection," in *7th International Symposium on Wireless Communication Systems (ISWCS)*, Sept 2010, pp. 461–465.

[131] Z. Hu, G. Zhu, Y. Xia, and G. Liu, "Multiuser subcarrier and bit allocation for MIMO-OFDM systems with perfect and partial channel information," in *IEEE Wireless Communications and Networking Conference (WCNC)*, March 2004, vol. 2, pp. 1188–1193.

[132] D. Niyato and E. Hossain, "Radio resource management in MIMO-OFDM- mesh networks: Issues and approaches," *IEEE Communications Magazine*, vol. 45, no. 11, pp. 100–107, November 2007.

[133] H. Yongqing, Q. Peng, and H. Shao, "Adaptive bit and power loading algorithm with low complexity in MIMO-OFDM systems," *Journal of Systems Engineering and Electronics*, vol. 19, no. 3, pp. 461–466, June 2008.

[134] W. W. L. Ho and Y. Liang, "Optimal resource allocation for multiuser MIMO-OFDM systems with user rate constraints," *IEEE Transactions on Vehicular Technology*, vol. 58, no. 3, pp. 1190–1203, March 2009.

[135] G. Scutari and D. P. Palomar, "MIMO cognitive radio: A game theoretical approach," *IEEE Transactions on Signal Processing*, vol. 58, no. 2, pp. 761–780, 2010.

[136] S. Hua, H. Liu, M. Wu, and S. S. Panwar, "Exploiting MIMO antennas in cooperative cognitive radio networks," in *Proceedings IEEE INFOCOM*, 2011, pp. 2714–2722.

[137] D. N. Nguyen and M. Krunz, "Spectrum management and power allocation in MIMO cognitive networks," in *Proceedings IEEE INFOCOM*, 2012, pp. 2023–2031.

[138] S. M. Perlaza, N. Fawaz, S. Lasaulce, and M. Debbah, "From spectrum pooling to space pooling: Opportunistic interference alignment in MIMO cognitive networks," *IEEE Transactions on Signal Processing*, vol. 58, no. 7, pp. 3728–3741, 2010.

[139] C.G. Tsinos and K. Berberidis, "Blind opportunistic interference alignment in MIMO cognitive radio systems," *IEEE Journal on Emerging and Selected Topics in Circuits and Systems*, vol. 3, no. 4, pp. 626–639, Dec 2013.

[140] L. Sboui, H. Ghazzai, Z. Rezki, and M.-S. Alouini, "Achievable rate of cognitive radio spectrum sharing MIMO channel with space alignment and interference temperature precoding," in *IEEE International Conference on Communications (ICC)*, 2013, pp. 2656–2660.

[141] N. Zhao, T. Qu, H. Sun, A Nallanathan, and H. Yin, "Frequency scheduling based interference alignment for cognitive radio networks," in *IEEE Global Communications Conference (GLOBECOM)*, Dec 2013, pp. 3447–3451.

[142] Y. Xu and S. Mao, "Stackelberg game for cognitive radio networks with MIMO and distributed interference alignment," *IEEE Transactions on Vehicular Technology*, vol. 63, no. 2, pp. 879–892, Feb 2014.

[143] T. Weiss, J. Hillenbrand, A. Krohn, and F. K. Jondral, "Mutual interference in OFDM-based spectrum pooling systems," in *IEEE 59th Vehicular Technology Conference*, 2004, vol. 4, pp. 1873–1877.

[144] Q. Zhao, S. Geirhofer, L. Tong, and B. Sadler, "Opportunistic spectrum access via periodic channel sensing," *IEEE Transactions on Signal Proceccing.*, vol. 56, no. 2, pp. 785–796, Feb 2008.

[145] T. Ban, W. Choi, B. Jung, and D. Sung, "Multi-user diversity in a spectrum sharing system," *IEEE Transactions on Wireless Communications*, vol. 8, no. 1, pp. 102–106, Jan 2009.

[146] G. Bansal, J. Hossain, and V. K. Bhargava, "Optimal and suboptimal power allocation schemes for OFDM-based cognitive radio systems," *IEEE Transactions on Wireless Communications*, vol. 7, no. 11, pp. 4710–4718, 2008.

[147] S. Chen and R. Cheng, "Clustering for interference alignment in multiuser interference network," *IEEE Transactions on Vehicular Technology*, vol. PP, no. 99, pp. 1–1, 2013.

[148] S. Ben Halima and A. Saadani, "Joint clustering and interference alignment for overloaded femtocell networks," in *IEEE Wireless Communications and Networking Conference (WCNC)*, 2012, pp. 1229–1233.

[149] P. Nikolaos and A. Theodore, "Bit and power allocation in constrained multicarrier systems: The single-user case," *EURASIP Journal on Advances in Signal Processing*, vol. 2008, 2007.

[150] W. Yu, W. Rhee, S. Boyd, and J. M. Cioffi, "Iterative water-filling for gaussian vector multiple-access channels," *IEEE Transactions on Information Theory*, vol. 50, no. 1, pp. 145–152, 2004.

[151] M. Pischella and E. Vivier, "Comparison of distributed space and frequency interference alignment," in *IEEE 21st International Symposium on Personal Indoor and Mobile Radio Communications (PIMRC)*, Sept 2010, pp. 532–537.

[152] L. Ma, T. Xu, and G. Sternberg, "Computational complexity of interference alignment for symmetric MIMO networks," *IEEE Communications Letters*, vol. 17, no. 12, pp. 2308–2311, December 2013.

[153] C. Sun, Y. Yang, and Y. Yuan, "Low complexity interference alignment algorithms for desired signal power maximization problem of MIMO channels," *EURASIP Journal on Advances in Signal Processing*, vol. 2012, no. 1, 2012.

[154] Y. J. Zhang and K. B. Letaief, "An efficient resource-allocation scheme for spatial multiuser access in MIMO/OFDM systems," *IEEE Transactions on Communications*, vol. 53, no. 1, pp. 107–116, Jan 2005.

[155] E. Lo, P. Chan, V. Lau, R. Cheng, K. B. Letaief, R. Murch, and W. Mow, "Adaptive resource allocation and capacity comparison of downlink multiuser MIMO-MC-CDMA and MIMO-OFDMA," *IEEE Transactions on Wireless Communications*, vol. 6, no. 3, pp. 1083–1093, March 2007.

[156] C. Suh and D. Tse, "Interference alignment for cellular networks," in *46th Annual Allerton Conference on Communication, Control, and Computing*, Sept 2008, pp. 1037–1044.

[157] C. Suh, M. Ho, and D. Tse, "Downlink interference alignment," *IEEE Transactions on Communications*, vol. 59, no. 9, pp. 2616–2626, September 2011.

[158] B. Nosrat-Makouei, J. G. Andrews, and R. W. Heath, "MIMO interference alignment over correlated channels with imperfect CSI," *IEEE Transactions on Signal Processing*, vol. 59, no. 6, pp. 2783–2794, June 2011.

[159] S. Jafar, "Blind interference alignment," *IEEE Journal of Selected Topics in Signal Processing*, vol. 6, no. 3, pp. 216–227, June 2012.

[160] R. T. Krishnamachari and M. K. Varanasi, "Interference alignment under limited feedback for MIMO interference channels," *IEEE Transactions on Signal Processing*, vol. 61, no. 15, pp. 3908–3917, Aug 2013.